

**UNIVERSITY OF GAZIANTEP
GRADUATE SCHOOL OF
NATURAL AND APPLIED SCIENCES**

**PROPERTIES OF SELF-COMPACTING CONCRETES MADE
WITH COLD BONDED FLY ASH LIGHTWEIGHT
AGGREGATES**

**Ph. D. THESIS
IN
CIVIL ENGINEERING**

**BY
HATİCE ÖZNUR ÖZ
JANUARY 2014**

**Properties of Self-Compacting Concretes Made with Cold Bonded
Fly Ash Lightweight Aggregates**

Ph. D. Thesis
in
Civil Engineering
University of Gaziantep

Supervisor
Assoc. Prof. Dr. Mehmet GESOĞLU

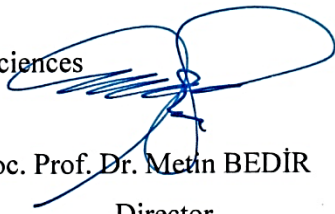
by
Hatice Öznur ÖZ
January 2014

© 2014 [Hatice Öznur ÖZ]


REPUBLIC OF TURKEY
UNIVERSITY OF GAZIANTEP
GRADUATE SCHOOL OF NATURAL & APPLIED SCIENCES
CIVIL ENGINEERING DEPARTMENT

Name of the Thesis: Properties of Self-Compacting Concretes Made with Cold
Bonded Fly Ash Lightweight Aggregates
Name of the Student: Hatice Öznur ÖZ
Exam Date : 15 January 2014


Approval of the Graduate School of Natural and Applied Sciences


Assoc. Prof. Dr. Metin BEDİR
Director

I certify that this thesis satisfies all the requirements as a thesis for the degree of
Doctor of Philosophy.


Prof. Dr. Mustafa GÜNAL
Head of Department

This is to certify that we have read this thesis and that in our opinion it is fully
adequate, in scope of quality as a thesis for the degree of Doctor of Philosophy.


Assoc. Prof. Dr. Mehmet GESOĞLU
Supervisor

Examining Committee Members

Assoc. Prof. Dr. Erhan GÜNEYİSİ

Assoc. Prof. Dr. Hanifi ÇANAKÇI

Assoc. Prof. Dr. Mehmet GESOĞLU

Assist. Prof. Dr. Ahmet ERKLİĞ

Assist. Prof. Dr. Kasım MERMERDAŞ

Signature


.....


.....


.....


.....


.....

I hereby declare that all information in this document has been obtained and presented in accordance with academic rules and ethical conduct. I also declare that, as required by this rules and conduct, I have fully cited and referenced all material and results that are not original to this work.

Hatice Öznur ÖZ

ABSTRACT

PROPERTIES OF SELF-COMPACTING CONCRETES MADE WITH COLD BONDED FLY ASH LIGHTWEIGHT AGGREGATES

ÖZ, Hatice Öznur

Ph.D. in Civil Engineering

Supervisor: Assoc. Prof. Dr. Mehmet GESOĞLU

January 2014

153 pages

In this thesis, an experimental program was conducted to investigate some mechanical, fracture, physical and durability properties of self-compacting concretes made with cold bonded fly ash aggregates. At first, dry powder mixture of 90% fly ash and 10% Portland cement by weight was pelletized through moistening in a revolving tilted pan at ambient temperature to produce lightweight fly ash aggregates which were then cured for 28 days. Thereafter, a total of seventeen self-compacting lightweight aggregate concretes (SCLCs) in which natural aggregates had been replaced with cold-bonded lightweight fine (LWFA) and coarse aggregate (LWCA) at different volume fraction of 10%, 20%, 30%, 40% and 50% were designed with a water/binder ratio of 0.32. The workability of SCLCs was observed through by slump flow time and diameter, V-Funnel flow time, and L-Box height ratio. Moreover, the rheological properties of fresh concrete mixes were determined via ICAR rheometer. Thereafter, the hardened properties of the concretes were measured by means of compressive strength, splitting tensile strength, fracture energy, water sorptivity, water permeability, rapid chloride permeability, and gas permeability tests. In addition, physical properties such as drying shrinkage, weight loss and the restrained shrinkage cracking were monitored.

Keywords: Lightweight aggregate; Pelletization method; Self compacting lightweight aggregate concrete; Fresh properties; Hardened properties.

ÖZET

SOĞUK BAĞLAMA YÖNTEMİ İLE ELDE EDİLEN UÇUCU KÜL HAFİF AGREGALI KENDİLİĞİNDEN YERLEŞEN BETONLARIN ÖZELLİKLERİ

ÖZ, Hatice Öznur
Doktora Tezi, İnşaat Mühendisliği Bölümü
Tez Yöneticisi: Doç. Dr. Mehmet GESOĞLU
Ocak 2014
153 sayfa

Bu tezde, soğuk bağlama yöntemi ile üretilen uçucu kül hafif agregalı kendiliğinden yerleşen betonların birtakım mekanik, kırılma, fiziksel ve durabilite özellikleri deneysel olarak incelenmiştir. İlk olarak, hafif uçucu kül agregaları üretmek için ağırlıkça %90 uçucu kül ve %10 çimentodan oluşan kuru toz karışım dönen eğimli bir diskte oda sıcaklığında ıslatma yoluyla peletlenmiş ve sonra 28 gün kürlenmiştir. Daha sonra, doğal agreganın soğuk bağlanmış ince ve iri agregayla %10, %20, %30, %40, 50% hacimsel oranlarda yer değiştirilmesiyle oluşan toplam on yedi kendiliğinden yerleşen hafif agregalı beton (SCLC) 0.32 su/bağlayıcı oranı ile tasarlanmıştır. Kendiliğinden yerleşen hafif agregalı betonların işlenebilirliği yayılma süresi ve çapı, V-hunisi akma süresi, L-kutusu yükseklik oranı deneyleriyle gözlemlenmiştir. Ayrıca, taze betonların reolojik özellikleri ICAR reometresi ile belirlenmiştir. Sonrasında, sertleşmiş betonların özellikleri basınç dayanımı, yarmada çekme dayanımı, eğilmede çekme dayanımı, kırılma enerjisi, kılcal su geçirimsizliği, basınçlı su geçirimsizliği, hızlı klor geçirimsizliği ve gaz geçirimsizliği testleri ile ölçülmüştür. Ek olarak, kuruma rötresi, ağırlık kaybı ve sınırlandırılmış rötire çatlağı gibi fiziksel özellikleri de incelenmiştir.

Anahtar Kelimeler: Hafif Agregası; Peletleme Yöntemi; Kendiliğinden Yerleşen Beton; Taze özellikler; Sertleşmiş Özellikler.

*To my husband and son,
Erçin and Mehmet Yiğit*

ACKNOWLEDGEMENT

First and foremost, I would like to express my deepest gratitude to my advisor, Assoc. Prof. Dr. Mehmet GESOĞLU for his helpful comments, criticisms, generous guidance and many creative insights offered during this thesis.

Special thanks are reserved Assoc. Prof. Dr. Erhan GÜNEYİSİ, Assoc. Prof. Dr. Hanifi ÇANAKÇI, and Assist. Prof. Dr. Ahmet ERKLİĞ for serving on the committee and their contributions and suggestions to improve the quality of the thesis.

This study received a financial support from Gaziantep University Scientific Research Projects Governing Unit under grant number MF09.08. I also would like to thank to Fly Ash Plant of Plato for supplying product from Çatalağzı Power Plant.

I would like to express my thanks to my family, especially to my sister Pınar ÖZEL, for their inspiration, unending support, and encouragement throughout my education and life.

I would like to extend my thanks to my colleagues Assist. Prof. Dr. Kasım MERMERDAŞ and Res. Assist. Süleyman İPEK as well as my students Diler Sabah ASAAD, İsmail ŞİMŞEK, Mehmet Yavuz TEZCAN and Ertan YAKAR for their precious helps in experimental phase of the study.

Last but not least, I will always be grateful to my husband Erçin ÖZ for his encouragement, endless support and assistance, and especially for his incredible love.

CONTENTS

ABSTRACT	v
ÖZET.....	vi
ACKNOWLEDGEMENT	viii
CONTENTS.....	ix
LIST OF FIGURES	xii
LIST OF TABLES	xvi
CHAPTER 1	1
INTRODUCTION	1
1.1 General	1
1.2 Research Significance	3
1.3 Outline of the Thesis	3
CHAPTER 2	5
LITERATURE REVIEW AND BACKGROUND.....	5
2.1 Fly Ash.....	5
2.1.1 Mineralogical Properties of Fly Ash.....	5
2.1.2 Chemical Properties	6
2.1.3 Physical Properties	7
2.1.4 Application and Uses of Fly Ash	8
2.2 Lightweight Aggregates	8
2.2.1 Lightweight Aggregate Production with Fly Ash.....	8
2.2.2 Pelletization Theory	10
2.3 Lightweight Aggregate Concrete	13
2.3.1 Mechanical Properties of Lightweight Aggregate Concretes	16
2.3.2 Interface between Lightweight Aggregate and Cement Paste	20
2.3.3 Fracture of Lightweight Aggregate Concretes.....	21
2.3.4 Shrinkage of Lightweight Aggregate Concretes	23
2.3.5 Durability of Lightweight Aggregate Concretes.....	25
2.4 Self Compacting Concrete	28
2.4.1 Self Compacting Lightweight Concretes	33
CHAPTER 3	36
EXPERIMENTAL STUDY.....	36

3.1 Materials.....	36
3.1.1 Cement and Fly ash.....	36
3.1.2 High Range Water Reducing Admixture	37
3.1.3 Aggregates.....	37
3.2 Self Compacting Lightweight Concrete Mix Properties	43
3.3 Concrete Casting	46
3.4 Tests for Fresh Properties.....	49
3.4.1 Slump Flow Test	49
3.4.2 V-funnel Test	50
3.4.3 L-box Test	50
3.4.4 Viscosity Test.....	53
3.5 Tests for Mechanical Properties.....	55
3.5.1 Compressive Strength Test	55
3.5.2 Splitting Tensile Strength Test.....	55
3.5.3 Fracture Energy	56
3.7 Tests for Physical Properties.....	58
3.7.1 Drying Shrinkage and Weight Loss	58
3.7.2 Restrained Shrinkage Cracking.....	60
3.8 Determination of the Durability Performance of SCCs	62
3.8.1 Water Sorptivity	62
3.8.2 Water Permeability.....	63
3.8.3 Rapid Chloride Permeability Test.....	63
3.8.4 Gas Permeability	66
CHAPTER 4	70
TEST RESULTS AND DISCUSSIONS	70
4.1 Fresh Properties of Self Compacting Lightweight Concretes.....	70
4.1.1 Fresh Density	70
4.1.2 Slump Flow Time and Slump Flow Diameter	72
4.1.3 V-funnel Flow Time.....	73
4.1.4 L-box Height Ratio	79
4.1.5 Rheological Parameters of Self Compacting Lightweight Concretes.....	80
4.2 Mechanical Properties of Self Compacting Lightweight Concretes	85
4.2.1 Compressive Strength	85
4.2.2 Splitting Tensile Strength.....	92
4.2.3 Net Flexural Strength	96
4.3 Fracture Parameters of Self Compacting Lightweight Concretes.....	98
4.3.1 Fracture Energy	98

4.3.2 Characteristic Length	104
4.4 Physical Properties of Self Compacting Lightweight Concretes	108
4.4.1 Drying Shrinkage and Weight Loss	108
4.4.2 Restrained Shrinkage	110
4.5 Durability Properties of Self Compacting Lightweight Concretes	116
4.5.1 Water Sorptivity	116
4.5.2 Water Permeability.....	121
4.5.3 Rapid Chloride Permeability.....	125
4.5.4 Gas Permeability	129
CHAPTER 5	133
CONCLUSIONS.....	133
REFERENCES.....	138

LIST OF FIGURES

Figure 2.1 Mechanism of pellet formation (Jaroslav and Ruzickova, 1987).....	11
Figure 2.2 Process of ball nuclei forming (water components below ideal position) (Jaroslav and Ruzickova, 1987)	12
Figure 2.3 Process of ball nuclei forming (water components above ideal position)	12
Figure 2.4 Strengths following up on an individual pellet while pelletization process continues (Pietsch, 1991)	13
volume fraction (Gesoglu et al., 2004)	19
Figure 2.6 Typical results of stress-strain curves of concretes in compression.....	23
Figure 2.7 Schematic diagram displaying uncommensures between porosity and permeability (Euro Light Concrete Project, 1998).....	26
Figure 2.8 Differential rheological properties of conventional and self-compacting concretes (Koehler, 2009)	31
Figure 2.9 IBB Rheometer and impeller (Koehler and Fowler, 2004)	31
Figure 2.10 Velocity field in BRTHEOM rheometer (Koehler and Fowler, 2004)	32
Figure 2.11 ICAR rheometer	32
Figure 3.1 The general view of the pelletization disc	39
Figure 3.2 Artificial lightweight aggregate a) Self-curing process and b) Artificial fine and coarse lightweight aggregates.....	40
Figure 3.3 Crushing strength test apparatus	42
Figure 3.4 Crushing strength of lightweight aggregate.....	42
Figure 3.5 Aggregate grading for a) MC mixes, b) MF mixes and c) MCF mixes	45
Figure 3.6 LWAs in SSD condition	47
Figure 3.7 Photographic views of slump flow test a) Slump flow test plate and b) The measurement of slump flow diameter	51

Figure 3.8 Photographic view of V-funnel test a) Schematic representation of the V-funnel and b) Measurement of V-funnel flow time	52
Figure 3.10 The ICAR rheometer a) Principal dimensions and b) Device including vane (all dimensions are in mm)	55
Figure 3.11 Photographic view of universal testing devices and three point flexural testing fixture	57
Figure 3.12 Photographic view of notched beam specimen	58
Figure 3.13 Free shrinkage test a) Free shrinkage test set up and b) Test specimens	59
Figure 3.14 The dimension of restrained shrinkage ring specimen (in mm)	60
Figure 3.15 Restrained shrinkage test specimens	61
Figure 3.16 Photographic view of a cracked ring specimen (MF20).....	62
Figure 3.17 Water sorptivity test set up	64
Figure 3.18 Water permeability test set up	64
Figure 3.19 Schematic presentation of the test set up for RCPT	65
Figure 3.20 Photographic view of the RCPT test set up	66
Figure 3.21 Photographic view of the gas permeability test set up	68
Figure 3.23 Schematic presentation of the pressure cell and test specimen	69
Figure 4.1 Variation in the fresh density of SCLCs.....	71
Figure 4.2 Fresh density differences (%) for SCLCs with respect to CM.....	71
Figure 4.3 Slump flow diameter of a) CM and b) MCF100	75
Figure 4.4 Variation of HRWRA demand with increasing LWA content.....	76
Figure 4.5 Variation of slump flow diameter and slump flow classes for SCLCs	76
Figure 4.6 Variation of $T_{500\text{ mm}}$ slump flow time and viscosity classes for SCLCs	77
Figure 4.7 Variation of V-funnel flow time and viscosity classes for SCLCs.....	78
Figure 4.8 Variation of viscosity classes with $T_{500\text{ mm}}$ slump flow and V-funnel times for SCLCs.....	78
Figure 4.9 Variation of L-box height ratio values for SCLCs	80
Figure 4.10 Flow curves for a) MC group mixes, b) MF group mixes and c) MCF group mixes	83
Figure 4.11 Variation of plastic viscosity with increasing LWA content.....	84
Figure 4.12 Compressive strengths of SCLCs at a) 28 days and b) 90 days	89

Figure 4.13 Effect of replacement level of LWA on compressive strength of SCLCs at a) 28 days and b) 90 days (Compressive strength for control concrete is 100%)	90
Figure 4.14 Structural efficiency of SCLCs.....	91
Figure 4.15 Splitting tensile strength of SCLCs at a) 28 days and b) 90 days	94
Figure 4.16 Effect of replacement level of LWA on splitting tensile strength of SCLCs at a) 28 days and b) 90 days (Splitting tensile strength for control concrete is 100%).....	95
Figure 4.17 Net flexural tensile strength values for SCLCs at 90 days	97
Figure 4.18 Effect of replacement level of LWA on net flexural strength of SCLCs at 90 days (Net flexural strength for control concrete is 100%).....	98
Figure 4.19 Fracture energies of SCLCs at 90 days.....	101
Figure 4.20 Effect of replacement level of LWA on fracture energy of SCLCs at 90 days (Fracture energy for control concrete is 100%)	101
Figure 4.21 Typical load versus displacement curves of CM and MCF100.....	102
Figure 4.22 Typical load versus displacement curves of a) MC concretes, b) MF concrete and c) MCF concretes	103
Figure 4.23 Modulus of elasticity of SCLCs at a) 28 days and b) 90 days.....	107
Figure 4.24 Characteristic lengths of SCLCs.....	107
Figure 4.25 Effect of replacement level of LWA on characteristic lengths of SCLCs at 90 days (Characteristics length for control concrete is 100%)	108
Figure 4.26 Drying shrinkage strain development of a) MC concretes, b) MF concretes and c) MCF concretes	113
Figure 4.27 Variations in weight loss of a) MC concretes, b) MF concretes and c) MCF concretes	114
Figure 4.28 Shrinkage cracking performance of a) MC concretes, b) MF concretes and c) MCF concretes	116
Figure 4.29 Water sorptivity test results at a) 28 days and b) 90 days	119
Figure 4.30 Effect of replacement level of LWA on sorptivity index of SCLCs at a) 28 days and b) 90 days (Sorptivity index for control concrete is 1)	120
Figure 4.31 Water penetration depths of SCLCs at a) 28 days and b) 90 days	123
Figure 4.32 Effect of replacement level of LWA on water penetration depth of SCLCs at a) 28 days and b) 90 days (Water penetration depth for control concrete is 1)	124

Figure 4.33 RCPT test results of SCLCs at a) 28 days and b) 90 days.....	127
Figure 4.34 Effect of replacement level of LWA on chloride resistance of SCLCs at a) 28 days and b) 90 days (Charge passed for control concrete is 1)	128
Figure 4.35 Variation of apparent gas permeability coefficients of SCLCs at a) 28 days and b) 90 days	131
Figure 4.36 Effect of replacement level of LWA on apparent gas permeability of SCLCs at a) 28 days and b) 90 days (Apparent gas permeability coefficient for control concrete is 1)	132

LIST OF TABLES

Table 2.1 Classification of lightweight concretes according to compressive strength-density relationship (Clarke, 1993).....	16
Table 2.2 List of test methods for workability properties of SCC (EFNARC, 2005)	30
Table 3.1 Chemical compositions and physical properties of Portland cement and fly ash	38
Table 3.2 Properties of High Range Water Reducing Admixture (HRWRA).....	38
Table 3.3 Sieve analysis and physical properties of natural and lightweight aggregates.....	43
Table 3.4 Aggregates volume fractions for SCLCs	46
Table 3.5 Concrete mix proportions in kg/m ³	48
Table 3.6 Slump flow, viscosity, and passing ability classes with respect to EFNARC (2005)	52
Table 3.7 Interpretation of the test results obtained using RCPT test (ASTM C1202, 2012).....	65
Table 4.1 Slump flow, V-funnel and L-box properties of SCLCs	74
Table 4.2 Plastic and relative viscosity values for SCLCs	85
Table 4.3 Compressive strength of SCLCs	88
Table 4.4 The variations of air dry density and structural efficiency for SCLCs	91
Table 4.5 Splitting tensile strength of SCLCs.....	93
Table 4.6 Ultimate load and flexural strength of SCLCs.....	97
Table 4.7 The variations of final displacements and fracture energy of SCLCs	100
Table 4.8 Modulus of elasticity and characteristic length of SCLCs.....	106
Table 4.9 Drying and restrained shrinkage performance of SCLCs	111
Table 4.10 28 and 90 days sorptivity values of SCLCs	118
Table 4.11 Water penetration depths measured at 28 and 90 days	122
Table 4.12 Total charge values measured at 28 and 90 days	126

Table 4.13 Apparent gas permeability coefficient average of that value for 150,
200, and 300 kPa inlet pressures as recommended per RILEM (1999)..... 130

LIST OF SYMBOLS/ABBREVIATIONS

μ	Plastic viscosity
A	Cross-sectional area of the sample
a	The notch depth of beam
B	The width of beam
CC	Conventional Concrete
E	Static modulus of elasticity
FA	Fly Ash
f_c	Cylinder compressive strength
f_{flex}	Net flexural strength
f_{st}	Splitting tensile strength
g	Gravitational acceleration,
G_F	Fracture energy
HRWRA	High Range Water Reducing Admixture
I	Cumulative infiltration
ITZ	Interfacial Transition Zone
K	Gas permeability coefficient
L	Height of sample
l_{ch}	Characteristics length
LEFM	Linear Elastic Fracture Mechanics
LVDT	Linear Variable Displacement Transducer
LWA	Lightweight Aggregate
LWC	Lightweight Concrete
LWCA	Lightweight Coarse Aggregate
LWFA	Lightweight Fine Aggregate
m	Mass
N	Rotational speed
NFM	Nonlinear Fracture Mechanics
NWA	Normal Weight Aggregate
NWC	Normal Weight Concrete

NWCA	Normal Weight Coarse Aggregate
NWFA	Normal Weight Fine Aggregate
P_1	Inlet gas pressure
P_2	Outlet gas pressure
P_{\max}	Fracture load
q	Air dried density of concrete
Q	Rate of flow of air bubble
R	Radius of the disc
S	The span of beam
S'	Sorptivity index
SCC	Self Compacting Concrete
SCLC	Self Compacting Lightweight Aggregate Concrete
SSD	Saturated Surface Dry Condition
t	Time
T	Torque
$T_{500\text{mm}}$	The time required to reach 500 mm slump-flow
U	The length of beam
V	The slope of the line
w	Centrifugal acceleration
W	The depth of beam
X	Distance between loading points
Y	The intercept of the line with the torque axis
β	Angle of the disc's plane to normal
γ'	Shear rate (rotation speed)
δ_s	The specified deflection of the beam
η	Viscosity of oxygen
σ	Crushing strength
τ	Shear stress
τ_o	Yield stress
ν	Coefficient of friction between the pellet and the disc

CHAPTER 1

INTRODUCTION

1.1 General

Concrete is the world's most widely used structural material which has superior properties such as excellent versatility, availability and economy. Despite all advantages, the use of concrete is restricted in some structures due to its high own weight and high qualified workmanship with respect to other structural materials. Therefore, in recent years there has been a tremendous interest to develop new high performance structural materials such as self-compacting concrete (SCC) and lightweight concrete (LWC) to provide the needs of the construction sector (Bentur et al., 2001; Kılıç, 2003; Kim et al., 2010).

Since the second half of the twentieth century, LWCs has been used for many structural applications, and became a very convenient alternative in the terms of thermal insulation and unit weight when compared with Conventional Concrete (CC). In addition to the recycled industrial wastes, naturally existing scoria, volcanic cinders, tuff, and diatomite are also used as lightweight aggregate (LWA) in the concrete manufacture. However, commercially available LWAs such as shale or expanded clay, and sintered fly ash can be easily acquired via heat treatment at 1000°C to 1200°C (Gesoglu, 2004; Koçkal, 2008). By utilizing such type of LWAs, structural LWCs can be produced in the strength range of 30-80 MPa (Chang and Shieh, 1996; Yang, 1997).

Increasing use of LWC brought the need for the production of artificial lightweight aggregates so the waste materials derived from industrial products such as fly ash (FA), blast furnace slag, are used for LWA production. Although almost 15 million tons of FA is generated from thermal coal-fired power plants annually in Turkey, a very small amount of it is utilized in the construction industry (Turkish Statistical

Institute, 2010). Environmental impacts and economic considerations have had great role in the utilization of waste material as well as better performance characteristics. Using waste materials for the production of LWA has a promising future due to the increasing interest and the need for recycling waste product (Metha, 1998; Videla and Martinez, 2002). Artificial lightweight aggregates made from waste materials have a positive influence on the environment, the community, and the construction industry. The benefits of using waste materials can be summarized as follows: First, without using natural aggregates (NWA), the natural resources are not depleted and the damaging activities of aggregate mining are prevented. The aggregates produced with waste materials can be lighter compared to the natural aggregate, which in turn leads to lightweight concrete produced using such aggregates. In addition, the emissions of green house gases reduce as the need for large quantities of cement is decreased (Kayali, 2008). Cold bonding, autoclaving or sintering procedures are the most commonly applied techniques for manufacturing artificial aggregates (Gesoglu, 2004; Arslan and Baykal, 2006; Manikandan and Ramamurthy, 2008; Joseph and Ramamurthy, 2009). Cold-bonding or pelletization method is the agglomeration of fines that has cementitious property either by them and/or by blending those with a mineral additive. This method requires minimum energy consumption for making pellets, a ball like shape of material made by agglomeration of moisturized fines with water acting as a coagulant in a rotating disc (Baykal and Döven, 2000; Gesoglu, 2004; Arslan and Baykal, 2006).

Incorporations of mineral and chemical admixtures in CC contributed in the existence of new trends in construction sector. Thus, at the early 1990s, self-compacting concrete has brought a revolution in concrete technology which led to improve the concrete quality, enhanced the conditions of working on the site and increased productivity (Zhu and Bartos, 2003). SCC is a highly flowing concrete that can spread through congested reinforcement, fills restricted areas without segregation and bleeding, places and gets consolidated under self-weight (Khaleel et al. 2011; Safiuddin et al., 2011). Although having favorable properties, the usage of SCC can be limited in some structures by the reason of high self-weight. Self-compacting lightweight aggregate concrete (SCLC) is a kind of high performance concrete developed by combining the favorable properties of SCC and LWC. The use of SCLC can be beneficial to obtain a significant reduction in the total mass of

the structure which can result in size reductions of sections and simplify the construction (Kim et al., 2010). Furthermore, the segregation of LWA in place of SCC can be prevented by skipping the process of vibration.

Due to occupation of 60-70% of the concrete volume, LWAs play a main role in affecting the workability, strength, dimensional stability, and durability as well as the cost of SCLC (Khaleel et al. 2011; Safiuddin et al., 2011). The wide diversity of source and production methods for LWAs caused distinctive behavior among SCLCs. Therefore, the characteristics of SCLCs have to be examined individually for each type of LWA. Many researchers studied the effects of the particle shape, specific gravity, unit weight, particle size, strength, moisture content, and absorption of the LWA on the properties of LWC (Baykal and Döven, 2000; Gesoğlu et al., 2007; Kayali, 2008; Joseph and Ramamurthy, 2009; Gesoğlu et al., 2012a, Gesoğlu et al., 2012b). However, so far, there are only a few studies on use of LWA in the production SCLC. Compared with SCC, there was no significant difference in the design of SCLC except for the aggregate used (Müller and Haist, 2002). However, spherical shaped of aggregate with smooth surface are preferred because they more readily flow past each other as reducing of specific surface area requires less cement and water (EFNARC, 2005; Hela and Hubertova, 2005; Lo et al., 2007b; Wu et al., 2009; Bogas et al., 2012).

The main objective of the thesis presented herein is to investigate the properties of the self-compacting concretes made with the fly ash lightweight coarse and fine aggregates produced by cold bonding process. For this purpose, an experimental program was conducted in two stages. The first part covered the manufacturing of artificial lightweight coarse and fine aggregates by cold-bonding pelletization of fly ash and cement at room temperature. In the second part of the study, natural coarse and fine aggregates of conventional SCC were partially substituted by LWAs at six volume fractions from 0% to 100% by 20% increments. Thus, a total of seventeen different SCLC mixtures were designed with constant water-binder ratio (w/b) of 0.32 and the total binder content of 550 kg/m³. Fresh properties of SCCs were observed through slump flow time and flow diameter, V-funnel flow time, L-box height ratio. The rheological properties of each mixture were also determined by using ICAR rheometer equipment. Hardened properties of SCCs were tested for

compressive strength, splitting tensile strength, net flexural strength, sorptivity, water permeability, chloride ion permeability, gas permeability, and drying shrinkage performance. Moreover, fracture energy was determined for each SCLC.

1.2 Research Significance

The characteristic properties of the LWCs are mainly based on the properties and amount of LWA utilized. Therefore, various studies were conducted to examine how the mechanical properties of LWCs are affected by the special features of LWA used, but most of the research has focused on natural and commercially available LWA. Although the cold-bonded fly ash aggregates have been easily used in the production of LWCs, its usage in SCCs has not received adequate attention in previous studies. Incorporation of LWA in SCC can increase quality and produce high-strength LWCs while preventing the segregation of LWA. Also the use of fly ash aggregate in SCC can reduce the negative environmental effects of thermal coal-fired power plants and the consumption of limited natural resources. Thus, to achieve more sustainable and environment friendly concretes, the use of fly ash lightweight aggregates may be an alternative to CC.

1.3 Outline of the Thesis

This thesis consists of five chapters. **Chapter 2** presents a literature review and general background on the types and sources of lightweight aggregate, the characteristic properties of lightweight concrete incorporating lightweight aggregates, and the effect of lightweight aggregates on production of self-compacting concrete.

Chapter 3 includes the experimental program conducted throughout this study. Properties of cement, aggregates, mineral, and chemical admixture used in the concrete production as well as the tests on fresh and hardened properties of SCLCs are described.

Chapter 4 provides the results of testing program. Moreover, how the gradation size and volume fraction of lightweight aggregate affect the fresh, mechanical, durability and fracture properties of self-compacting lightweight aggregate concrete are

explained in this chapter. List of results, figures, evaluation are presented and discussed.

Chapter 5 gives conclusions of the thesis.

CHAPTER 2

LITERATURE REVIEW AND BACKGROUND

2.1 Fly Ash

Pozzolans including siliceous and/or alumina materials hold little or no cementitious value by themselves. However, in existence of humidity, in a finely divided shape, it reacts with calcium hydroxide in chemical way in order to create composites with cementitious features at any temperature. Fly ash is the best known, and one of the most commonly used pozzolans in the world. Fly ash is inorganic waste product generated during the firing of (nearly 1200°C) powder coal particles in thermal power stations, which is capable of reacting with $\text{Ca}(\text{OH})_2$ at room temperature so as to create cementitious composites. The presence of SiO_2 and Al_2O_3 in amorphous form affects the pozzolanic activity of fly ash (Baker, 1984; Naik and Singh, 1995; Baykal et. al, 1997). Characteristics of the fly ash depends on numerous factors, such as type of power plant, the composition of feed coal, chemical composition of the coal and burning system, and conditions of deposition of fly ash.

2.1.1 Mineralogical Properties of Fly Ash

Fly ashes are fine powders, heterogeneous in nature. They consist of mainly rounded or spherical glassy particles of varying silica, alumina and iron oxide content. Also irregular and angular particles are found in fly ashes which include both unburned coal remnants and mineral particles. The majority of mineral matter consists of clays, pyrite and calcite.

The coal composition, combustion conditions, ash collection systems and other variables, highly influence the compound of the fly ashes. The compound of FA is affected by the rate of cooling.

It is composed mainly (50-90%) of mineral substance shaped as glassy particles, and also a small amount occurs in the form of crystals. The most important minerals in FA obtained from bituminous coal are magnetite, hematite, quartz, mullite and free CaO. The other minerals like goethite, pyrite, calcite, anhydrite and periclase range within trace amounts to 2.5% (Ramadan, 1995; Döven, 1996; Gesoğlu, 2004).

2.1.2 Chemical Properties

During fly ash substance is being hung in the exhaust gases, an induration starts among these substances at the end; it is collected from chimney via electrostatic filters during cooling period. The main components of FA are silica (SiO_2) consisting of two forms: amorphous, whose structure is spherical and soft, and the other type is crystalline, alumina (Al_2O_3) and iron oxide (Fe_2O_3).

Fly ashes, consisting of a blend of glassy particles with diverse definable crystalline phases such as quartz, mullite as well as alkali oxides such as MgO and SO_3 are considerably heterogeneous in normal conditions. However, the chemical structure of FA can show distinctions owing to the obtaining from different locations of coal. Therefore, silica and alumina may be considered the main components of FA (Satapathy, 2000; Matsunaga et al., 2002).

Depending on its chemical compositions including calcium, silica, alumina, and iron content, fly ash is classified into two class; Class F and Class C with respect to ASTM C 618 (ASTM C618, 2000). Class F fly ash take part just in pozzolanic reaction because of necessitating a cementing agent, such as Portland cement, quicklime, or hydrated lime, when water is available in the environment, so as to have a reaction and generate cementitious composites. This type of fly ash is also known as low calcareous ash due to having less than 10% of CaO. However, Class C fly ash generated from the igniting of younger lignite or sub bituminous coal includes more than 20% lime (CaO). This fly ash is classified as pozzolanic and also cementitious. Class C fly ash can be growing stronger in time in the presence of water. In general, Class C fly ash has higher $\text{CaO}+\text{MgO}+\text{SO}_3$ and lower $\text{Al}_2\text{O}_3+\text{SiO}_2$ compared to Class F fly ash. Owing to the high CaO content, Class C fly ash participates in both cementitious and pozzolanic reactions, whereas Class F fly ash

takes place only in the pozzolanic reactions during the hydration process (Döven, 1996; Gesoğlu, 2004).

2.1.3 Physical Properties

The properties of concrete are affected by the shape, fineness, particle size distribution, densities, and compound of fly ash particles. Dimension of fly ash particle and properties of its shape are rely upon the source and consistency of the coal, the grade of powder prior to burning, the combustion surroundings, consistency of combustion, and the category of collection system (utilized mechanical separators, bag filters, or electrostatic precipitators). The particles vary in shape (spherical, rounded, irregular and angular) as well as in size by the examination of FA under optical instruments and scanning electron microscopy studies. Irregular and angular particles are larger in general also spherical and rounded particles are between 0.5 and 200 μm . The great part of fly ash particles is gleaming and round (Bradbury, 1982; Alonso and Wesche, 1991; Erdoğan, 1993). Because of agglomeration of fly ash molecules in liquefied phase, the allocation of the grain size distribution for the fly ash and the pulverized coal differs during the combustion process. Individual particles of fly ash range in size from less than 1 μm to greater than 1mm.

Fineness, one of the physical properties of fly ash that relates to its pozzolanic activity, is described as the percentage by weight of the material retained on the 0.044 mm (No. 325) sieve. Very fine particles have high specific surface area. The superficial section for fly ash is able to be measured using the Blaine apparatus. The Blaine fineness of fly ash varies from 2500 to 5500 cm^2/g .

The specific gravity of solid fly ash particles ranges from 1.9 to 2.9. Because of containing high amounts of unburned coal and hollow spherical particles, called cenospheres, FA has low specific gravity. Because of fly ash high in iron, it tends to have higher specific gravity. The bulk density of dry fly ash is about 7.9-9.5 kN/m^3 (Raask, 1968; Myers et. al., 1976; Bradbury, 1982; Alonso and Wesche, 1991).

Fly ash diversifies in color from light cream to dark brown, dark gray or black. The color of FA is affected by the quantity of carbon capacity, the iron-rich particles and moisture. The carbon content in fly ash is responsible of gray or black appearance of

FA, and the carbon capacity in FA may range from 0.5% to 12%. The amount of Fe_2O_3 is responsible of giving brown color to FA.

2.1.4 Application and Uses of Fly Ash

Because of its pozzolanic quality, spherical shape, and relative uniformity, fly ash may be reused as an engineering material. The recycling FA is used as in construction of raw feed for cement clinkers, Portland cement, grout, road subbase for subgrade stabilization, as landfill shelter, land renewal, and flowable ash slurry, waste stabilization and solidification, mineral reclamation, productions of bricks, blocks and paving stones, mineral filler in asphaltic concrete, loose application on rivers to melt ice, loose application on roads and parking lots for ice control, lightweight aggregate and concrete production, production of roller compacted concrete, autoclaved cellular concrete, material recovery, fillers for polymer matrix compounds, metal matrix compounds, and other filler applications (Döven, 1996; Gaarder, 2010; Josephson, 2010).

2.2 Lightweight Aggregates

Lightweight aggregates are a granular material with a bulk density not exceeding 1200 kg/m^3 , or with a particle density not exceeding 2000 kg/m^3 . Some lightweight aggregates are naturally found; others are manufactured (Gonzalez-Corrochano et al., 2009). LWAs are generally classified with respect to production process and method. Natural lightweight aggregates are generally of volcanic basis and, therefore, are available just in particular areas of the world. Artificial aggregates may be produced from wastes materials and industrial by products such as glass, fly ash, and dross (Baykal and Döven, 2000; Videla and Matinez, 2002; Kim et al., 2005; Mahmood, 2012). Lightweight aggregates, both natural and artificial, should meet the requirements of ASTM C330 (2009).

2.2.1 Lightweight Aggregate Production with Fly Ash

The usage of fly ash for concrete technology goes back to 1930s (Şengül, 2005). It is estimated that about 450 million tons of FA is produced worldwide every year, however just 6% of the total available is used as pozzolan in blended cements or in concrete mixtures (Baker, 1984). In Turkey, there are twelve active coal-burning

power plants with annual fly ash fabrication of about 15 million tons. The main aim using FA for LWA production is a feasible way for recycling of waste materials. Manufacturing fly ash lightweight aggregates can be achieved by sintering, autoclaving and cold-bonding methods (Hwang, 1992; Döven, 1996; Gesoğlu, 2004; Koçkal, 2008). The cold bonding process is more economical process because of lower energy consumption.

2.2.1.1 Sintering Method

It is a process of burning aggregates in industrial furnaces to vitrification. Artificial lightweight fly ash aggregates are produced by the use of sinter strand. At first, fly ash with clay is mixed with water and pelletized. Then, this is followed by firing on a travelling grate or on a sintering strand to about 1100°C. The pellets are gone through the process of drying, grinding, sintering and cooling; the process is ending up with a fly ash lightweight aggregate. At the end of the strand, the last pellets are in a natural or in a mechanical way distinguished. Aggregates, passing from 2.5 mm sieve, are pulled off and the others, remaining on 2.5 mm sieve, are used for the production of lightweight concretes (Ramadan, 1995; Koçkal and Özturan, 2010).

2.2.1.2 Autoclaving (Hydrothermal Treating) Method

Fly ash pellets are hardened by using pressurized saturated steam curing and this application is known autoclaving (hydrothermal treating). In the autoclaving method, 45% quartz sand, 47% fly ash, 4.5% lime, 2.0% additives and 1.5% water by weight are used to fly ash aggregates manufacturing. The whole admixture is pelletized and then inflated in the presence of high moisture and then fired up for 6.5 hours at 200°C so as to generate LWA that gets its first usage in brick laying parts (Bremner and Thomas, 2004; Koçkal, 2008).

2.2.1.3 Cold Bonding

Cold bonding is a kind of bonding which explains the capacity for FA to react with calcium hydroxide at ambient temperature. The main manufacturing process of fly ash LWA consists of pelletizing (also called agglomerating) in which fly ash, Portland cement and water, and curing for several days (Döven, 1996; Gesoğlu, 2004; Koçkal, 2008; Booya, 2012; Güneyisi et al., 2012).

2.2.2 Pelletization Theory

The idea of pelletization process was first put forward by A. G. Anderson, a Swedish researcher, in 1912, and then by C. A. Brackelsberg in Germany, who devised a similar balling process, it was a revised process with the addition of binder to the fines agglomerated and the pellets strengthened at elevated temperatures during production. Studies on pelletization process started in United States in 1920's due to the necessity of sintering concentrates that were used in Taconite-ore dressing procedure. The concentrates were finer than the size that would enable efficient sintering procedure and the pelletization methodology was started to be used upon the success obtained in pelletization process to enlarge the size of fines. This study was improved by agglomerating the fines in a drum and sintering them at 500°C, at ores fusing point, by E. P. Barret and S. R. Dean. A devised methodology in which the pellets would be sintered in shaft-furnace immediately after production in balling drum as a continuous process was carried out by E. A. Davies and his colleagues. Applications were realized on magnetite and other ores. For agglomerating fine-grained concentrate the pelletization process became economically feasible method in 1950s and the first pelletization plant was established in Sweden with 10-60 tones daily capacity. In 1955, the world's first huge plant started to produce 6 million tons of annual pellet operation and later followed by the others in USA and other countries in time (Jaroslav and Ruzickova, 1987; Döven 1996; Gesoğlu, 2004).

The pelletization theory investigates the mechanical forces being exert on the pellets while the process goes on, and the effect of these forces to cohesion of the structure. The studies indicated that the interpretation of the pelletization process is function of the engineering properties of the substance pelletized, amount of moisture of the medium, the angle of disc to the normal and the rotation speed (Jaroslav and Ruzickova, 1987).

When a substance of fine-grained is moisturized, a slim moist film is occurred on exterior of particles by the meniscus among the grains. Materials similar to bridges are shaped crescent among fragments by this film (Figure 2.1 a). In the form of the revolving the particles in a balling disc, the spherical shaped structures are formed by the augmented bonding forces among particles because of centrifugal and gravitated forces (Figure 2.1 b and c) (Baykal and Döven, 2000). Throughout the pelletization

process, the air among the grains is taken out by the developed force on the pellets. Thus the free spaces are being filled with water as well as grains. If the particles and water fill air between grains, the structure of pellets is denser. As a result of this, a denser pellet inspires closer packed particles that enhance the structural coherence and create intensive and strengthened fresh pellets for handling and storing (Pietsch, 1991).

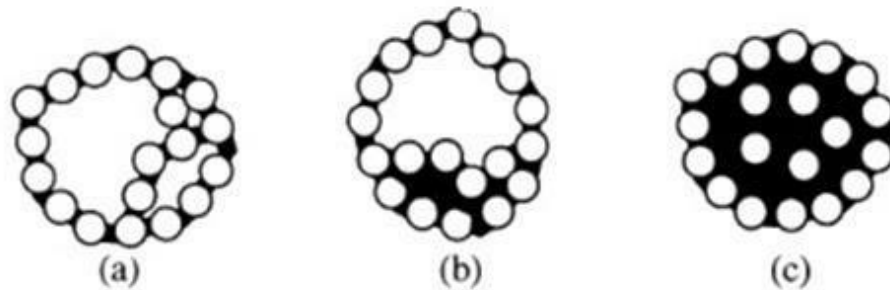


Figure 2.1 Mechanism of pellet formation (Jaroslav and Ruzickova, 1987)

The force of new pellets is influenced by the outcome of pressure which is being arised on the pellets by capillary forces as well as the pelletization procedure parameters. The previous experimental studies are concluded that the greatest force of the cured pellets can be achieved only if the all capillaries are completed with water in the generation. The filling of intergranular spaces with water is impressed three stages in pelletization process (Döven, 1996; Gesoğlu, 2004):

- The pendular state, only the contact point of the particles has water,
- The funicular state, in addition to situations occurred in previous stage, the water fills some of pores completely,
- The capillary state, the water fills all intergranular spaces completely and water film on the pellets surfaces is not occurred.

During the pelletization process, the granulometric distribution of fresh pellets can be adjusted by controlling the water components and the feeding amount of binders. In order to minimize of void ratio for the end output, a wider range of granulometric distribution should be used. However, during pelletization process, the amount of spraying water content which determined by binder type is significantly important to obtain the optimum water content of fresh pellets. Otherwise, as seen Figure 2.2 and

Figure 2.3, the desired strength of final product cannot be acquired by the water components below or above ideal position.

The rotation speed of disc which managed by gravitational force and centrifugal force at low and high speeds respectively is affected by the angle of disc plane to normal and diameter of the disc. As seen Figure 2.4, in order to refrain from prepotency of gravitational or centrifugal forces, the forces following up on an individual pellet while the pelletization process continues in a pelletization disc with radius "R" must be in equilibrium (Pietsch, 1991).

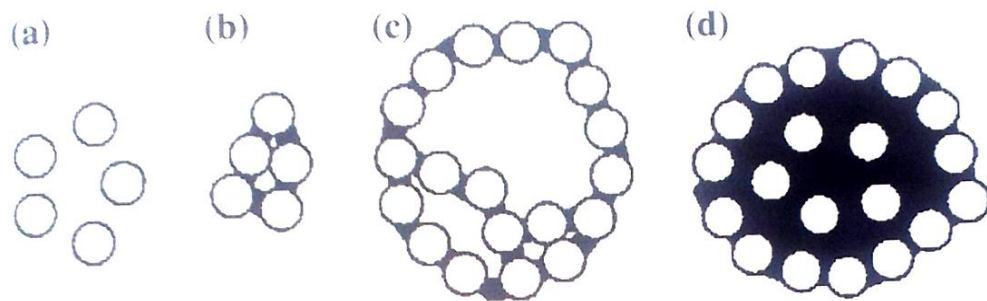


Figure 2.2 Process of ball nuclei forming (water components below ideal position)
(Jaroslav and Rurickova, 1987)

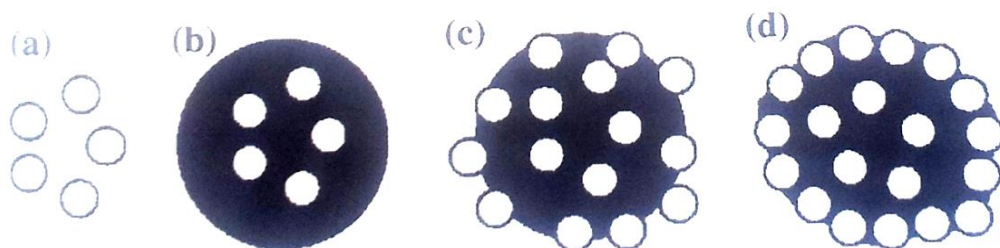


Figure 2.3 Process of ball nuclei forming (water components above ideal position)
(Jaroslav and Rurickova, 1987)

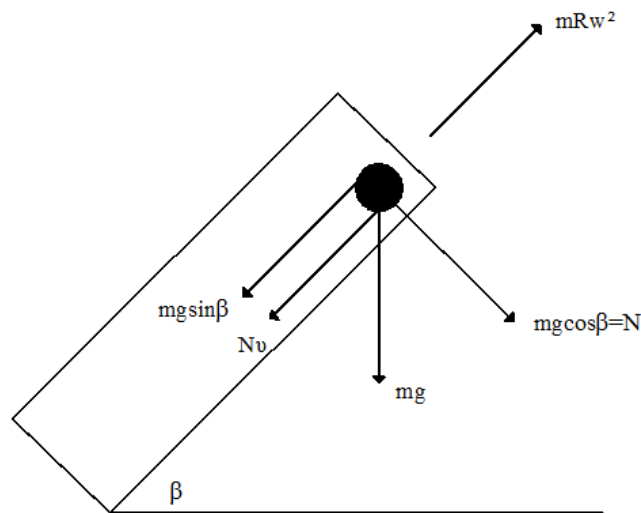


Figure 2.4 Strengths following up on an individual pellet while pelletization process continues (Pietsch, 1991)

Where, m corresponds to the mass of the independent pellet, g indicates the gravitational acceleration, β stated the angle of the disc's plane to normal in degrees, ν is the coefficient of friction between the pellet and the disc, R shows the radius of the disc, w is the centrifugal acceleration in radians/sec².

2.3 Lightweight Aggregate Concrete

One method for producing structural lightweight concrete is to replace, totally or partly, natural aggregates in concrete mixture with aggregates comprising great part of voids, with respect to the ACI Committee 213 (2003). Such concrete are usually defined as lightweight aggregate concretes (LWCs). The qualities and the attributes of LWAs may change differently because they are able to be generated from a great kind of raw materials by using different methods. Only the aggregates manufactured from fly ash, clay, shale, slate, and blast-furnace slag possess sufficient strength properties for structural concrete applications.

Zhang and Gjorv (1991a) studied an investigation of some high-strength lightweight aggregates available in European markets. Depending on the particle shape, surface texture, and pore structure, the aggregates properties varied within wide limits. Because of the open pores in the lightweight aggregates, they can absorb water so much. In this study, more than half of the 24 hr absorption was observed after the first

30 min although most of the water absorption took place within the first 2 min. However, surface treatments for LWA particles are used to decrease the water absorption and to increase the wearing resistance. It was suggested that coating the aggregate grains with water glass, polymer treatments, heating the surface above sintering temperature, and immersing the aggregates in silica fume or cement slurry were used successfully for the ways of surface treatments (Nielsen et al., 1995; Yang, 1997).

Yamashita et al. (1992) inspected the correct sintering conditions for the pelletized fly ash. The mixture with fly ash (93%), clay (2%) and water (5%) were fed into a disc pelletizer, and then the fresh pellets were manufactured by agglomerating. The result was shown that the sintering temperature of the pelletized fly ash influenced the quality of LWAs. The specific gravity and compressive strength became maximum at a sintering temperature. Optimum sintering temperature was slightly lower than this maximum temperature. The particular gravitation for the fly ash LWA was about 1.40.

Ramadan (1995) investigated the possibility of producing high performance fly ash aggregate by adding different low melting point metals and sintering process. In this study, it can be concluded that producing LWA from high calcium fly ash without any heating process was possible. This process was believed to be economical and simple with minimum energy consumption. Adding 5% lime by weight to FA for producing aggregate improved both physical and mechanical properties.

Videla and Martinez (2002) evaluated inventions in the production of fly ash lightweight aggregates using a cold bonded production technique. The aggregate mixtures were planned in view of 3, 5 and 7% by weight of the next binders: lime and two rapid-hardening cements such as portland cement and blended portland cement with 19% of natural pozzolan, respectively. For a 20 mm maximum size aggregate, the best size distribution was acquired with a 57° angle and 21 rpm speed in the disc with a diameter of 150 cm. Experiments showed that the aggregates manufactured with 5% weight of portland pozzolans cement indicated the greatest viability for use at structural concrete production.

Manikandan and Ramamurthy (2007) observed the influence of fineness for FA getting from two thermal power plants on the agglomeration method. Finer fly ash showed greater agglomeration productivity as contrasted to coarser fly ash. The agglomeration productivity of coarser fly ash was improved by adding of clay binders similar to bentonite and kaolinite. The class of binder utilized (with fly ash having a fineness of $257 \text{ m}^2/\text{kg}$), was impressed by quantity of binder content and capacity of humidity. Clay binder content altered the relative influence of pelletization factors.

Manikandan and Ramamurthy (2008) also discussed the influence of three type curing conditions such as normal water curing, autoclaving and steam curing on the properties of a typical class-C fly ash aggregate. In order to achieve maximum pelletization efficiency, the optimum levels of angle, speed for disc and moisture content for binder was found to be 55° , 55rpm, and 31% by the weight of binder, respectively. Normal water cured aggregate resulted in better increasing in the qualities when compared to autoclaving and steam curing. Among the accelerated curing methods, autoclaved aggregate have qualities similar to that of the normal water cured aggregate because of the intense microstructure generation. After the aggregates were initially subjected to accelerate curing, the continuation of normal water curing was showed simply a great extent improvement in the qualities.

Döven (1996), Arslan and Baykal (2000), Gesoğlu (2004), and Koçkal (2008) produced lightweight fly ash aggregates by using the same cold-bonding pelletization methods. The most efficient production revealed the optimum angle 43° and revolution speed 45 rpm with a moisture content 24% for the pelletizer with a diameter of 40 cm and a depth of 15 cm. Döven (1996) used three groups of mixtures, formed of fly ash only group, cement blended fly ash group (92% fly ash+8% cement, by weight), and lime blended fly ash group (92% fly ash+8%lime, by weight). Arslan and Baykal (2000) investigated the material properties of four groups of aggregate mixture; Fly ash only group, FC10 (10% fly ash+90% cement, by the weight), FC20 and FC30. Moreover, Gesoğlu (2004) preferred to apply the surface treatment method by either water glass ($\text{Na}_2\text{O nSiO}_2$) or cement-silica fume slurry to the artificial aggregates made from the fly ash with a cement/fly ash ratio of 0.1 by weight. The surface treatments of LWAs with water glass impart improved

strength and much water resistance while the cement-silica fume slurry impregnation remarkably decreased the water absorption and slightly increase the aggregate crushing strength. Only Koçkal (2008) used sintering method for lightweight fly ash aggregates after pelletization.

2.3.1 Mechanical Properties of Lightweight Aggregate Concretes

Lightweight concrete has similar properties as normal weight concrete (NWC) in the plastic state. After mixing, slump loss can be a severe problem when the aggregate continue to absorb large quantities of water because of its porous structure. This condition can generally be avoided by using air entraining agent simultaneously. Usage an air entraining agent will impact the water sorption of the concrete or reaching the aggregate saturated surface dry condition before adding the cement and the balance of the water. To prevent segregation of the lightest coarse aggregate particles, slump should be limited to a maximum of 100 mm value (Mindness, 2003).

The materials used in LWC mix design determine its engineering properties. The density of LWCs changes in a range of approximately 300-2000 kg/m³, comparable cube strengths from nearly 1 to over 60N/mm². These measures are able to be got comparison with those for NWC of roughly 2100-2500kg/m³, 15 to greater than 100 N/mm² (Newman, 2003). Structural lightweight concrete has high compressive strength in relation to density. The compressive strength of such concrete is noticed to rise with increasing density (Gambhir, 2003). RILEM/CEB (Clarke, 1993) has proposed a classification which defines the relation between compressive strength and density range as displayed in Table 2.1.

Table 2.1 Classification of lightweight concretes according to compressive strength-density relationship (Clarke, 1993)

Property	Class and Type		
	Structural	Structural/Insulating	Insulating
Compressive strength (MPa)	>15	>3.5	>0.5
Density range (kg/m ³)	1600-2000	<1600	«1450

In spite of high porosity and inherent weakness of LWA, compressive strength of 50-63 MPa can be obtained for LWCs. To obtain higher strengths in structural lightweight concrete, higher cement and mineral admixture content are needed compared to NWC of the same strength. However, it is precisely difficult to calculate the w/b ratio of the paste due to the high absorption of LWAs. Compressive strength and also tensile strength of LWAs are affected by the same factors. The flexural strength is more influenced than the cylinder splitting strength (Clarke, 1993; Mindness, 2003).

Lightweight aggregates have low moduli of elasticity (E) due to their high porosity. The measured modulus elasticity of LWCs is nearly halved compared to NWCs of the same strength (Hammer and Sandvik, 1995). The lower elastic modulus of lightweight aggregates would also suggest less restraint to time dependent deformations such as drying shrinkage and creep.

Zhang and Gjorv (1991a) produced high-strength lightweight concrete up to 100 MPa with a density of 1865 kg/m³ with unconventional species of lightweight aggregates. The force of the aggregates appears to be the fundamental component controlling the strength of the produced concretes. The measured elastic modulus of concretes varied from 17.8 to 25.9 GPa that is much lesser than when compared to that of reference concrete.

Al-Khaiyat et al. (2007) carried out a research program on long term strength development and durability of lightweight concrete in hot marine exposure conditions prevalent in Kuwait. They aimed at casting two structural lightweight concrete of 35 and 50 MPa for 100 mm cube strength at 28 days by using Lytag (sintered fly ash aggregate available in U.K.). For comparison, 50 MPa normal weights concrete was manufactured by the natural aggregates (NWC50). Before exposed to seaside conditions, the specimens were subjected to an initial curing ranged from 1 to 7 days. The generated LWCs of 35 and 50 MPa for 28 day compressive strength with a unit weight of 1800 kg/m³ are workable and cohesive. The best strength development of LWC50 occurred on seaboard exposure after 7 days primary curing rather than under continuous water curing. However, for NWC50 the finest strength development occurred under a continuous water-curing regime. The indirect tensile strength, modulus of rupture, and modulus of elasticity

of NWC50 was approximately 20, 50, and 30% greater when compared to the matching value of the LWC50, respectively, at the age of 9 months.

Ke et al. (2009) showed that the elastic modulus and the compressive strength of LWC including expanded shale and clay are strongly affected by the volume fraction of aggregate of which density less than 1000 kg/m^3 . The mechanical properties of LWA were not only affected by its density but also its outer shell thickness, macro porosity and broken grains percentage affected the aggregate strength.

Torres and Ruiz (2009) reported the influence of lightweight materials like expanded perlite, expanded glass, hollow micro-spheres and expanded polystyrene on density, sorptivity, water absorption, and mechanical strength. The experiments showed that mechanical strength, sorptivity, and water absorption were influenced by the lightweight material type and the dose utilized. Certain mechanical characteristics of the lightweight mortars reduced owing to using expanded polystyrene and expanded perlite depending on their density. The durability of mortars prepared enhanced glass or hollow micro-sphere cement mortars is likely superior when compared to expanded perlite or polystyrene.

Since the artificial fly ash aggregates were weaker than the matrix, the increasing amount of lightweight cold bonded fly ash aggregate resulted in gradually decreasing of compressive strength as reported by Gesoğlu et al. (2004). As shown in Figure 2.5, a decrease in the water/cement ratio from 0.55 to 0.35 resulted in a substantial increase in the compressive strength by 86%, 60%, and 40% for the concretes with 30%, 45%, and 60% coarse aggregate volume, respectively. However, Koçkal and Özturan (2010) found that lightweight concretes are able to generate with cold-bonded and sintered fly ash aggregates with densities in the interval of 1860-1943 kg/m^3 . Moreover, the 28-day compressive strength of lightweight concretes and splitting tensile strength altered in the range of 42.3 to 55.8 MPa and 3.7 to 4.9 MPa, respectively. Modulus of elasticity of the lightweight concretes was found between 22.4 and 28.6 GPa by using cold-bonded and sintered fly ash aggregates.

Shannag (2011) investigated the qualities of LWC including volcanic tuffs of scoria origin. The compressive strength of mixes ranged from 22.5-43 MPa with air dry densities of 1935-1995 kg/m^3 . However, Smadi and Migdadi (1991) showed that it is

possible to manufacture high-strength concrete with 55-60 MPa compressive strength with 1880 kg/m^3 of unit weight by using high-strength tuff lightweight aggregate. The poisson's ratio was close to 0.21. They also developed empirical equations for the estimation of the splitting tensile strength and the modulus of rupture on the basis experimental results.

Liu et al. (2010; 2011) separated expanded glass and expanded clay into four size fractions to investigate the transport properties. The outcomes of study showed that the use of size fraction smaller than 1.18 mm fine LWA reduced the resistance of the all-LWC to water and chloride-ion penetration in comparison with the sand LWC which has the same coarse LWA. Water sorptivity and permeability of LWC were increased by pre-soaked coarse LWA in comparison with NWC for alike w/b ratio. An increment in porosity of the coarse LWA gave rise to a decrease in water permeability and chloride-ion penetration for the sand lightweight concrete. Water sorptivity, permeability coefficient, and resistance to chloride ion penetration were more particularly associated with the water accessible porosity when compared to the whole porosity of the concrete.

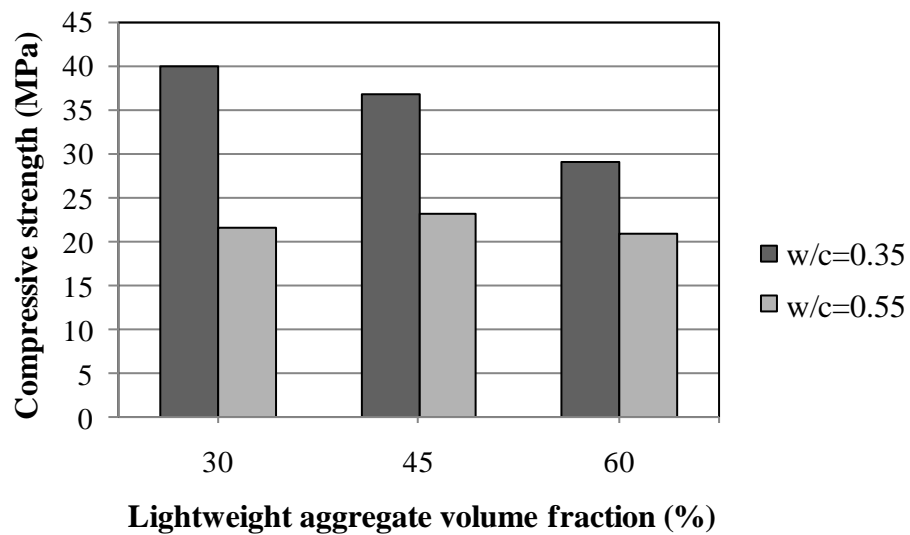


Figure 2.5 Variation in compressive strength for different lightweight aggregate volume fraction (Gesoglu et al., 2004)

2.3.2 Interface between Lightweight Aggregate and Cement Paste

Concrete which can be defined as a three phased combination comprised of coarse aggregate, cement mortar, and interfacial transition zone between coarse aggregate and cement mortar. The interfacial transition zone (ITZ) is defined as a region of weakness in concrete compound, both with regard to strength and permeation of fluids. The interfacial transition region between aggregate and cement mortar in concrete is critically important. The most significant differences between LWC and NWC stem from fracture path and water absorption. LWC will collapse through the lightweight aggregate particle, because the matrix will be the stronger when compared to the LWA. Thus the LWA fracture path moves around into the particle. In the case of natural aggregate this fracture path moves around into the particle due to the particles will be more powerfully when compared to the matrix and the fracture path will go around the NWA, i.e. through the matrix. The whole water content is extremely for LWA owing to the high absorption. Tensile strength is reduced in drying situations by greater moisture gradients although this effect is somewhat relieved by the effects of increased hydration (Mindness et al., 2003).

The interfacial zone between cement paste and aggregate has a significant position in examining mechanical characteristics of concrete. Schneider and Chen (1992) investigated the morphology of the interface between the expanded clay grains and the hardened cement paste by using scanning electron microscopy. It was displayed that the rough surface and porous structure of the aggregate are advantageous properties for using in cement paste. Zhang and Gjorv (1990) found that because of diversity of LWA, the case of ITZ between aggregate and cement paste may be dissimilar from another based on the micro structural characteristic of LWAs. Husem (2003) showed that the bond strength of aggregate-cement paste bond is improved by pores of LWA. Additionally, Lo et al. (2007a) indicated that the adhesion of the aggregate between cement paste was influenced by the pore size and surface characteristics of LWAs.

Wesserman and Bentur (1997) examined the resulting effects on the concrete strength by modifying the aggregate properties. It was concluded that the strength of concrete produced with different LWAs did not essentially correlate with that of the aggregates despite the matrix was always of the same effective w/b ratio. In another

study of Wesserman and Bentur (1996) the adhesion of sintered fly ash LWAs to the cement matrix were examined to analyze the other factors apart from aggregate strength which have an effect on the concrete strength. It was noticed that the difference in concrete strength could not constantly related the aggregate strength. These inclinations could be relation with physical and chemical processes occurred in ITZ, which affect on the whole strength unlike from that of strength for aggregate. The physical reaction had an influence at early ages determined as the densification of the ITZ owing to water absorption of LWAs. However, the chemical procedure was related to pozzolanic activity of LWA; this process was effective only in the later stages, beyond 28 days. The improvement in strength because of these effects arranged between 20 and 40 percent. Such effects should be taken into consideration in the design of LWC of optimum features.

2.3.3 Fracture of Lightweight Aggregate Concretes

Fracture mechanics is a science which investigates the strain replacement and stress around the cracks. Because of progress in fracture mechanics, engineers and designers have gained new concept about crack propagation and residual strength of structures containing crack. In the last two decades, fracture mechanics has reached to the certain stage of application, where it can be utilized in engineering design to avoid suddenly brittle failure of high-strength materials. The mechanical behavior of used materials is affected significantly by the properties and mechanical behavior of materials used in structures. The compressive strength theory is considered in the designing of concrete in application, whereas and the brittleness of concrete is disregarded. Therefore, the definition of the fracture parameters for concrete has to be determined depending on its brittleness (Akçay, 2007). The fracture mechanics researched the propagation of present cracks of which the places, formation and circumstances of failure. For this reason, there are two theory developed which are Linear Elastic Fracture Mechanics (LEFM) and Nonlinear Fracture Mechanics (NFM). LEFM can be applied to brittle and homogenous materials such as glass, however NFM is the modified state of LEFM due to being inefficient of LEFM for quasi-brittle and heterogeneous materials like concrete (Taşdemir et al., 1996).

When the aggregate is stronger than the matrix, crack propagates mainly through the matrix, around the stronger particles and the concrete strength is not very dependent

on the aggregate strength. However, in LWC, fracture invariably passes through virtually all the relevant aggregate particles and their properties and volume concentration are of great significance (Lydon and Balendran, 1980). As a result, the mechanism of crack deflection is not expected to be an important toughening mechanism in LWC. On the other hand, microcrack shielding is expected to remain an important toughening mechanism. Furthermore, the mechanism of aggregate/ligament bridging is expected to be present in LWC, except that its contribution to toughness will not be as large as in NWC (Li and Maalej, 1996; Akçay, 2007).

In the studies presented, there are few examinations on the fracture mechanics of the LWC (Chang and Shieh, 1996; Zhou et al., 1998; Akçay, 2007; İpek, 2013). In both studies of Chang and Shieh (1996) and Zhou et al. (1998), the relevant fracture properties were determined by the well-known size-effect law. The study made by Chang and Shieh (1996) showed that the fracture energies for LWC incorporating sintered and cold-bonded fly ash aggregates were 34.42 N/m and 37.2 N/m, respectively. However, the size effect curves indicate that the fracture behavior of the concrete made with sintered aggregate is similar to the straight line determined by LEFM. Zhou et al. (1998) performed research on high-strength lightweight concrete with sintered fly ash aggregate. It was shown that Bazant's size effect law gives a significant consistency to the flexural strength of LWC measured from the beams of different sizes.

Also, Taşdemir et al. (2002) showed that particle size of LWA had influence on the stress-strain behavior of semi-lightweight concrete in compression as shown in Figure 2.6. It was concluded that concretes with coarser LWAs have smaller compressive strength values than those with finer LWAs, although both have similar moduli of elasticity. In addition, Akçay (2007) reported that the low volume of LWAs increased the fracture energy, while further addition decreased. The size of LWAs has been found more effective than its volume on fracture energy of concrete.

Moreover, İpek (2013) reported that the fracture energies of LWC designed with 0.4 water/ cement ratio were 42 and 34.4 N/m for 45% and 60% replacement of LWA, respectively. This lower fracture energy at 60% LWA utilization as compared with

45% LWA utilization was caused due to artificial fly ash aggregates being weaker than the matrix. However, the characteristic lengths of LWC of 45% and 60% LWA were 382 and 311 mm, respectively. The concrete with 60% LWA had lower characteristic length than concrete with 45% LWA; it was due to having the concrete with 45% LWA higher modulus of elasticity and fracture energy than concrete with 60%. Increasing the amount of normal weight coarse aggregate resulted in increasing the compressive strength, and this makes the concrete more brittle.

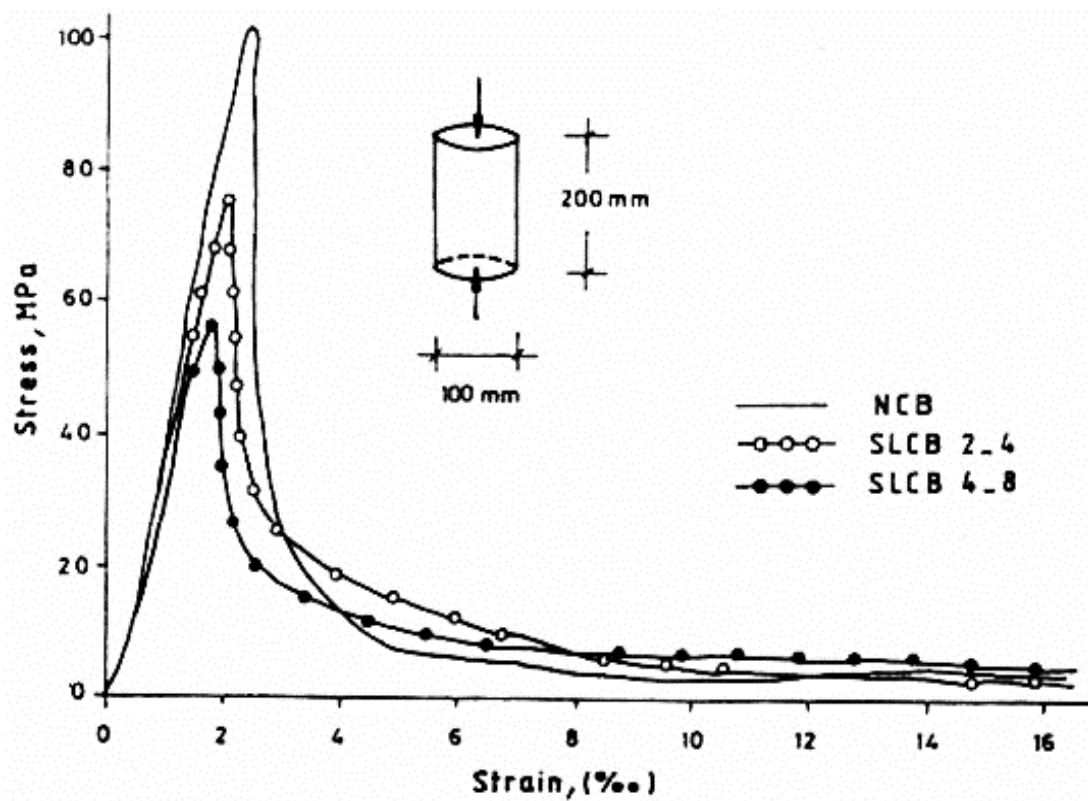


Figure 2.6 Typical results of stress-strain curves of concretes in compression (Taşdemir et al., 2002)

2.3.4 Shrinkage of Lightweight Aggregate Concretes

The developing interest in the usage of LWA increases concern over the long-term performance of concrete related to shrinkage. Shrinkage is a phenomenon that causes a reduction in concrete volume over time by internal and external drying of concrete. Internal drying of concrete results in self-desiccation by the water consumption in hydrated cement paste. However, external drying of concrete occurs owing to water migration from concrete surface to room temperature. The free water evaporation

from the fresh concrete surface can lead to plastic shrinkage and further water loss from hardened concrete can cause to drying shrinkage (Wittmann, 1976; Cohen et al. 1990, Lura et al., 2007).

To obtain required performance, LWC generally designs with low w/b ratio to right the weakness of LWA. In the literature review, less restrain to time dependent deformations such as drying shrinkage and creep is observed. Neville (1997) and Gesoğlu (2004) indicated that the average creep and shrinkage strains of LWC tend to be higher when compared to NWA. The reason of higher shrinkage values can be concluded by the lower modulus of elasticity of the aggregate, and the greater voids content of that higher proportion of the fine aggregate. However, the different types of LWA display very different behavior in terms of drying shrinkage (Nielsen and Aitcin, 1992; Gesoğlu, 2004; Kayali et al., 1999).

Nielsen and Aitcin (1992) demonstrated that LWC including expanded shale had 30 to 50% less drying shrinkage in comparison with NWC concrete. It was found that shrinkage values for NWC was approximately 203 microstrains while these values of LWC varied between 34 and 230 microstrain after 28 days of curing and 56 days of drying, respectively. This conclusion might be attributed to existence of water in the LWA particles. The usage of expanded shale aggregate as internal water reservoir reduced the drying shrinkage of high performance concrete. It was stated that low replacement level of LWA was in effective on mitigation of drying shrinkage as the measured shrinkage was significantly reduced with higher replacement level of LWA (Hwang and Khayat, 2008).

Kayaliet al. (1999) investigated the drying shrinkage of fiber-reinforced LWC including sintered fly ash aggregate (Lytag) strengthened with either polypropylene or steel fibers. Although the tensile strength was improved by the fibers, the compressive strength was not. The compressive strength tests accompanied with the modulus of elasticity and indirect tensile tests were conducted on 150x300 mm and 100x200 mm cylinder specimens, respectively. Drying shrinkage tests were implemented on prism specimens of 75x75x284 mm dimensions in a controlled room of 23°C temperature and 50% relative humidity. Test results have revealed that LWC including a total binder content of 785 kg/m³ showed approximately a half value than that of NWC including total binder content of 495 kg/m³ as far as a long term drying

shrinkage. Even though the compressive strength of the LWCs was around 63 MPa, the long-term drying shrinkage of these concretes concluded in 1000 microstrain which may not be applicable for certain constructional applications. As the modulus of elasticity of concrete increased, the shrinkage value decreased. It was believed that the reduced shrinkage cracking was affected by the higher the tensile strength combined with the low modulus of elasticity.

Al-khaiyat and Haque (1998) investigated the drying shrinkage of LWC as part of an extensive experimental research program. The long-term strength development and durability characteristics of LWC having a 50 MPa compressive strength were examined in curing conditions such as severe hot and dry, hot-coastal and salt-laden exposure conditions. The drying shrinkage of this concrete measured on 50x50x285 mm specimens was noticed to be excessively than 600 microstrains in the first three months' duration.

Kabay and Aköz (2012) researched that the drying shrinkage of LWC incorporating with pumice aggregate depending on the effect of three different prewetting methods. The results showed that LWC including presoaked aggregates had the highest shrinkage value of 794 microstrains at 189 days. However, the water soaked and vacuum-soaked pumice aggregates acting as internal curing reservoir decreased the drying shrinkage of LWC.

2.3.5 Durability of Lightweight Aggregate Concretes

The structures ensure long term durability as well as the high-strength/weight ratio. Permeability is one of important factors affecting the durability. Concrete with high permeability will provide easily to reach harmful substances via water into concrete in which resulting the deterioration of either concrete or steel reinforcement. Due to comprising of coarse and fine aggregates in a cement paste matrix, the durability of concrete is impressed by the aggregate, cement paste, interfacial transition zone. Generally, porosity and pore structural are essential in formation of the permeability. However, micro cracks occurred in the matrix can subscribe subsequently to the permeability. The difference between permeability and pore structure is presented in Figure 2.7.

Kayali (2008) examined the efficiency of concrete manufactured from lightweight aggregates by sintering method. Concrete generated produced with these aggregates is approximately 22% lighter and at the same time 20% more durable when compared to NWC. In addition, LWC including sintered and crushed fly ash aggregates had better performance in terms of strength as well as lower carbonation and lower chloride penetration. These aggregates contributed to the vigorous bonding properties between the aggregates and the cement paste.

Chia and Zhang (2002) conducted a study in order to compare the water permeability and chloride ion penetrability of LWC to that of high-strength NWC with or without silica fume. The conclusions displayed that the water permeability of the high-strength LWC and NWC had the identical results regardless whether silica fume was incorporated. The 28-day compressive strength of the high-strength LWC was about 50-55 MPa, whereas that of the high-strength NWC was about 80-90 MPa. The durability of LWC to the chloride penetration was parallel to that of the matching NWC in the normal-strength and in the high-strength levels. From the results, it appears that the property of the mortar matrix is the most significant parameter that controls the permeability of the high-strength concrete regardless of the coarse aggregate used. The results showed that the durability to the chloride penetration does not strike to be correlated with the water permeability of the concrete.

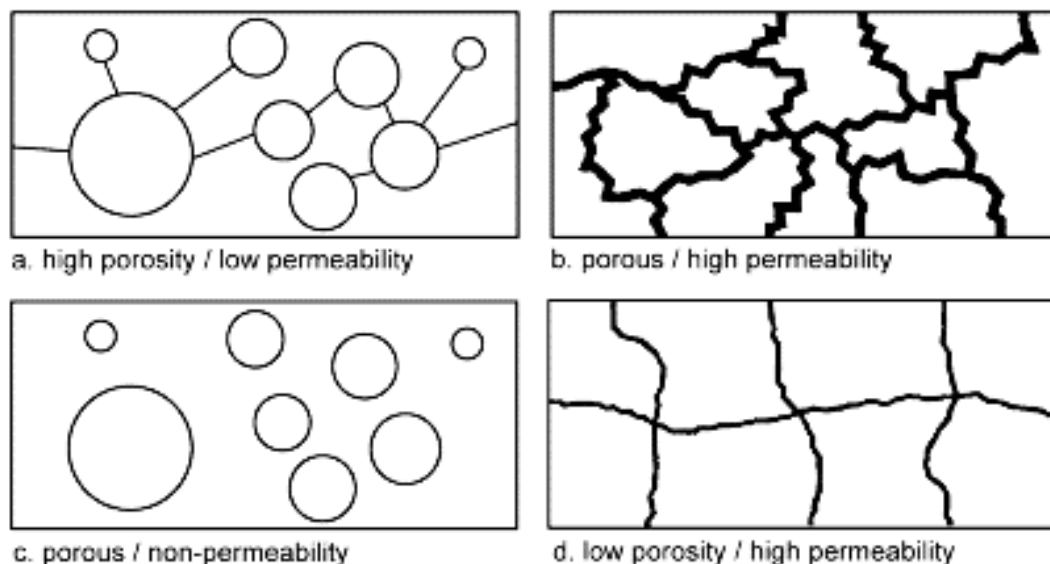


Figure 2.7 Schematic diagram displaying uncommenseness between porosity and permeability (Euro Light Concrete Project, 1998)

Hammer and Sandvik (1995) examined the permeability and resistance to chloride ingress of LWC for Norwegian marine structures. In the study, the permeability has been characterized by water intrusion due to capillary absorption of fresh and sea water respectively. All results, both using fresh and sea water, showed that water depths equal to normal density concretes with similar paste compositions. The lightweight aggregates do not contribute to the water absorption due to lower driving force as LWA pores are coarser and already contain water. The test was repeated with the Liapor 6 concrete but now with an external water pressure of 4 MPa. The results showed no significant difference between LWC and NWC with nearly equal paste compositions. Consequently, the type of aggregate used does not strike to influence the permeability of concrete. However, the tests have been performed on sound, well-cured specimens. Any deterioration of the paste (bad curing, cracking, etc.) that allows an easy access of water to LWA will probably increase the permeability. The chloride intrusion depths found from the sea water capillary absorption tests also are not significantly different between LWC and NWC with equal binder composition. However, it is noted that LWA may contribute to the chloride diffusion in cases of high initial water content of the lightweight aggregate. The measured electric resistance of the concretes was generally very high and far above an empirical limit for negligible rate of corrosion. Again, the type of aggregate does not seem to have any significant effect.

Zhang and Gjørsvik (1991b) evaluated the water penetration and accelerated chloride penetration for high-strength lightweight concrete having a compressive strength between 50 to 100 MPa. The conclusions showed that the porosity of the mortar matrix had a more important effect on the permeability of concrete than the porosity of LWA. Even though some lightweight aggregates were rather porous, the permeability of these concretes was as low as that of the concretes made from denser aggregates. Moreover, optimum cement content for the permeability was observed, where too-high cement content increased the permeability. The use of natural sand instead of lightweight sand reduced the permeability. No direct relationship was obtained between water permeability and electrical conductivity. But there was a relation directly between water permeability and accelerated chloride penetration. Hence, accelerated testing of chloride penetration appears to be a more valuable way of testing the permeability than testing the electrical conductivity.

2.4 Self Compacting Concrete

EFNARC (2005) defined SCC as “Concrete that has ability of flowing under its own weight and fill the formwork totally, even in the existence of packed steel reinforcement.” According to Okamura (1999), SCC is a modern type of high performance concrete that has excellent segregation resistance and deformability. In addition, it can flow through and fill the gaps between the reinforcements and corners of moulds by itself without the need of compaction or vibration.

From many other researches and the experimental work of this study, this definition can be suggested for SCC: “High performance self-compacting concrete that is capable of flowing under its own weight up to leveling, totally fill the formwork even in the existence of packed steel reinforcement, airs out, compacts and consolidates without the need of any vibration, whilst maintaining homogeneity due to high resistance to segregation.”

Fresh properties of SCC is significant in that the ability of the concrete placing may be evaluated in a satisfied way so that the practical requirements needed are obviously different from that of conventional fresh concrete. In order to obtain the workability performance of SCC, EFNARC (2005) recommended some important characteristics as described in the following:

- **Filling ability** which is the ability of concrete to fill the formworks and encapsulation of reinforcement with maintained homogeneity.
- **Passing ability** which is the ability of concrete to pass between narrow openings and enclosed spaced of formwork such as the areas of packed reinforcement with blockage caused by interlock aggregate particles.
- **Resistance to segregation** which is the ability of the concrete to maintain the homogeneity during mixing and transportation as well as the high fluidity without blocking owing to aggregate lock.

So as to determine the fresh properties of SCC, many different test methods have been brought out. Workability tests for SCC can be mainly divided into three classes, such as filling ability, passing ability, and segregation resistance tests. Each test is suitable for one or more of these classes. According to EFNARC (2005), test methods to enhance the workability are presented in Table 2.2.

Rheology is the study of flow process that deals with relations between stress, strain and their time dependent behavior. In fact, the workability of self-compacting concrete that flows readily under its own weight via the incorporation of special chemical admixtures as well as the usage of enhanced particle size distributions must be determined and monitored carefully by using the concrete rheometer (Koehler and Fowler, 2004). The rheology of fresh concrete, however, is frequently determined by the Bingham model. In this model the flow curve has an intercept on the stress axis, indicating a minimum stress which is required to start the flow (Tattersall and Banfill, 1983). As soon as the concrete begins to flow, shear stress increases in linear way with an increasing in strain rate defined as plastic viscosity. Therefore, in order to characterize the rheological properties of fresh concrete by the Bingham model two parameters, namely the plastic viscosity and the yield stress are necessary (Ozawa and Maekawa,1989). The rheological behavior of concrete can be simulated by the Bingham model as given in Equation 2.1.

$$\tau = \tau_0 + \mu \gamma' \quad (2.1)$$

Where, τ : shear stress (Pa), τ_0 : yield stress (Pa), μ : plastic viscosity (Pa s), γ' :shear rate (rotation speed) (1/s). Due to the thixotropy and loss of workability of the fresh concrete, the parameters in the Bingham equation, particularly yield stress also viscosity, are not constant in time (Wallevik, 2003; Roussel, 2005; Roussel, 2006). Moreover, the apparent viscosity increases by increasing shear rate, which is due to the preferential orientation of the particles resulting in the more rapid increase of the shear stress than the shear rate (Douglas, 2004; Roussel, 2006).

Because it is designed to flow under its own weight, resist segregation and meet other requirements, SCC, compared to CC, needs to have lower yield stress and comparable viscosity to impart high fluidity and retain kinetic energy. As it is also observed in Figure 2.8, yield stress for CC ranges from about 500 Pa to a many thousand Pa and that for SCC varies from zero to about 60 Pa, whereas the viscosity of CC and SCC vary similarly from 20 Pa.s to over 100 Pa.s (Nielsson and Wallevik, 2003;Wallevik, 2003; Koehler, 2009).

Rheology is significantly used as a tool to accurately describe the workability of SCC, and it can also aid in the design of future SCC mixtures. A design methodology for SCC was proposed by Saak et al. (2001a) based on the assumption that reduced viscosity with minimized yield stress are required for restraining segregation. Schwartzentruber et al. (2006) studied the rheological response of fresh cement pastes designed for SCC. They evaluated the torque value at an extremely low speed over a constant duration to determine the highest value of the shear stress corresponding to the yield stress. However, the rheological properties of the concrete mixtures are generally measured by using three rheometers; the IBB, the BTRHEOM and the ICAR instruments (Figures 2.9-2.11). The IBB rheometer is formed by a cylindrical container with an H-shaped impeller driven through the concrete in a planetary motion. The BTRHEOM is a parallel plate rheometer in which the bottom side is stationary and whereas the top side has as rotation with changeable speed (Sadran, 2000). However, as seen Figure 2.11, the ICAR rheometer placed on standard container can be controlled by hand. It is able to evaluate a flow curve or perform a stress growth test and, however, it is suitable for approximately the full range of concrete workability ranging from a slump flow diameter of nearly 2 inches for SCC. The rheological parameters can be computed utilizing the Bingham equation implemented to the torque and rotation rate data. Because the simple geometry of the vane, it is probable to figure out the conclusions in fundamental units, i.e., (Pa) for yield stress and (Pa.s) for viscosity (Koehler and Fowler, 2004).

Table 2.2 List of test methods for workability properties of SCC (EFNARC, 2005)

Property	Method
Filling ability	Slump-flow by Abrams cone
	T _{500mm} slump-flow
	Ormit
Passing ability	J-ring
	L-box
	U-box
	Fill-box
Segregation resistance	GTM screen stability test
	V-funnel and T _{500mm}
Filling ability + Segregation resistance	V-funnel

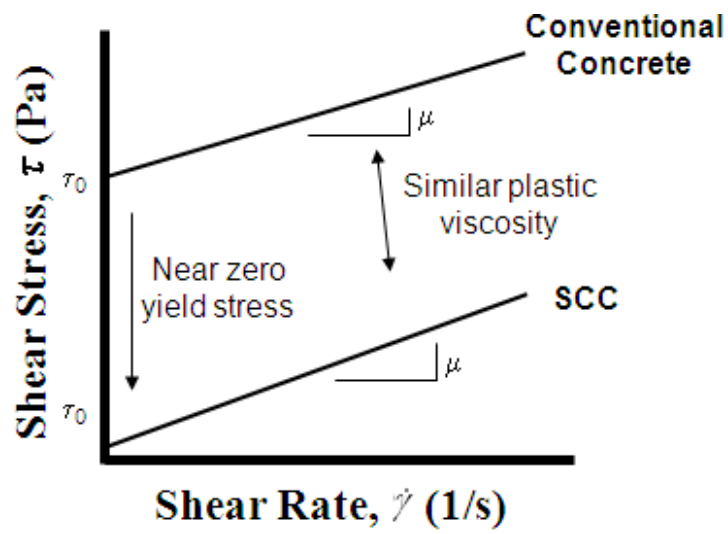


Figure 2.8 Differential rheological properties of conventional and self-compacting concretes (Koehler, 2009)



Figure 2.9 IBB Rheometer and impeller (Koehler and Fowler, 2004)

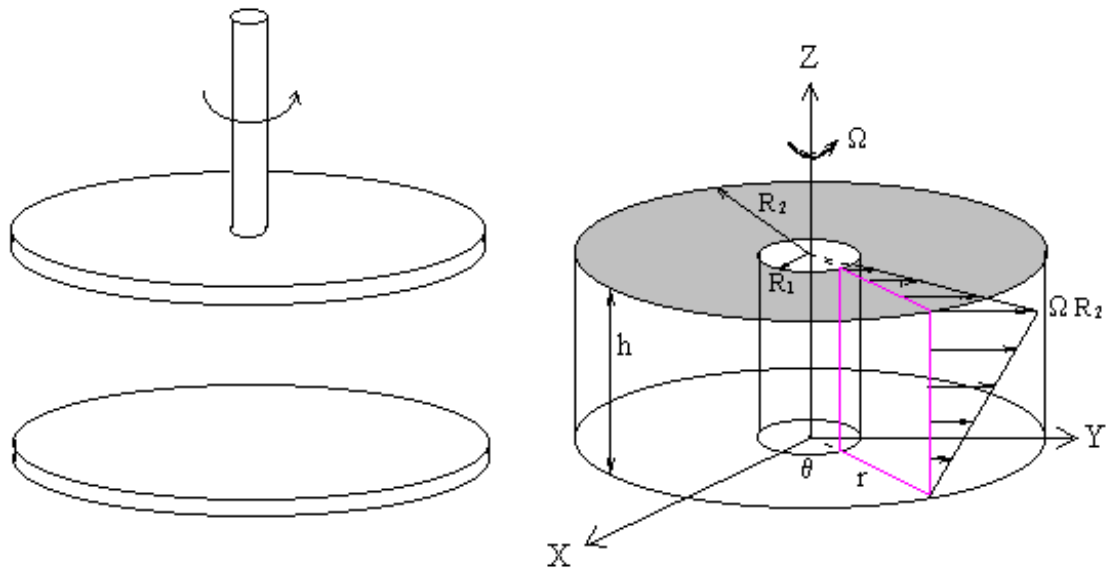


Figure 2.10 Velocity field in BRTHEOM rheometer (Koehler and Fowler, 2004)



Figure 2.11 ICAR rheometer

2.4.1 Self Compacting Lightweight Concretes

Self-compacting lightweight aggregate concrete is an innovative type of concrete which unifies the favorable properties of LWC and SCC. SCLC can place without vibration, fill the formwork and enclose reinforcement without any bleeding or segregation (Wu et al., 2009). The use of SCLC can be useful to obtain the significant reduction in the total mass of structure which can result in reduced structural members sections and facilitate construction (Kim et al., 2010). Furthermore, the segregation of LWA in place of SCC can be prevented by skipping the process of vibration.

There is a lack of information in the literature where LWA used in SCLC. Most of the studies focused on the mix design method and fresh properties of SCLC. Some researchers designed SCLC mixes by the most popular method introduced by Okamura. Okamura's method is based on the cement paste and mortar test prior to changing the properties of the superplasticizer, cement, fine aggregate and pozzolanic material. However, it is difficult to apply for producing the ready mixed concrete. To avoid this obstacle, some researchers used a new mix design method suggested by Nan-Su. In spite of its simplicity, this method had some problems about the fluctuating range of packing factor (PF). For this, Choi et al. (2006) modified PF and applied to design the high-strength SCC of which comprising LWA. The test results were evaluated with respect to the standard of second class rating of JSCE. All mixes satisfied the expected capacity in the tests of slump flow and time required to reach 500 mm of slump flow (s) of SCC. However, time required to flow through V-funnel (s) satisfied only with the mixes in which used 25% and 75% lightweight coarse aggregate (LWCA) and 25% lightweight fine aggregate (LWFA), respectively. For the mechanical properties of SCCs, SCC with 75% LWCA had a decrease of 6% with respect to reference concrete whereas SCC with 100% LWCA showed 31% decrease. However, SCC with 50% LWFA caused a decrease of 6% in comparison with reference concrete while the higher replacement of LWFA than this level provided 8% to 20% increase in the compressive strength owing to filler effect of LWFA. The elastic moduli of SCCs ranged between 24-33 GPa.

Wu et al. (2009) designed two SCLC depending on the water absorption rate of expanded shale via the overall calculation method with constant fine and coarse

aggregate contents. Fresh properties were tested by the slump flow, V-funnel, L-box, U-box, wet sieve segregation, and surface settlement tests as well as the column segregation test and the cross-section images for the uniformity of distribution of LWAs along the specimen. The results showed that two types of fresh SCLCs was satisfactory in the terms of good fluidity, deformability, filling ability, uniform aggregate distribution and minimum resistance to segregation

Wang (2009) produced SCLC including two types of LWA made from dredged silt with particle densities of 800 kg/m^3 and 1060 kg/m^3 respectively. To improve hardened properties of SCLC, pozzolanic materials such as fly ash and slag was added to the fresh mix, thus three different w/b ratio (0.28, 0.32 and 0.40) with three different volumes of mixing water (140 , 150 and 160 kg/m^3) were designed. It was observed that slump and slump flow diameter of SCLC ranged between 26-27 cm and 51-58 cm, respectively. The hardened SCLCs reached 70% or more of their compressive strength at 7 days, regardless of w/b ratio. Splitting tensile strength reached to value changing between 1.5-2.2 MPa at 91 days. SCLC with low w/b ratio ensured higher chloride penetration resistance, a decreasing number of cracks, and lower weight loss as well as the better ultrasonic pulse velocity. The results indicated that SCLC with good hardening and durability characteristics can be produced by dredged silt.

Kim et al. (2010) evaluated the properties SCLC incorporated two type LWAs, first type (LWA1) with a density of 1.58 g/cm^3 produced with rhyolite fine powder, and the other type (LWA2) with a density of 2.07 g/cm^3 produced from wastes such as screening sludge. It was revealed that when the density of LWCA decreased, the segregation resistance deteriorated however the flowability improved. Moreover the filling ability was not affected by the density of LWCA. Replacing natural coarse aggregate with LWA up to 75% gave a decrease of 10% in compressive strength than that of the reference concrete. However, SCLC including 100% LWA2 had 10% lower compressive strength than that of reference concrete, while the compressive strength of SCLC including 100% LWA1 was 31%.

Türkmen and Kantarcı (2007) applied five different cure conditions to SCLCs including 5%, 10% and 15% expanded perlite aggregate. In air curing condition the compressive strength of SCLCs incorporated 5%, 10% and 15% expanded perlite

aggregate was higher than those of reference concrete. It was showed that the capillarity coefficient value depended on the curing time, curing conditions, and the percent of expanded perlite aggregate. For lime saturated water curing condition capillarity coefficient decreased with time. The increment of expanded perlite aggregate cured in air for 28 days resulted in an increase of apparent porosity.

Topçu and Uygunoğlu (2010) investigated the effect of pumice, volcanic tuff and diatomite on the properties of SCLC. The SCLC mixtures were designed by preparing different combinations of w/b ratio with the total constant powder content and super plasticizer dosage levels. The results showed that, the decreasing ratio of unit weight for SCLCs were ranged between 30-35%, 22-31% and 34-38% by replacing crushed limestone with pumice, tuff and diatomite, respectively. The decreasing w/b ratio resulted an increase in compressive strength and splitting tensile strength of SCLCs. Moreover, the decreasing ratio of flexural strength was lower than that of compressive strength and splitting tensile strength.

Bogas et al. (2012) produced the SCLC having a compressive strength within the range of 37.4-60.8 MPa. For this, two different expanded shale aggregate having particle densities 1068 kg/m^3 and 1290 kg/m^3 , respectively were replaced with NWA. The slump flow diameter and slump flow time altered between 66-75 cm and 10-15 s for SCLCs. Additionally, the effect of the volume for coarse aggregate, the volumetric ratio of fine aggregate to mortar and fine material to fine aggregate, water content to fine materials were discussed. The results showed that deformation capacity of SCLCs was hardly altered by the fine materials and fine aggregate ratio but the aggregates influenced the rheology of cement paste and mortar. The volume of coarse aggregate affected the filling and passing ability of SCLCs due to having higher sphericity of LWA. It was recommended that the ratio of water content to fine materials and fine material to fine aggregate varied between 0.8-1 and 0.41-0.49, respectively to obtain self compactability. The elastic modulus of SCLC was found to be slightly higher than SCC including NWA. This might be attributed to the stiffness of LWA.

CHAPTER 3

EXPERIMENTAL STUDY

In this thesis, two-part experimental program was conducted to investigate the properties of the self-compacting concretes made with fly ash (fine and coarse) lightweight aggregates. In the first stage, artificial lightweight fly ash aggregates were produced through the pelletization of fly ash and cement at ambient temperature. After the fresh pellets were cured for 28 days, the hardened fly ash aggregates were sieved into fractions of 0.25-4 mm and 4-16 mm sizes to utilize in the production of SCLCs. The slump flow diameter, slump flow time, V-funnel time, L-box height ratio, and viscosity tests were carried out to identify the required properties and the characteristics of fresh SCLC mixes. The concretes were also tested for the mechanical, physical, and durability properties. The hardened concretes were tested for the compressive strength, splitting tensile strength at 28 and 90 days for the evaluation of mechanical properties. Moreover, the fracture test was performed on the notched beams to characterize the ductility of SCLCs at 90 days. Drying shrinkage accompanied by the water loss and restrained shrinkage were also monitored for a drying period of 60 days. Apart from those, the durability tests were conducted to investigate the resistance to chloride permeability, water sorptivity, water permeability, and gas permeability at the ages of 28 and 90 days. Therefore, evaluations and comparisons of SCLC were made in regard to the volume fraction and the maximum particle size of LWAs.

3.1 Materials

3.1.1 Cement and Fly ash

In this study, ordinary Portland cement CEM I 42.5 R was utilized for producing both artificial lightweight aggregates and fresh concrete mixes. Type F fly ash, supplied from Çatalağzı Thermal Power Plant, Zonguldak, Turkey, was utilized both

as a secondary binder material at a 20% replacement level by weight of cement in producing SCCs and in producing LWA. Physical and chemical characteristics of cement and FA are given in Table 3.1.

3.1.2 High Range Water Reducing Admixture

High Range Water Reducing Admixture (HRWRA) with a specific gravity of 1.07 g/cm³ was used to obtain the required workability in SCCs. The properties of HRWRA are presented in Table 3.2.

3.1.3 Aggregates

3.1.3.1 Lightweight Aggregates

Cold bonding process was utilized for producing the lightweight aggregates. The pelletization disc is consisting of three parts as given Figure 3.1. A speed controller unit is able to control the revolution speed of disc. The angle between the disc plane and the normal is arranged between 30°-92° degrees by the way of hydraulic system. The water content will be added the mixture is regulated by the pressurized water injection system providing from the water reservoir. The sticking of any mix to the disc surface is prevented by scrapping blades which creates an energy barrier being ensured more compacted pellet. However, the scrapping blades allows different size distribution of spherical material in which coarse size material moves in interior path whereas fine size moves in outer path (Baykal and Döven, 2000; Gesoğlu, 2004). It is considerably significant to identify the angle between disc plane and the normal, the rotational speed of the disc as well as the required moisture content for efficient production. An optimization study was carried out to find the relationship between the optimum rotational speed and the slope angle of disc. From this study, the optimum rotational speed and the slope angle of disc are found to be 42 rpm and 45° respectively, for the pelletizer with a diameter of 80 cm and a depth of 35 cm.

Table 3.1 Chemical compositions and physical properties of Portland cement and fly ash

Analysis Report (%)	Cement	Fly ash
CaO	62.58	2.04
SiO ₂	20.25	57.2
Al ₂ O ₃	5.31	24.4
Fe ₂ O ₃	4.04	7.1
MgO	2.82	2.4
SO ₃	2.73	0.29
K ₂ O	0.92	3.37
Na ₂ O	0.22	0.38
Loss on ignition	3.02	1.52
Specific gravity(g/cm ³)	3.15	2.04
Blaine fineness(m ² /kg)	326	379

Table 3.2 Properties of High Range Water Reducing Admixture (HRWRA)

Properties	HRWRA
Name	Glenium 51
Color tone	Dark brown
State	Liquid
Specific gravity (kg/l)	1.07
Chemical description	Modified polycarboxylic polymer
Recommended dosage	1-2% (% binder content)

Dry mixture of fly ash and Portland cement at 90% and 10% weight proportions, respectively, was pelletized by moistening in an inclined rotating pan. Pelletization was completed at about 20 min. The initial water spraying on the dry mixture at about 22% by weight of the total binder mixture took about 10 min. The remaining time was spared for growing up and stiffening of the freshly formed pellets. The last step in the manufacture of the LWAs was the agglomerated fresh pellets, which were self-cured in closed plastic bags that were kept for hardening in a curing room having 70% relative humidity and temperature of 20°C and during 28 days (Ke et al., 2009; Gesoğlu et al., 2012). Thereafter, the hardened fly ash aggregates were sieved to groups into size fractions of 0.25-4 mm as lightweight fine aggregate and 4-16 mm as lightweight coarse aggregate. Figure 3.2 shows self-curing process of the agglomerates and hardened lightweight aggregates.

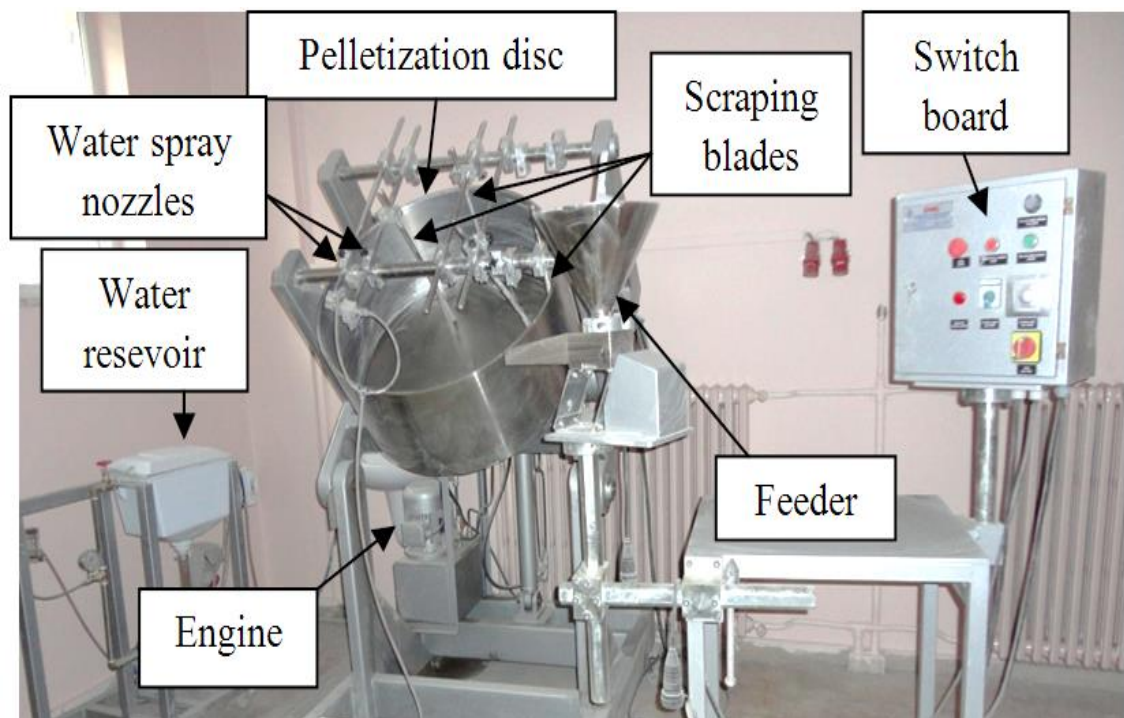
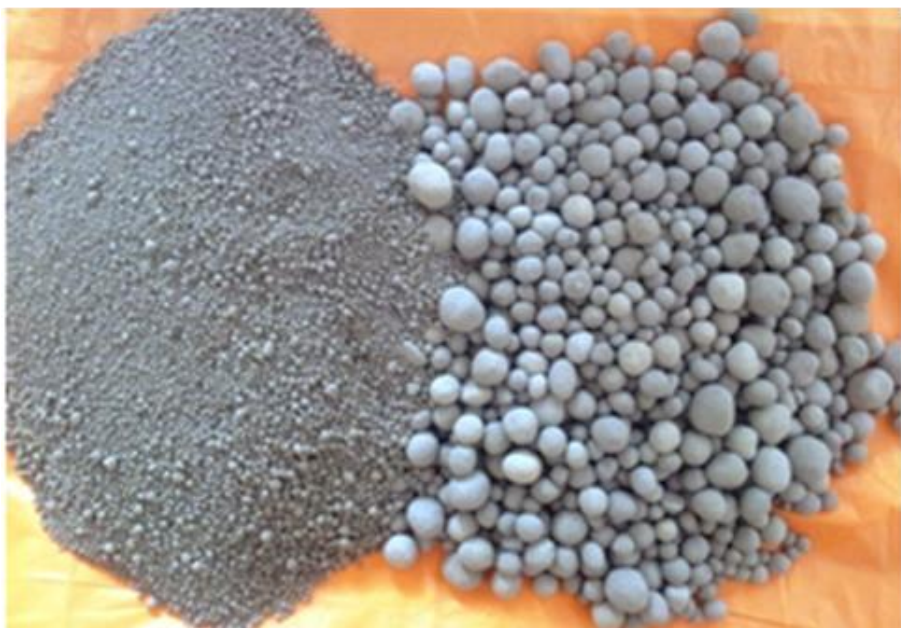


Figure 3.1 The general view of the pelletization disc



a)



b)

Figure 3.2 Artificial lightweight aggregate a) Self-curing process and b) Artificial fine and coarse lightweight aggregates

The specific gravity and the water absorption capacity for LWA were determined according to ASTM C127 (2007). It was found that water absorption of the coarse aggregate after 24 hrs of soaking in water was about 17.1% while the specific gravity of the LWCA for bulk, apparent and saturated surface dry conditions were 1.5, 2.0, and 1.76 g/cm³, respectively. Water absorption of the fine aggregate was about 21.2%, while the specific gravity of the LWFA for bulk, apparent and saturated surface dry conditions were 1.46, 2.1, and 1.76 g/cm³, respectively.

Moreover, crushing strength of LWAs was determined according to BS 812, part 110 (1990). The crushing force was measured by a dial gage and it was transformed to the load. Figure 3.3 gives the sketch of crushing strength test apparatus. The statistical force applied at for failure for a number agglomerates statistically representative is defined the crushing strength or more often called as crushing value. The crushing strength test results calculated by following Equation 3.1 is presented in Figure 3.4.

$$\sigma = \frac{2.8P_{max}}{\pi X^2} \quad (3.1)$$

Where X, is the distance between loading points and P_{max} is the fracture load (Yashima et al., 1987; Li et al., 2000; Mangialardi, 2001; Cheeseman et al., 2005).

3.1.3.2 Normal Weight Aggregates

Natural fine (NWFA) and coarse aggregates (NWCA) were used together with LWFA and LWCA in order produce SCLC. In this study, natural fine and coarse aggregates were replaced by LWFA and/or LWCA, respectively to manufacture SCLC mixtures. For natural fine aggregate, a mixture of crushed lime stone and natural river sands with a maximum size of 4 mm was used. As coarse aggregate, natural river having a maximum size of 16 mm was used. The particle size distribution and physical properties of natural aggregates and LWAs are shown in Table 3.3.

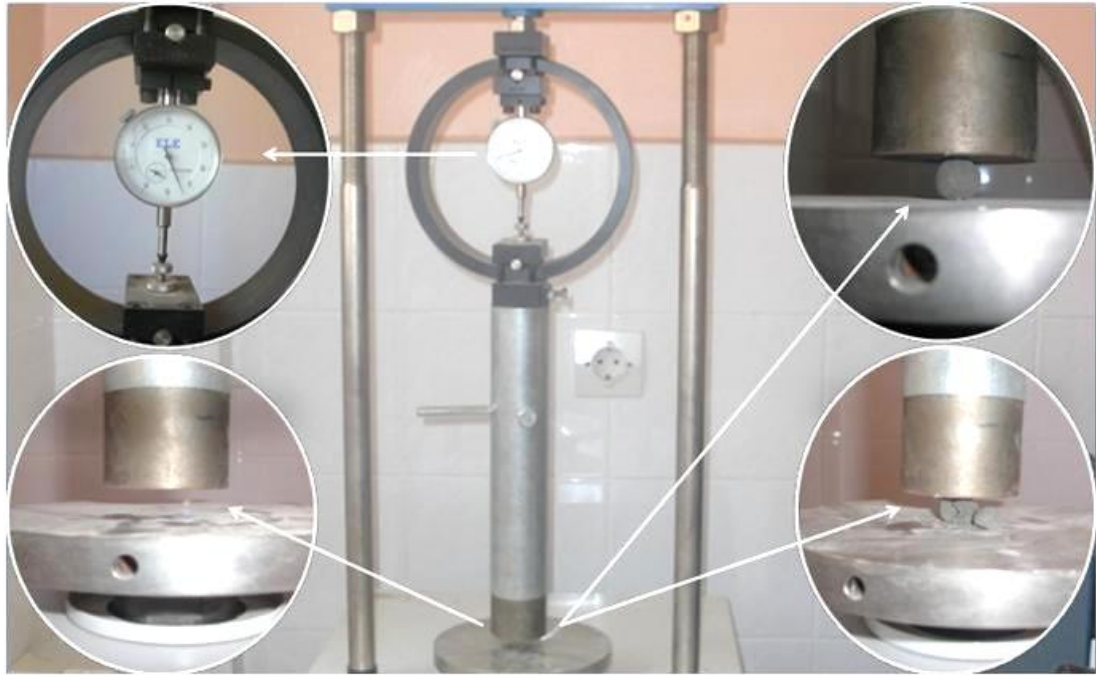


Figure 3.3 Crushing strength test apparatus

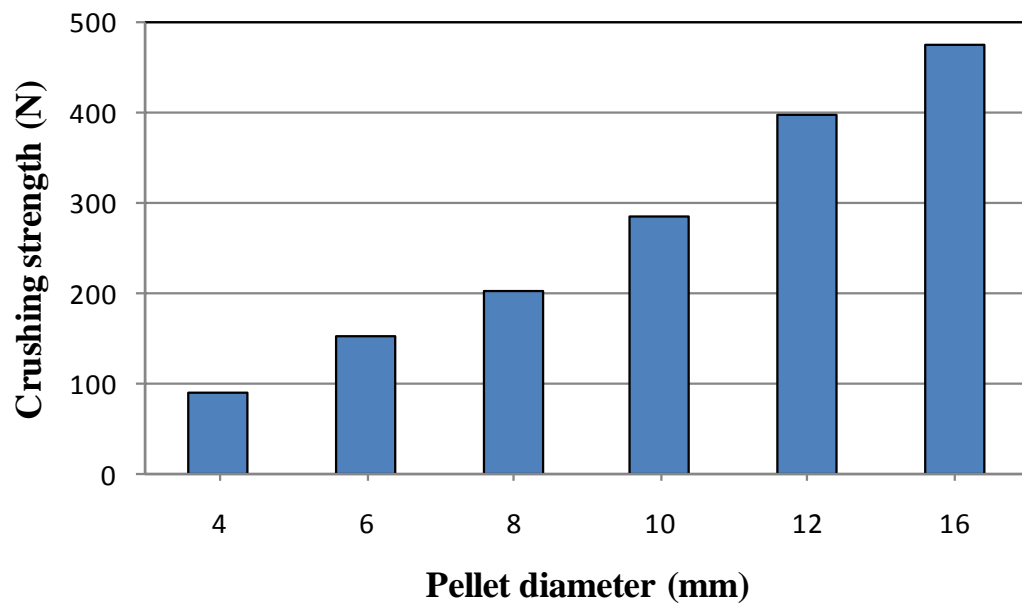


Figure 3.4 Crushing strength of lightweight aggregate

Table 3.3 Sieve analysis and physical properties of natural and lightweight aggregates

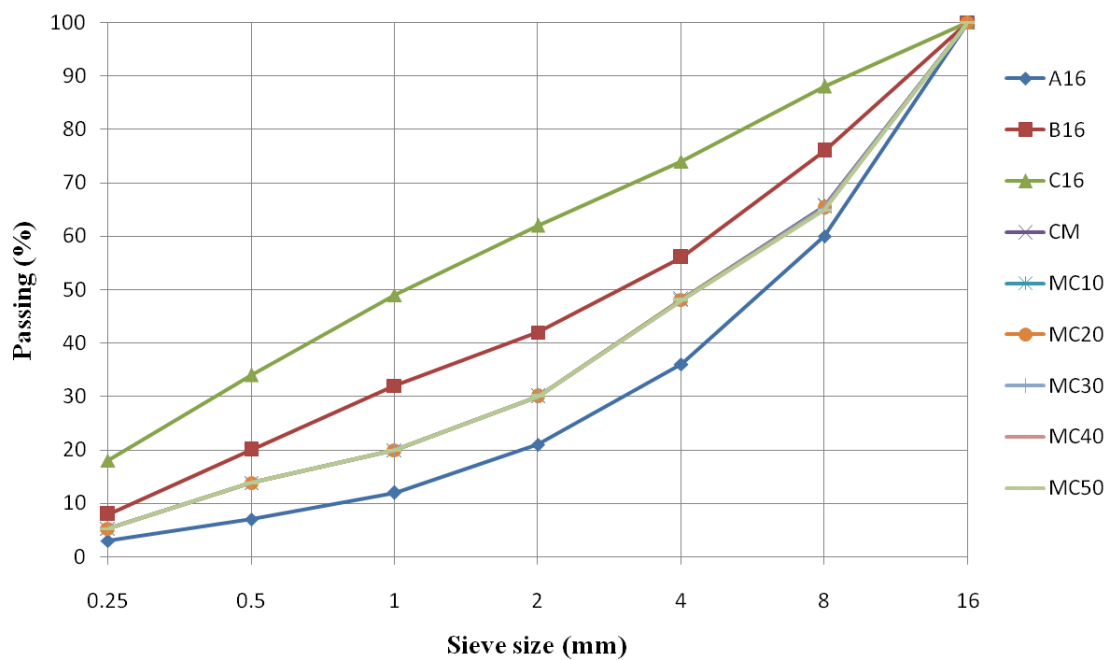
Sieve size (mm)	Normal weight aggregate			Lightweight aggregate	
	River sand	Crushed Sand	Natural Coarse	LWFA ^a 0.25-4 mm	LWCA ^b 4-16 mm
	16	100	100	100	100
8	99.7	100	31.5	100	79.9
4	94.5	99.2	0.4	100	0
2	58.7	62.9	0	75.5	0
1	38.2	43.7	0	28.9	0
0.5	24.9	33.9	0	12	0
0.25	5.4	22.6	0	4	0
Fineness modulus	2.79	2.38	5.68	2.79	5.20
Specific gravity (g/cm ³)	2.66	2.45	2.72	1.76	1.76

a: Lightweight fine aggregate, b: Lightweight coarse aggregate.

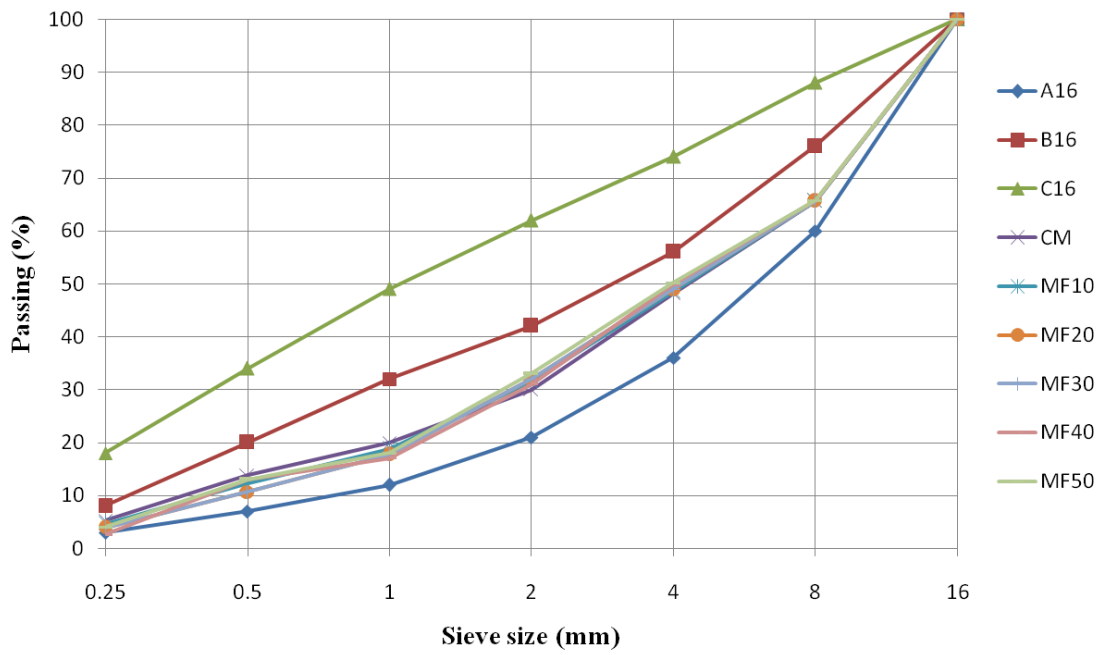
3.2 Self Compacting Lightweight Concrete Mix Properties

A total of seventeen SCLC mixtures were designed with a constant w/b ratio of 0.32 and a total cementitious material content of 550 kg/m³ by incorporating binary cementitious blends of 20% FA with 80% Portland cement in SCLCs. The mixes were all the same except for the natural aggregate being replaced by artificial LWA, for both fine and coarse fractions at different proportions as illustrated in Table 3.4. The process of replacement was carried out in 20% increments by volume of coarse, fine, and both (at equal proportions) natural aggregates. The control mix (CM) contained 100% natural aggregates including 50% natural coarse aggregate, 35% natural sand and 15% crushed sand by the total aggregate volume. However, SCLC designed with LWFA and/or LWCA constitute 50% of the total aggregate volume in a typical SCLC mixture. For each volume concentration, a grading curve was generated to be used in the final concrete mixture regarding the regions recommended by TS 706 (2009). In order to obtain the best fit, LWCA was divided into two volume fraction such as 35% of 8-16 mm and 15% of 4-8 mm by the total LWCA volume. The grading curves for MC group are shown in Figure 3.5 a for

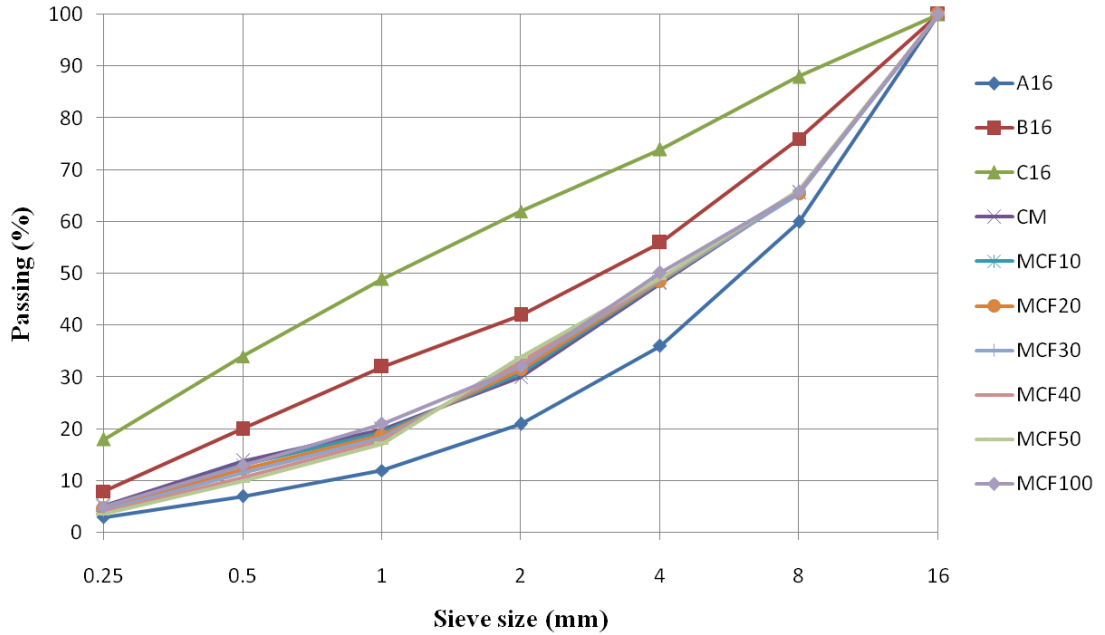
volume percentages of 0, 10, 20, 30, 40 and 50 respectively. In a similar way, the aggregate grading curves of MF and MCF group are depicted in Figure 3.5 b and 3.5 c, respectively. Thus, concrete mixes were scheduled as three groups: first, MC group in which coarse lightweight aggregate replaced coarse normal weight aggregate, namely MC10 to MC50 mixes; second, MF group in which LWFA replaced fine natural aggregate resulting in MF10, MF20, MF30, MF40, and MF50 mixes; third, MCF group in which LWFA and LWCA replaced in equal proportions the fine and coarse natural aggregates resulting in MCF10, MCF20, MCF30, MCF40, and MCF50. Moreover, MCF100 mix was designed to have full replacement of natural aggregates by lightweight aggregates. The mixture proportions and HRWRA used in varying amounts to provide the desired workability for all mixes were presented in Table 3.5.



a)



b)



c)

Figure 3.5 Aggregate grading for a) MC mixes, b) MF mixes and c) MCF mixes

Table 3.4 Aggregates volume fractions for SCLCs

Code Number	Coarse aggregate (%)		Fine aggregate (%)	
	NWCA	LWCA	NWFA	LWFA
CM	100	0	100	0
MC10	80	20	100	0
MC20	60	40	100	0
MC30	40	60	100	0
MC40	20	80	100	0
MC50	0	100	100	0
MF10	100	0	80	20
MF20	100	0	60	40
MF30	100	0	40	60
MF40	100	0	20	80
MF50	100	0	0	100
MCF10	90	10	90	10
MCF20	80	20	80	20
MCF30	70	30	70	30
MCF40	60	40	60	40
MCF50	50	50	50	50
MCF100	0	100	0	100

3.3 Concrete Casting

To prevent early slump loss of LWA owing to its high water absorption feature, a special method was employed. Before mixing, considering the high water absorption of LWAs, they were immersed in water for 30 minutes to ensure saturated surface dry condition (SSD) (Gesoglu, 2004; Joseph and Ramamurthy, 2009; Gesoglu et al., 2012). The extra water on the surface of the pellets was dried up manually by a towel (Figure 3.6). Laboratory mixing pan with capacity of 30 liter was used to mix all concrete with following the special procedure for batching and mixing. At first, LWA in SSD was mixed with binder then natural coarse and fine aggregate were added to the mixer. After homogenizing of the aggregates and the binder for 30 s of mixing, roughly one third of mixing water was added gradually into the mix for one

more minute. Lastly, the remaining water and HRWRA were added through the mixing for three minutes and after that the mix was left for 2 minutes to rest. Finally, additional two minutes of mixing adapted to complete the sequence of the mixing. The slump flow diameter of SCLCs was designed to be in the range of 720 ± 20 mm to provide EFNARC (2005) limitation. So, test batches were cast for each type of mixture by using HRWRA at varying amounts to obtain the target mentioned slump flow diameter.

After the mixing procedure had completed, fresh concrete mixtures were tested for workability, passing ability, and viscosity. The compressive strength, splitting tensile strength, net flexural strength, fracture test, water sorptivity, water permeability, rapid chloride permeability, gas permeability, free and restrained shrinkage of SCLCs were also determined in the hardened state. All of the specimens were cast without any vibration or compaction.



Figure 3.6 LWAs in SSD condition

Table 3.5 Concrete mix proportions in kg/m³

Code Number	w/b	Cement	Fly ash	Water	Coarse aggregate			Fine aggregate			HRWRA
					NWA	LWA		NWA		LWA	
					4-16 mm	4-8 mm	8-16 mm	natural sand	crushed sand		
CM	0.32	440	110	176	853.7	0.0	0.0	582.3	229.8	0.0	7.1
MC10	0.32	440	110	176	683.0	33.0	77.1	582.3	229.8	0.0	5.9
MC20	0.32	440	110	176	512.2	66.0	154.1	582.3	229.8	0.0	5.4
MC30	0.32	440	110	176	341.5	99.1	231.2	582.3	229.8	0.0	4.4
MC40	0.32	440	110	176	170.7	132.1	308.2	582.3	229.8	0.0	4.0
MC50	0.32	440	110	176	0.0	165.1	385.3	582.3	229.8	0.0	4.0
MF10	0.32	440	110	176	853.7	0.0	0.0	465.8	183.9	110.1	6.1
MF20	0.32	440	110	176	853.7	0.0	0.0	349.4	137.9	220.2	5.3
MF30	0.32	440	110	176	853.7	0.0	0.0	232.9	91.9	330.2	4.0
MF40	0.32	440	110	176	853.7	0.0	0.0	116.5	46.0	440.3	3.3
MF50	0.32	440	110	176	853.7	0.0	0.0	0.0	0.0	550.4	3.1
MCF10	0.32	440	110	176	768.3	16.5	38.5	524.0	206.9	55.0	5.9
MCF20	0.32	440	110	176	683.0	33.0	77.1	465.8	183.9	110.1	4.7
MCF30	0.32	440	110	176	597.6	49.5	115.6	407.6	160.9	165.1	4.5
MCF40	0.32	440	110	176	512.2	66.0	154.1	349.4	137.9	220.2	4.1
MCF50	0.32	440	110	176	426.9	82.6	192.6	291.1	114.9	275.2	3.8
MCF100	0.32	440	110	176	0.0	165.1	385.3	0.0	0.0	550.4	3.0

Specimens were cast from each mixture consisting of the following:

- Six 150 mm cubes for the compressive strength evaluation at 28 and 90 days;
- Six 100x200 mm cylinders for splitting tensile strength at 28 and 90 days;
- Four 150 mm cubes for water permeability test at 28 and 90 days;
- Four 100x200 mm cylinders for rapid chloride permeability at 28 and 90 days;
- One 150x300 mm cylinder for gas permeability test at 28 and 90 days;
- Four 100x100x500 mm prisms for determination of fracture energy and net flexural strength at 90 days;
- Three 70x70x280 mm prisms for evaluation of drying shrinkage and weight loss;
- Two ring-shaped specimens to display restrained shrinkage cracking.

Immediately after casting, drying and restrained shrinkage test specimens were cured for 24 hr in a cabinet having 100% relative humidity and temperature of 20°C during 28 days. Following this curing period, as soon as the outer mould of the ring specimen had been removed, the top surface of the concrete ring was covered via a silicone rubber, so that the drying would be permitted only by the outer circumferential surface. Meanwhile, the free shrinkage test prisms were demoulded. After the gage length was fixed on each specimen via the glued pins on the face of prisms, its initial weight was recorded to monitor the weight loss during drying period. Then, the both ring and prisms specimens were subject to drying at 23±2°C and 50±5% relative humidity for about 60 days. After the demoulding of all the other specimens, they were cured by water until testing age.

3.4 Tests for Fresh Properties

3.4.1 Slump Flow Test

Slump flow defines the flowability of a fresh mix in unconfined conditions. It is a sensitive test that can normally be specified for all self-compacting concretes, as the primary check that the fresh concrete meets the specification in terms of flow. To measure the slump flow, an ordinary slump flow cone is filled with SCC without any compaction and leveled. The cone is lifted and average diameter of the resulting concrete spread is measured as seen Figure 3.7. The slump flow diameter of SCLCs

was fixed at about 72 ± 2 cm while the slump flow time was observed as the measured time for the concrete to attain the 500 mm circle diameter ($T_{500\text{mm}}$). Visual observations during the measurement of $T_{500\text{ mm}}$ provide additional information about the uniformity and tendency of the segregation for SCLCs. According to EFNARC (2005); there are three typical flow classes for different application areas of these classes as given in Table 3.6.

3.4.2 V-funnel Test

V-funnel test was conducted in evaluating the viscosity and the passing ability of SCLCs to replace its pathway and to pierce in restricted region (Figure 3.8). The procedure of determining the flow time is filling the V-shaped funnel with fresh concrete, thereafter, the hinged trapdoor is released and the flow time measured until it completely becomes empty.

$T_{500\text{ mm}}$ and V-funnel flow time can be used together to assess the viscosity of the produced SCCs. These values do not measure the viscosity of SCC directly but they give the related information about the rate of flow. There are two viscosity classes in the EFNARC (2005) according to the measured V-funnel and $T_{500\text{ mm}}$ slump flow times as given in Table 3.6.

3.4.3 L-box Test

The L-box is an L shaped apparatus having a rectangular section of which a vertical and horizontal parts with a moving gate. Two or three reinforcing bars put in front of the gate to represent an obstruction for the concrete to move (Figure 3.9). The test procedure is pouring the fresh concrete in the vertical section and then the gate is opened and let the concrete flows to horizontal section through the gaps between the obstructing bars. When the movement stopped, the depths of concrete that are directly behind a gate (H_1) and at the extreme of the horizontal part of L box (H_2) are measured and the ratio of H_2/H_1 is computed. This is a symptom of the capability of the concrete to get through narrow openings such as restricted reinforcement sections. The classes of passing ability according to L-box height ratio are also given in Table 3.6.



a)



b)

Figure 3.7 Photographic views of slump flow test a) Slump flow test plate and b) The measurement of slump flow diameter

Table 3.6 Slump flow, viscosity, and passing ability classes with respect to EFNARC (2005)

Class		Slump flow diameter (mm)
Slump flow classes		
SF1		550-650
SF2		660-750
SF3		760-850
Viscosity classes		$T_{500\text{mm}}$ (s) V-funnel time (s)
VS1/VF1	≤ 2	≤ 8
VS2/VF2	> 2	9-25
Passing ability classes		H_2/H_1 ratio
PA1		≥ 0.8 with two bar
PA2		≥ 0.8 with three bar

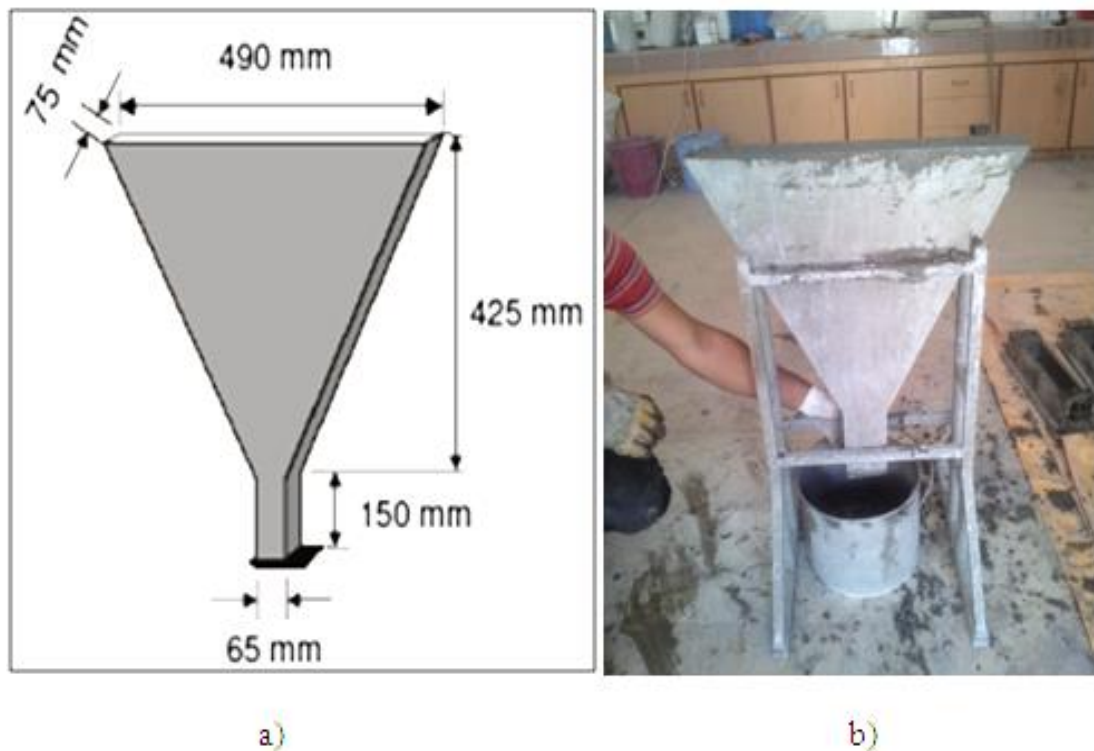


Figure 3.8 Photographic view of V-funnel test a) Schematic representation of the V-funnel and b) Measurement of V-funnel flow time



Figure 3.9 Photographic views of the L-box apparatus and test procedure

3.4.4 Viscosity Test

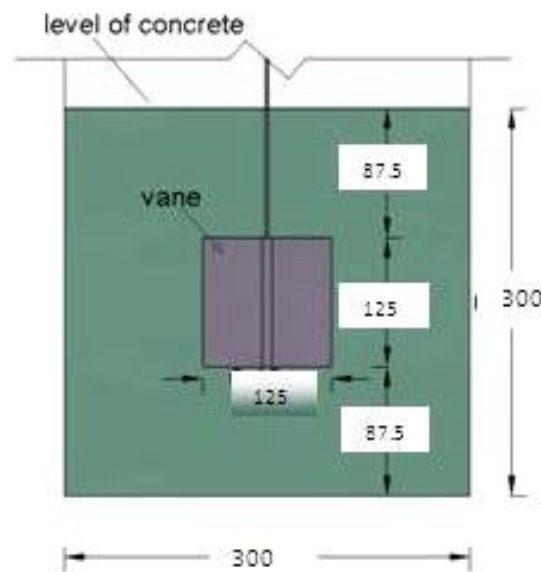
ICAR rheometer was used to characterize the rheology of SCLCs as shown in Figure 3.10. Fresh self-compacting concrete was poured up to a height of 300 mm in to 300 mm diameter container in which a 125 mm diameter and 125 mm height four-bladed vane was placed in the centre of the container with a 87.5 mm spacing above and below the vane. Flow curves for every fresh concrete mixture was obtained after entering breakdown speed and time, number of points, time per point, initial speed, and final speed as input. The vane was first rotated at a speed of 0.5 rps for an interruption time of 20 sec. Depending on seven speeds, torque measurements were then recorded varying in decreasing range from 0.5 rps to 0.05 rps.

For analyzing rheological parameters of the fresh concrete properties, Equation 3.2 was used for plotting the flow curves in relative units.

$$T=Y+VN \quad (3.2)$$

Where ; V denotes the slope of the line (Nm.s) related to plastic viscosity, Y is the intercept of the line with the torque axis (Nm) which is related to yield stress, N is rotational speed, and T is the torque (Koehler and Fowler 2004; Koehler, 2004).

The resultant data were evaluated depending on the Bingham model in order to specify the plastic viscosity into basic units in analytical way by fitting a straight line to the plot of torque, τ (Pa), versus rotation speed, γ (rad/s) data as given in Equation 2.1. The intercept, τ_0 (Pa), and the slope, μ (Pa.s), of this line were taken into account to be interrelated with yield stress and plastic viscosity, correspondingly.



a)



b)

Figure 3.10 The ICAR rheometer a) Principal dimensions and b) Device including vane (all dimensions are in mm)

3.5 Tests for Mechanical Properties

3.5.1 Compressive Strength Test

For compressive strength measurement of SCLC, cubical samples of 150 mm were tested with respect to ASTM C 39 (2012). The test is conducted on three cube samples from each SCLC mix at 28 and 90 days. The compressive strength was computed by averaging the results from the three tested samples at each testing age.

3.5.2 Splitting Tensile Strength Test

According to ASTM 496 (2011), splitting tensile strength of the concrete was measured by using the cylindrical samples of 100x200 mm at 28 and 90 days. The splitting tensile strength was obtained by averaging the results from the three tested cylindrical samples.

3.5.3 Fracture Energy

In order to obtain the fracture energy (G_F) of SCLCs, the test was carried out coinciding with of RILEM 50-FMC (1985). The measurement of displacement was observed simultaneously via a linear variable displacement transducer (LVDT) at midpoint of span. A testing machine (Instron 5590R) having a highest performance of 250 kN for applying to load was used (Figure 3.11). The details of the testing machine and specimen as well as placing LVDT are shown in Figure 3.12.

The beams having length of 500 mm and cross-section of 100x100 mm were cast for the fracture energy test. The opening notch was achieved through reducing the effective cross section to 60x100 mm via a saw so as to locate large aggregates in more denseness. Thus, the notch versus depth ratio (a/D) of beams was 0.4. However, the distance between supports of the specimens was 400 mm.

After obtaining the curve of load versus deflection at the midpoint of span (δ) for each beam, the area under this load versus displacement at midpoint of span (W_o), G_F was calculated via the following formulation (Equation 3.3) by RILEM 50-FMC (1985).

$$G_F = \frac{W_o + mg \frac{S}{U} \delta_s}{B(W-a)} \quad (3.3)$$

In this formula, the width, depth, notch depth, span, length, mass, specified deflection of the beam and gravitational acceleration are presented as B , W , a , S , U , m , δ_s , and g , respectively. For each SCLC, four specimens were tested at 90-day. For SCLCs calculation of fracture energy is dependent on the area under the whole load versus displacement at midpoint of span curve as much as a limited displacement 1.5 mm displacement chosen as cut-off point. The beams were loaded at a constant rate of 0.02 mm/min.

The notched beams were used to calculate the net flexural strength (f_{flex}) by the given formulation (Equation 3.4) assuming no notch sensitivity, where P_{max} is the ultimate load.

$$f_{flex} = \frac{3P_{max}S}{2B(W-a)^2} \quad (3.4)$$

By the following expression, the brittleness of materials can be determined in terms of characteristic length (Hillerborg, 1985):

$$l_{ch} = \frac{EG_F}{f_{st}^2} \quad (3.5)$$

Where, f_{st} , E , and G_F are the splitting tensile strength, static modulus of elasticity, and fracture energy, respectively. In this study, splitting tensile strength was used instead of direct tensile strength.



Figure 3.11 Photographic view of universal testing devices and three point flexural testing fixture

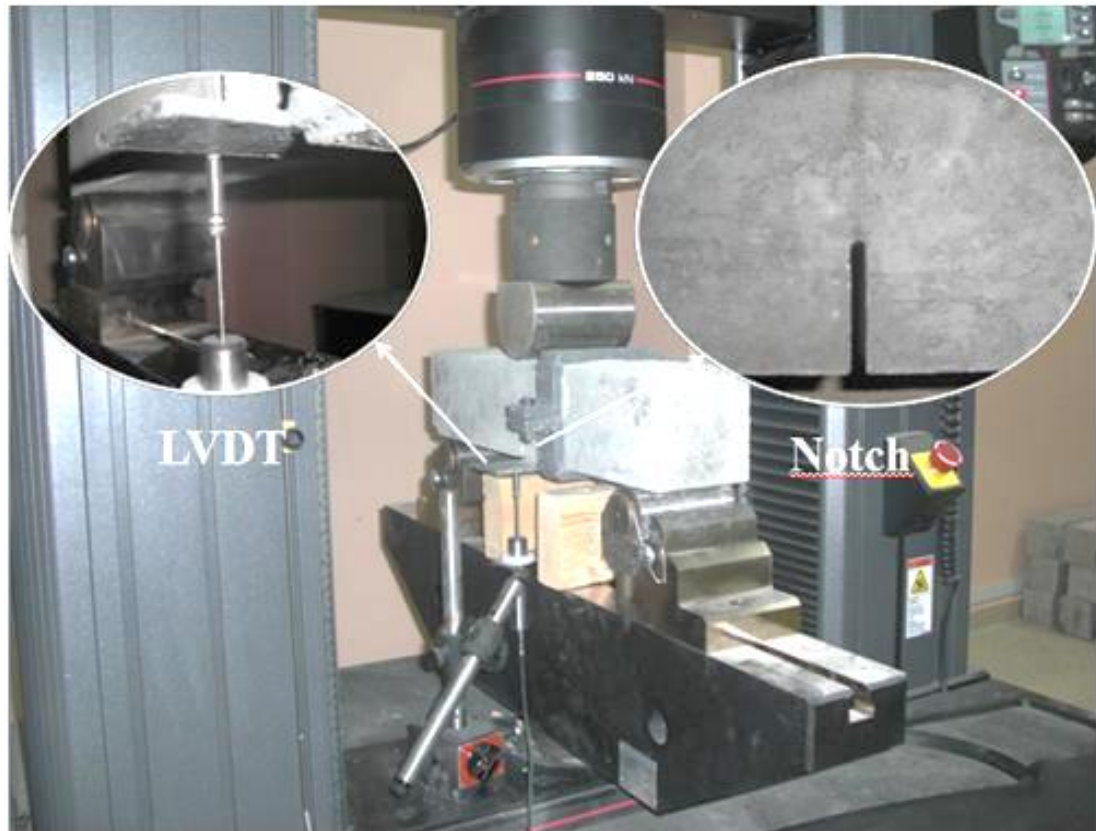
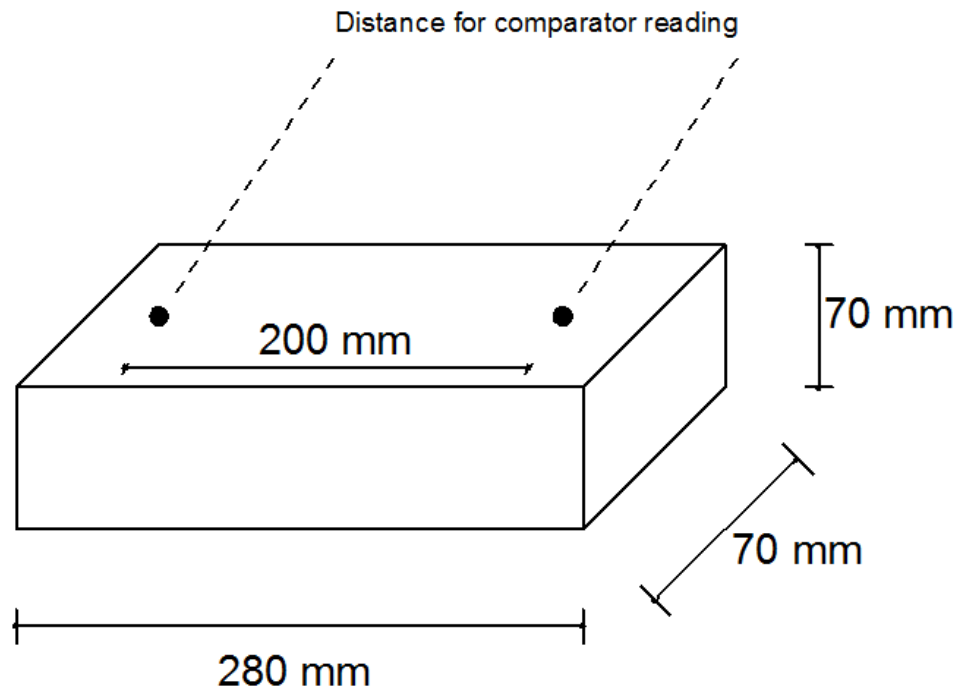


Figure 3.12 Photographic view of notched beam specimen

3.7 Tests for Physical Properties

3.7.1 Drying Shrinkage and Weight Loss

In order to observe the drying shrinkage and weight loss of the SCLCs, three 70x70x280 mm prisms with respect to ASTM C 157 (2008) were used as shown in Figure 3.13. As soon as the prisms being demoulded, the gage length was fixed on each specimen by the means of the glued pins on the face of prisms. The length change was measured via a dial gage extensometer which had a quantity of 200mm gage length with the 0.002 strain for measuring. Measurements were implemented for the first 3 weeks as every 24 h and then 3 times a week. Meanwhile, measurements of weight loss were operated on the identical prism, too. The variety of the drying shrinkage strain and the weight loss were followed during drying period for the 60-days at $23\pm 2^{\circ}\text{C}$ and $50\pm 5\%$ relative humidity. The test results for each property were evaluated by the average measurement of three prism specimens.



a)



b)

Figure 3.13 Free shrinkage test a) Free shrinkage test set up and b) Test specimens

3.7.2 Restrained Shrinkage Cracking

In this study, the ring-shaped specimens were utilized in order to determine the shrinkage stimulated cracking of SCLCs. For the ring with dimensions in Figure 3.14, it was shown that, when an interior pressure stimulated by the restricting internal steel ring exposed to the concrete, the variation between the values of the tensile hoop stress on the external and the internal surface of the ring specimen was about 10%. At that time, approximately 20 percentage of the maximum hoop stress consisted of the greatest rate of the radial stress. Therefore, it was able to be accept that the ring-shaped specimen was fundamentally exposed to a uniform, uniaxial tensile stress in which concrete specimens was restrained by the steel ring whose thickness (35 mm) corresponds to four times lesser than its width (140 mm) (Grzybowski and Shah, 1990; Shah et. al., 1992; Wiegrink, 1996)

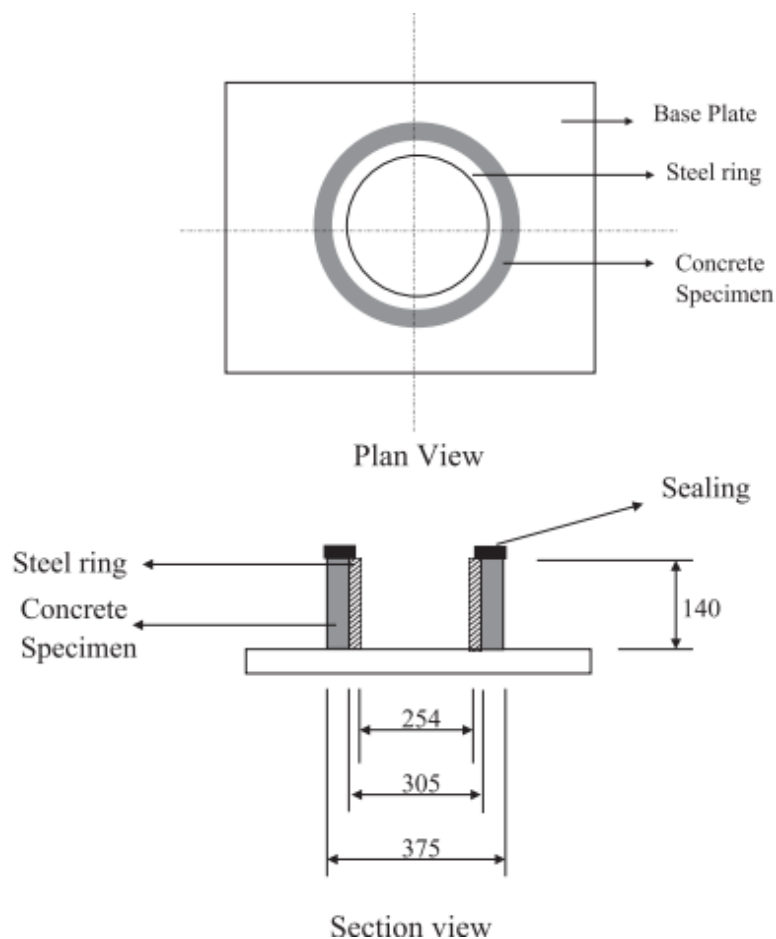


Figure 3.14 The dimension of restrained shrinkage ring specimen (in mm)

After the outer mould of the ring specimen had been removed, and then the top surface of the concrete ring was covered via a silicone rubber, so that the drying would be permitted only by the outer circumferential surface (Figure 3.15). Thereafter, the ring specimens were subjected to drying in a cabinet with relative humidity of $50\pm 5\%$ and temperature of $23\pm 2^{\circ}\text{C}$, according to ASTM C157 (2008) during about 60 days. The width of the crack declared at this point were mean of three evaluations: one is at the midpoint for the ring and second one is at the midpoints of the top for the ring and last one is bottom half of the ring (Figure 3.16). After crack being occurred on the surface of specimen, the measurements of the widths for the existing crack were operated during first 7 days as every 24 hr, and then every 48 hr.



Figure 3.15 Restrained shrinkage test specimens



Figure 3.16 Photographic view of a cracked ring specimen (MF20)

3.8 Determination of the Durability Performance of SCCs

3.8.1 Water Sorptivity

Water sorptivity was measured on four specimens of 100 mm in diameter and 50 mm in length cut from the of $\text{Ø}100 \times 200$ mm cylinders. Before test, the specimens were dried in an oven at $100 \pm 5^\circ\text{C}$ till they reached the constant mass. The test was conducted on the surface of concrete which is in contact with a thin water layer while the sides of the specimens were covered by paraffin, so that capillary suction was considered the dominant invasion mechanism. The measurement was conducted on the specimens located on glass rods in a tray such that their underside as much as a height of 5 mm is got in touch water, as shown in Figure 3.17. Water sorptivity evaluated by the water uptake from the concrete per unit cross-sectional area with time. The test was implemented in 28 and 90 days.

3.8.2 Water Permeability

TS EN 12390-8 (2002) standard was adapted to examine the water permeability of SCLCs at 28 and 90 days. For this, the bottom side of the specimen was subject to a 500 ± 50 KPa for 72 hrs. When 72 hrs periods was completed, the cube specimens were cut into the middle section and the maximum water penetration depth was measured in mm. In order to qualify the concrete resistant against to the chemical attack, water does not pass through a depth of more than 50 mm in concrete probably to get in touch with vaguely aggressive media and not more than 30 mm if concrete is probably to get in touch with aggressive media (TS EN 12390-8, 2002). A photograph of the water permeability test equipment is given in Figure 3.18.

3.8.3 Rapid Chloride Permeability Test

An experimental setup meeting the ASTM C 1202 (2012) was followed to measure the resistance of SCLCs against chloride ion penetration as shown in Figure 3.19. Two specimens of $\varnothing 100 \times 200$ mm were tried out at the same time for each SCLC at 28 and 90 days. For this, two 50 mm thick disc samples were cut from the mid-section of each cylinder. Then, the discs were allowed to surface dry in air. In order to prevent evaporation of water from the saturated specimen, a rapid setting coating was applied onto the lateral surface of the specimens prior to a vacuum-saturation procedure for 2 hrs. Finally, the specimens were immersed in water in the curing room at 20°C and 50% relative humidity for 18 ± 2 hrs. Following this conditioning procedure, the disc specimens, whose one side got in touch with 0.30 N NaOH solution and the other side was in contact with 3% NaCl solution, were relocated in a test cell (Figures 3.19 and 3.20). A direct voltage of 60.0 ± 0.1 V was enforced between the faces by the power supply. Due to this applied voltage the chloride ions in the NaCl solution, being negatively charged, were attracted by the opposite positive electrode (+) and they penetrate through the pores of saturated concrete. The data was measured at every 30 minutes to record the current passing through the specimens over a 6 hour period. After being completed the test, current (in amperes) versus time (in seconds) were drawn for each specimen. And the area under the curve was computed to acquire the charge passed (in coulombs). Five classes from 'High' to 'Negligible' were categorized according to ASTM C1202 (2012) depending on total coulomb value as given in Table 3.7.

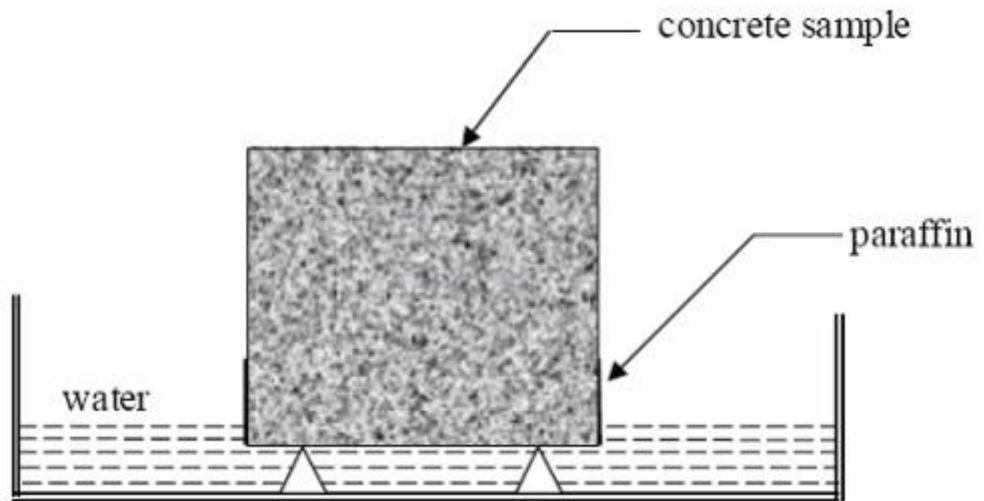


Figure 3.17 Water sorptivity test set up



Figure 3.18 Water permeability test set up

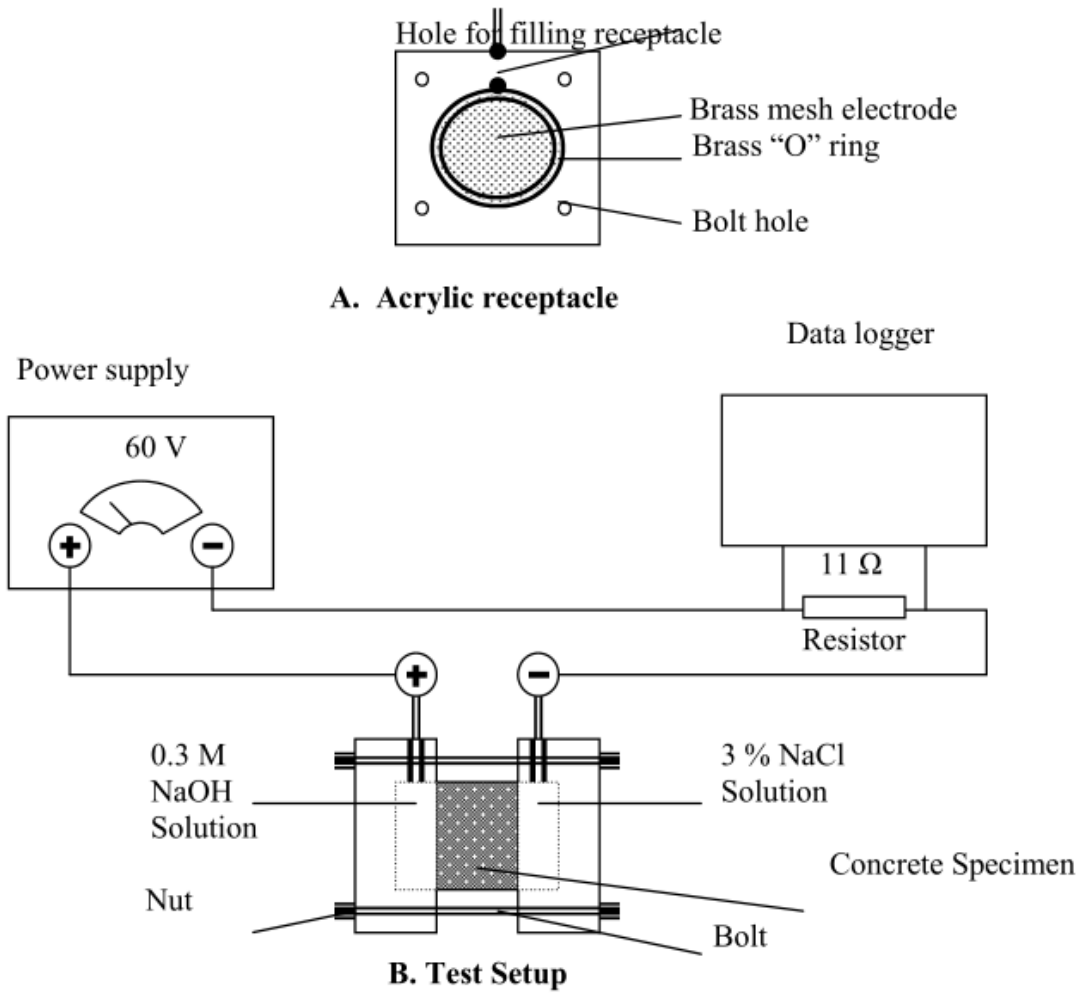


Figure 3.19 Schematic presentation of the test set up for RCPT

Table 3.7 Interpretation of the test results obtained using RCPT test (ASTM C1202, 2012)

Charged Passed (Coulombs)	Chloride Permeability
>4000	High
2000-4000	Moderate
1000-2000	Low
100-1000	Very Low
<100	Negligible



Figure 3.20 Photographic view of the RCPT test set up

3.8.4 Gas Permeability

A RILEM TC 116 (1999) recommendation, the CEMBUREAU method was conducted for measuring the gas permeability coefficients of concretes. The gas permeability was measured on 50 mm height and 150 mm diameter disk specimens cut from the midpoint section of $\text{Ø}150 \times 300$ mm cylinders. When the curing period of 28 and 90 days were ended, the specimens dried at $50 \pm 5^\circ\text{C}$ in oven to make sure each specimen weight change was less than 1%. Then, they were kept in a sealed box till test began. At each testing age, two specimens were investigated and the average of them was recorded. The photographic view and the schematic layout of the apparatus as well as the detail of the testing cell are shown in Figures 3.21-3.23. The steps of the gas permeability test are as follows;

1. Measure the diameter of the test specimen in 4 positions (two perpendicular diameters in both top and bottom faces) with a precision of 0.1 mm. The diameter D is the mean value of the four readings. The thickness L of the test

specimen is determined in four positions equally distributed along the perimeter.

2. Place the test specimen in the cell and assemble the apparatus.
3. Build up a minimum lateral pressure of 7 bar (0.70 MPa) on the rubber tube.
4. Select 3 pressure stages: start with 1.5 bar (0.15 MPa) and increase to 2.0 (0.20 MPa) and then 3.0 bar (0.30 MPa) absolute gas pressure. Correct the input pressure of gas if necessary within 10 minutes.
5. Wait for 30 minutes before measuring the first flow.
6. Measure the flow at each pressure stage until it becomes constant, as follows:
 - a. Moisten the capillary of the soap bubble flow meter 1 minute before creating the bubble for measurement.
 - b. Always start the time measurement when the bubble is at the lowest marking of the calibrated tube.
 - c. Select the measuring volume by choosing the appropriate soap bubble flow meter such that the time reading is more than 20 seconds.
 - d. Take provisional readings of the flow rate. If the difference between successive readings within 5 to 15 minutes is less than 3%, take at least 2 readings in quick succession and determine the flow rate. $Q_i = V/t_i$ (m^3/s) for the given pressure stage. If this condition is not reached within 3 hours (no constant flow is attained, *e.g.* very low-permeability concretes), take the previous value of the flow rate.
7. Increase the pressure to the next pressure level and repeat the procedure with steps (6a) through (6d). Ensure that there are no leaks during the tests: the coefficient K should decrease when the pressure increases. If this is not the case, check the test setup for possible leaks and repeat the measurements.

$$K = \frac{2P_2QL\eta}{A(P_1^2 - P_2^2)} \quad (3.6)$$

Where,

K: Gas permeability coefficient (m^2)

P_1 : Inlet gas pressure (N/m^2)

P_2 : Outlet gas pressure (N/m^2)

A: Cross-sectional area of the sample (m^2)

L: Height of sample (m)

η : Viscosity of oxygen ($2.02 \times 10^{-5} \text{Ns}/\text{m}^2$)

Q: Rate of flow of air bubble (m^3/sn)

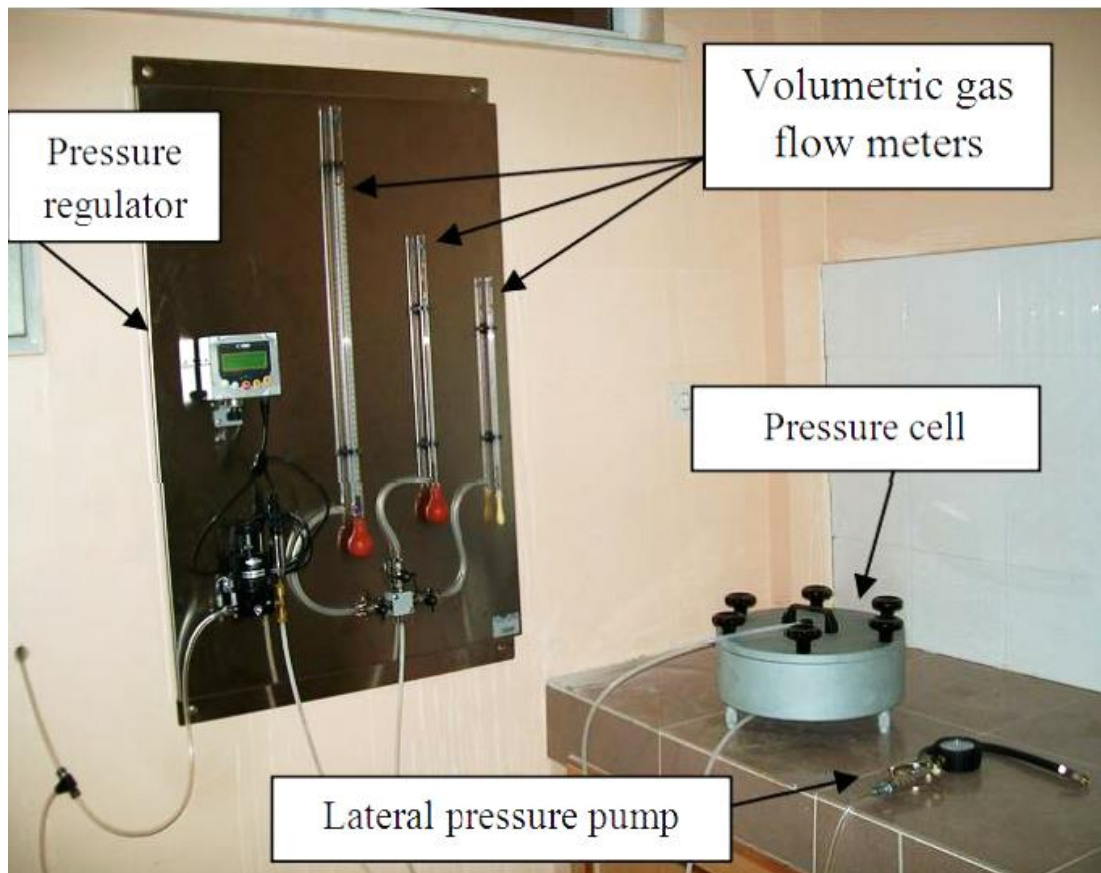


Figure 3.21 Photographic view of the gas permeability test set up

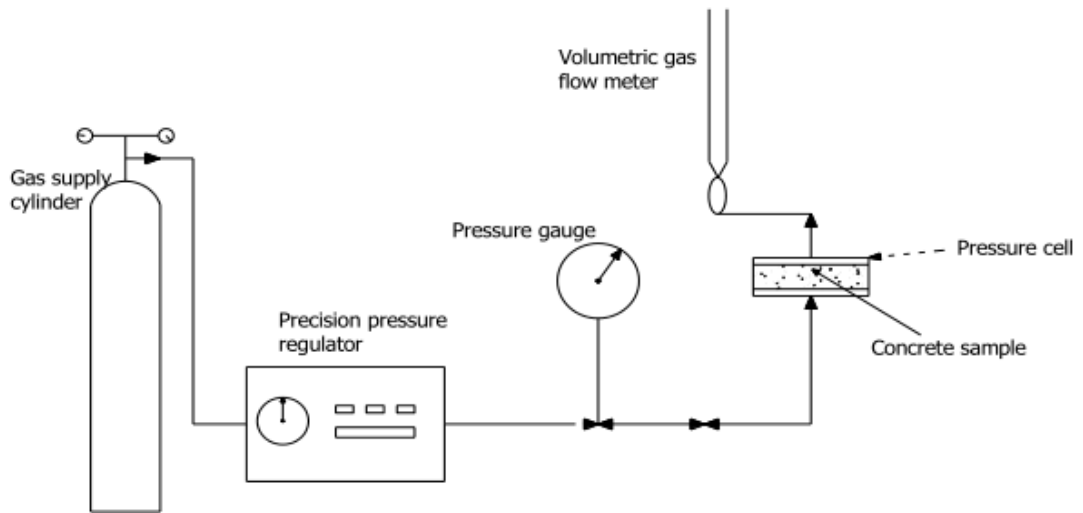


Figure 3.22 Schematic presentation of the gas permeability test set up

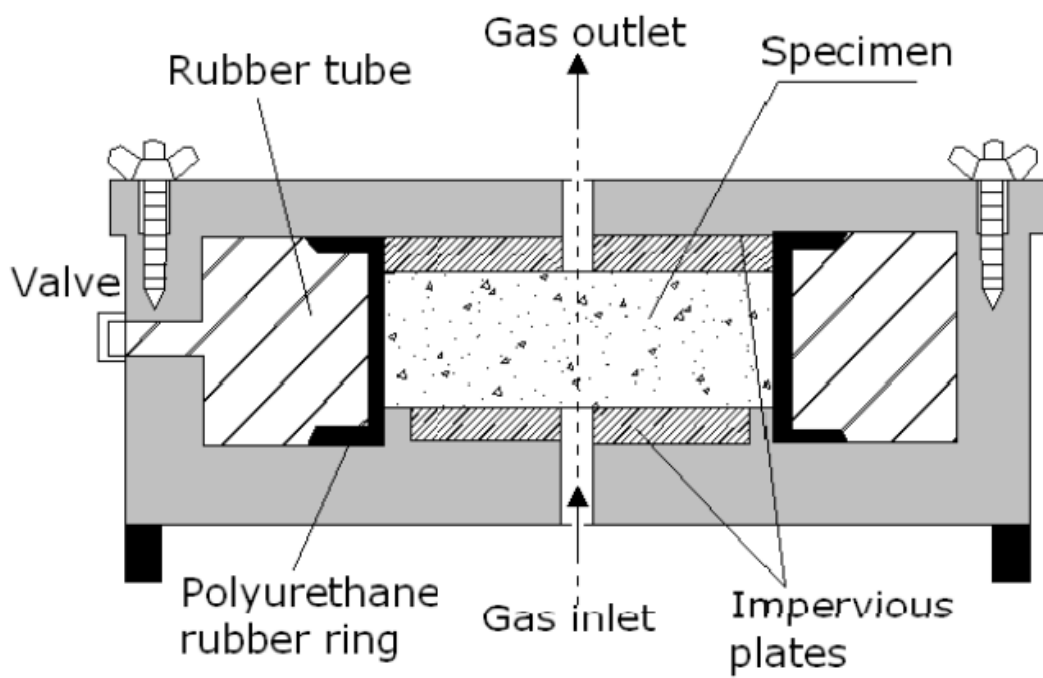


Figure 3.23 Schematic presentation of the pressure cell and test specimen

CHAPTER 4

TEST RESULTS AND DISCUSSIONS

4.1 Fresh Properties of Self Compacting Lightweight Concretes

4.1.1 Fresh Density

A preferable SCC should have good fluidity, deformability, and filling ability, as well as uniform aggregate distribution and maximum resistance to segregation, each of which being evaluated by one or more test methods (EFNARC, 2005; Wu et al., 2009). SCC requirements in accordance with a given application can be chosen from one or more of above mentioned characteristics and then specified by class or target value given in Table 3.6.

The concretes produced in the study had fresh densities ranging from 2337 to 2092, 2346 to 2133, and 2341 to 2113 kg/m³ for MC, MF and MCF mixes, respectively (Figure 4.1). It was observed that increasing the replacement level of LWFA and/or LWCA resulted in a reduction of fresh density. For instance, as seen Figure 4.2, fresh density of the SCLCs decreased by as much as 12.7%, 10.9%, 12% for MC50, MF50, and MCF50 mixes, respectively, compared with the control mixture (CM) containing fully natural aggregate. Furthermore, in the case of MCF100 (SCLC with %100 LWCA and LWFA) fresh density was as low as 23.6% with respect to CM. As it seen all the concretes except for MCF100 exceed the upper limit (1950 kg/m³ for air dried concrete) given by ACI Committee 213R (2003) for lightweight concretes. However, the concrete having an oven dried density between 800 and 2000 kg/m³ is specified as LWC in TS EN 206-1. Since the densities reported herein are fresh unit weights, most of concretes may conform to this limitation. But, due to their relatively higher fresh densities, SCLCs may be considered as semi-lightweight concretes except the MCF100 mix.

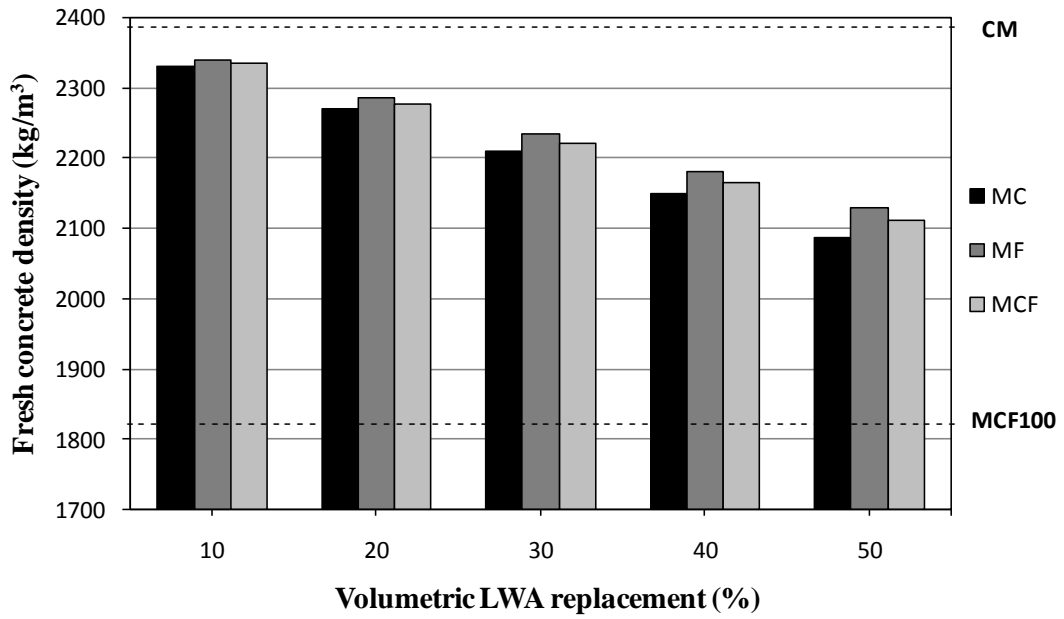


Figure 4.1 Variation in the fresh density of SCLCs

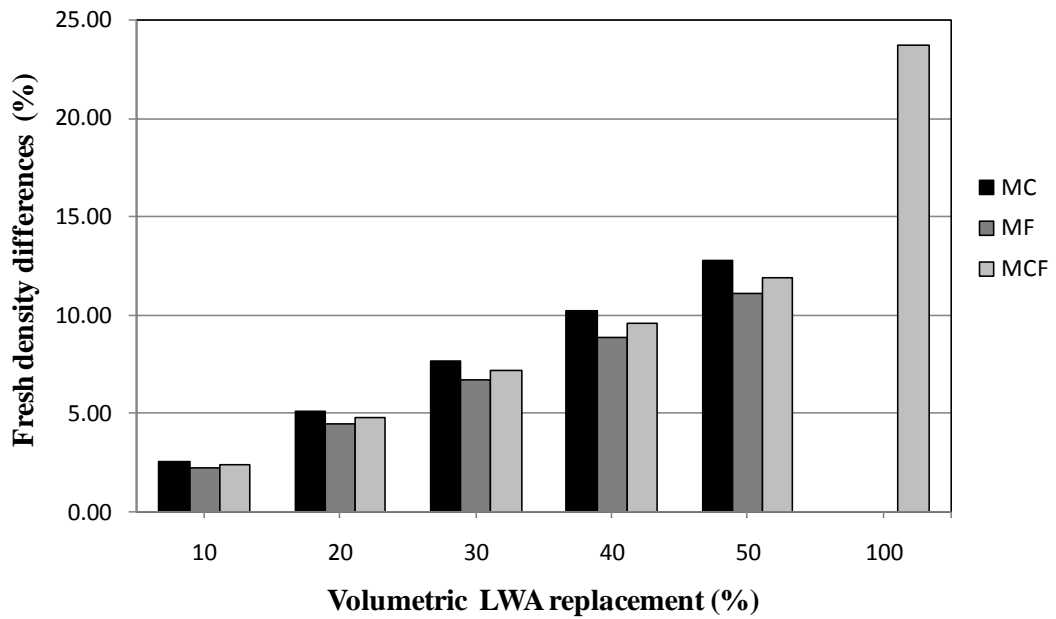


Figure 4.2 Fresh density differences (%) for SCLCs with respect to CM

Nevertheless, the higher unit weights might be attributed to three reasons. The low w/b ratio and high cement content kept the weight of fresh concrete heavy. Secondly, higher specific gravity of fly ash resulted in the production of artificial aggregates having a specific gravity of 1.76 (SSD condition) which was slightly heavier for use in LWC. However the main reason was the combined use of natural and lightweight aggregates which caused the fresh density of concretes to exceed the ACI limitation.

4.1.2 Slump Flow Time and Slump Flow Diameter

The slump flow diameters for SCLCs produced in this study ranged between 700 and 730 mm which were achieved by adjusting the amount of HRWRA used. Within this range, the lowest slump flow diameter was measured for the control concrete while the mixture (MCF100) with 100% LWCA and LWFA had the highest slump flow. As seen Figure 4.3, aggregate particles displayed regular and uniform distribution so that no bleeding and segregation were observed for all SCLCs, even for MCF100. The results of slump flow diameter and time for the produced SCLCs is indicated in Table 4.1. It was observed that the time required reaching 500 mm slump-flow decreased while slump flow diameter increased as the proportion of LWA increased.

Moreover, as demonstrated in Table 3.5, the required HRWRA to obtain the aimed slump flow substantially decreased with increasing the amount of LWCA and LWFA. In the case of control mixture, for instance, 7.1 kg/m³ of HRWRA was incorporated while MCF100 needed only 3 kg/m³ of HRWRA for a given slump flow diameter. Therefore, SCLCs incorporating LWCA and LWFA had better flow characteristics.

Furthermore, as observed in Table 3.5, SCLCs with LWFA generally needed less HRWRA than that of SCLC with LWCA for a given target slump flow diameter. For example, 4 kg/m³ of HRWRA was used in MC50 to get a slump flow diameter of 730 mm whereas MF50 gave a slump flow diameter of 720 mm with 3.1 kg/m³ of HRWRA.

It was observed that there was a good correlation between the need for HRWRA and volumetric replacement level of the aggregates as seen in Figure 4.4 which also indicated that for a constant slump flow diameter, the demand for HRWRA

decreased as more LWA replaced the natural ones. Indeed, for gaining the target slump flow of 720 ± 20 mm, HRWRA demand decreased by as much as 38%, 44%, and 37% for MC30, MF30 and MCF30 mixes, respectively. This may be attributed to the fact that the specific surface area plays an important role in decreasing the amount of HRWRA needed and LWFA has a bigger specific surface area than LWCA. Also, in MF group mixes, a reduction in NWFA content or an increment in LWFA content results in a reduction in the specific surface area of aggregates that must be coated with cement paste, thus, leading to a reduction in the resistance to flow. Moreover, in the MCF mixes, a further decrease in HRWRA was obtained to keep the same slump flow diameter due to the dual effect of fine and coarse lightweight spherical fly ash aggregates to provide ease in flow. As it is shown in Figure 4.5, slump flow classes of SCLCs fell in SF2 which indicated that SCLCs produced can be used in most of the structural members.

The time required to reach 500 mm slump-flow is shown graphically in Figure 4.6. $T_{500 \text{ mm}}$ slump flow was 3.03 s for the reference mixture (CM). However, $T_{500 \text{ mm}}$ slump-flow for MC50, MF50, and MCF50 was measured as 1.57, 1.85 and 1.2 s respectively. Furthermore, in the case of MCF100 mix, $T_{500 \text{ mm}}$ slump flow further decreased to 1.03 s. These results are in agreement with those observed by Lo et al. (2004) that for the same LWA proportions increasing the size of LWA to a certain limit results in higher flowability of SCLC.

4.1.3 V-funnel Flow Time

The flowability and viscosity of SCCs was evaluated by means of V-funnel flow time. According to EFNARC (2005), the concrete having a V-funnel flow time within 6 to 12 sec may be highly resistant to possible segregation. The variation of V-funnel flow time of the produced SCLCs is given in Table 4.1 and plotted in Figure 4.7. It was observed that, the V-funnel flow time was in the range of 6.50-11.54 s, depending mainly on LWA content.

Increasing the rate of LWA in SCLC accompanied with decreasing in the V-funnel time depending on the size group. For instance, there was a decrease in V-funnel time by as high as 31%, 26% and 32% for MC40, MF40, and MCF40 mixes, respectively, compared to CM. However, LWCA had more important effect on the

decreasing of V-funnel flow time. This may be attributed to the spherical shape as well as relatively smooth surface of LWCA and LWFA which provide ease in flow of the aggregate particles and paste (Kayali et al., 1999; Su et al., 2001). Similar to test results of slump flow, incorporating LWFA with SCC in MF mixes made the concretes more cohesive so that these concrete had higher flow times with respect to MC and MCF mixes. The main reason for this behavior may be attributed to the higher specific surface of the LWFA which in turn increased the flow time of the concretes.

Table 4.1 Slump flow, V-funnel and L-box properties of SCLCs

Code Number	Slump flow		V funnel flow time (s)	L-box (H_2/H_1)
	$T_{500\text{mm}}$ (s)	D (cm)		
CM	3.03	70.0	11.40	0.87
MC10	2.87	72.0	9.66	0.94
MC20	2.81	72.0	8.55	0.94
MC30	2.40	72.5	8.22	0.95
MC40	1.96	72.5	7.86	0.99
MC50	1.57	73.0	7.55	1.00
MF10	2.97	71.0	10.40	0.87
MF20	2.84	71.0	8.96	0.87
MF30	2.60	72.0	8.93	0.88
MF40	2.13	72.0	8.42	0.88
MF50	1.85	72.0	7.92	0.88
MCF10	2.87	72.0	9.85	0.86
MCF20	2.55	71.5	9.42	0.87
MCF30	2.08	72.0	8.31	0.89
MCF40	1.60	72.0	7.72	0.93
MCF50	1.20	72.5	7.00	0.94
MCF100	1.03	73.0	6.50	1.00



a)



b)

Figure 4.3 Slump flow diameter of a) CM and b) MCF100

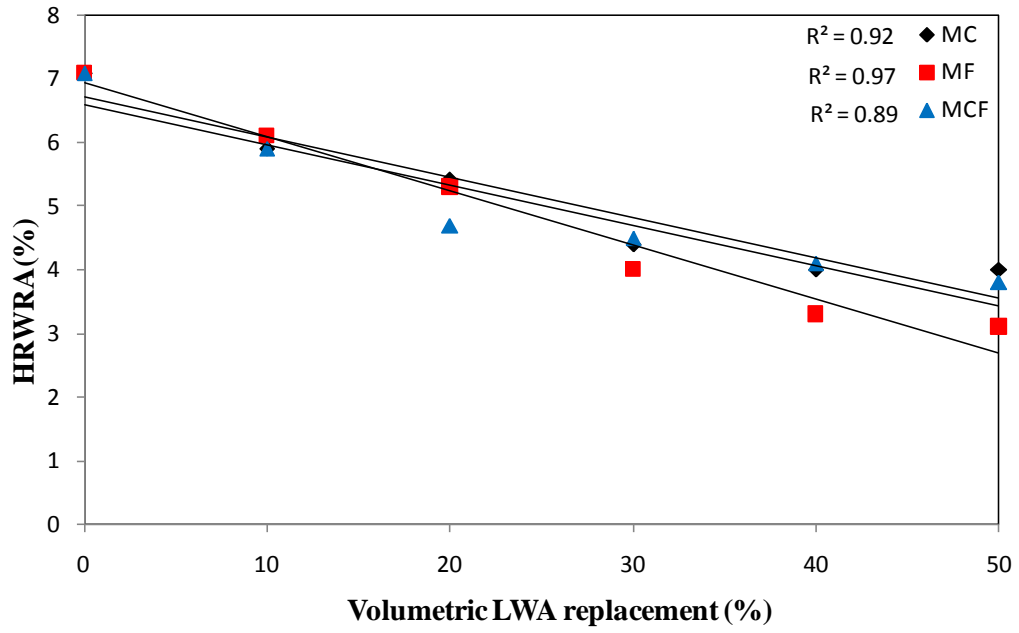


Figure 4.4 Variation of HRWRA demand with increasing LWA content

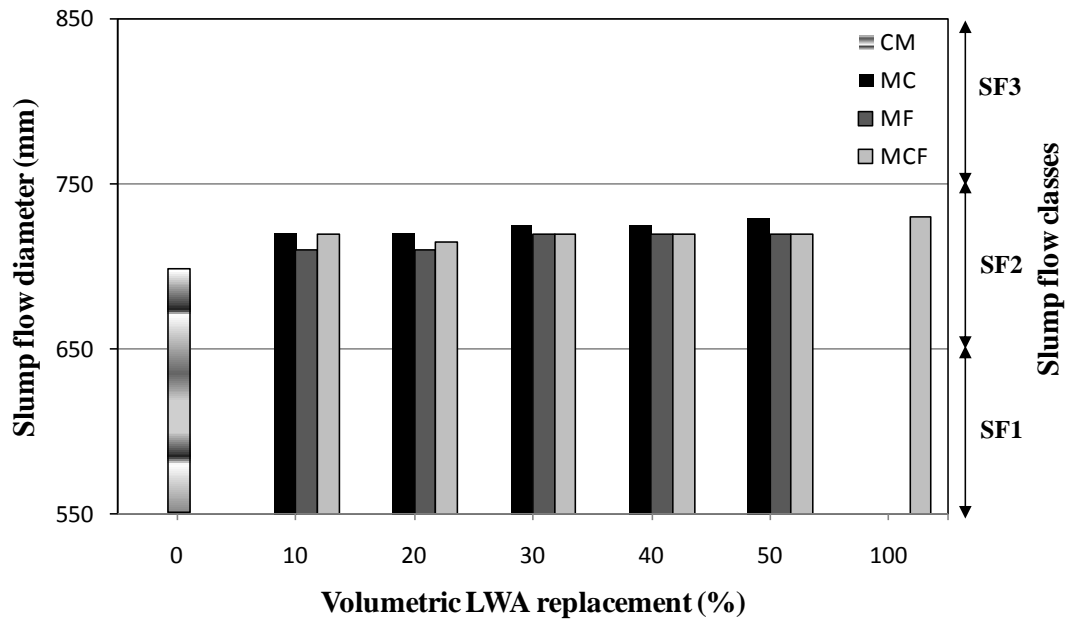


Figure 4.5 Variation of slump flow diameter and slump flow classes for SCLCs

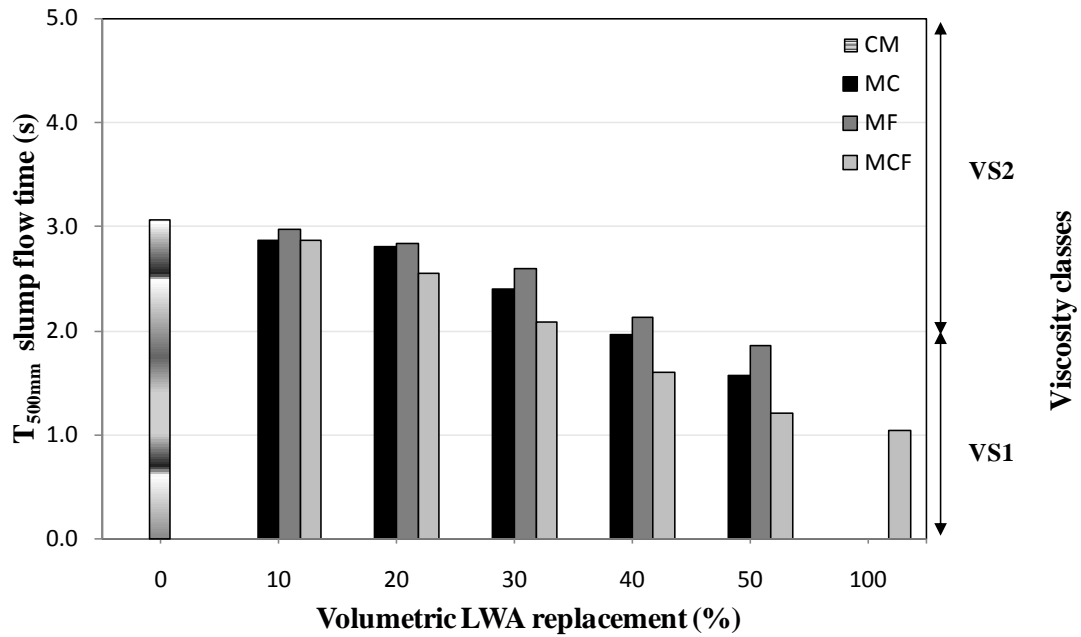


Figure 4.6 Variation of $T_{500\text{ mm}}$ slump flow time and viscosity classes for SCLCs

In the design of concrete, spherical shaped aggregates with smooth surface are preferred because they more readily flow past each other as well as the reduced specific surface area requires less cement and water (Tattersall, 1991; Quiroga, 2003). Moreover, according to EFNARC (2005) more spherical aggregate particles are less likely to cause blocking and the greater the flowability is because of reduced internal friction. In addition to the ease in flow of concrete due to replacement of fine and/or coarse aggregates by lightweight fly ash aggregates, this is probably because the driving force responsible for funnel flow increases with the concrete fresh density (Bogas et al., 2012).

In accordance with Table 3.6, the viscosity classes of the produced SCLCs are given in Figure 4.7. Considering EFNARC (2005) recommendation, viscosity should be specified only in special cases such as best surface finish and in limiting the formwork pressure or improving the segregation resistance. As obviously seen in Figure 4.8, when considering the seventeen SCLCs, the mixtures containing 40% LWA except MF40 were classified as VS2/VF2 while the other six (MC40, MC50, MF50, MCF40, MCF50 and MCF100) were in the category of VS1/VF1. The concretes having viscosity class of VS2/VF2 can be applied at the ramps and walls/columns with SF2 class slump flow. However, the concretes with VS1/VF1 viscosity class are the most suitable types for construction of wide span slabs.

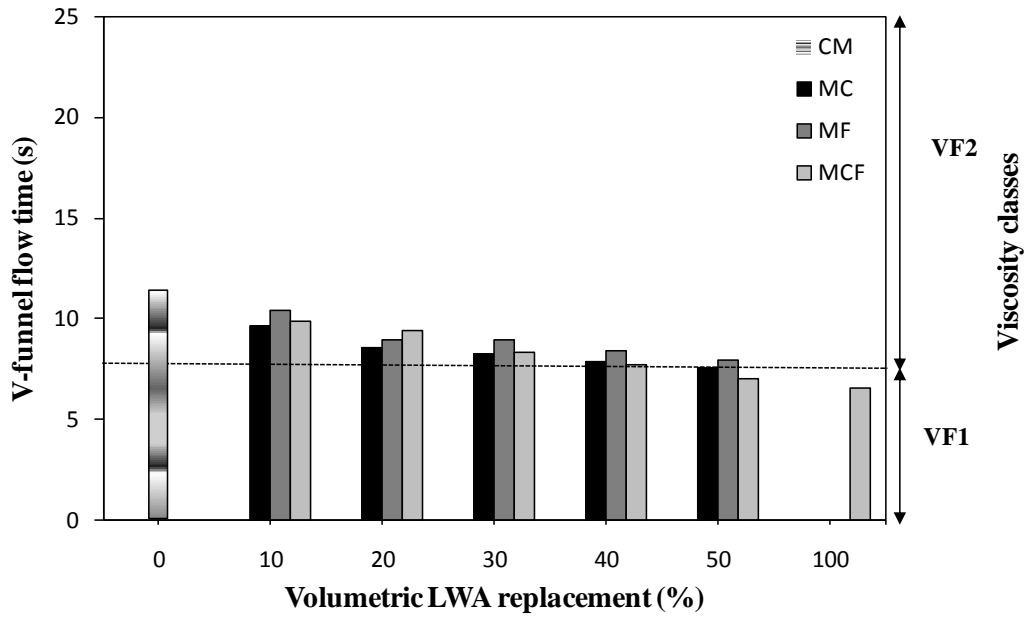


Figure 4.7 Variation of V-funnel flow time and viscosity classes for SCLCs

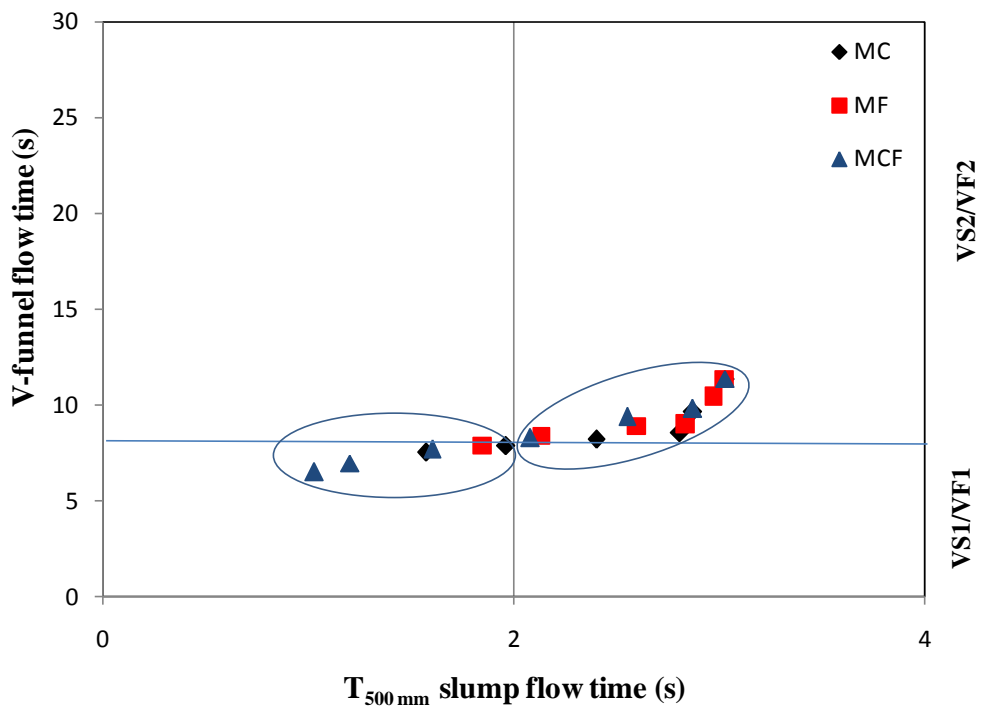


Figure 4.8 Variation of viscosity classes with $T_{500\text{mm}}$ slump flow and V-funnel times for SCLCs

4.1.4 L-box Height Ratio

The L-box test can be used to measure the passing ability of SCLC mixes such that the ratio of H_2/H_1 represents a measure of the passing ability among the reinforcing bars. The variation in the three bar L-box height ratio with LWA replacement ratio is presented in Table 4.1 and graphically depicted in Figure 4.9 for the SCLCs. To confirm that SCC has sufficient passing ability, L-box height ratio must be equal to or greater than 0.8.

It was clearly observed that almost all of the concretes satisfied the EFNARC (2005) limitation in terms of L-box height ratio. H_2/H_1 values ranged from 0.86 to 1.0 depending mainly on the volume fraction of lightweight aggregate used in the concrete production. As clearly seen in Figure 4.9, the reference mixture has the lowest H_2/H_1 ratio of 0.86. Especially, a perfect fluid behavior was observed in MC50 and MCF100 due to having H_2/H_1 ratio being 1.0. Findings of this test emphasized that incorporation of LWA provided a systematic increase in the L-box height ratio. The reason for lesser demand of HRWRA was the spherical shape of the lightweight aggregates which might have helped fresh concrete to be more flowable and more workable. Additionally, EFNARC (2005) specifies that the more the spherical aggregate particles the less the likelihood of blocking and the greater flow of the fresh mixture is because of the reduced internal friction. Therefore, the L-box height ratio of SCLCs including spherical shaped LWA increased with the increasing volume ratio of LWA that conformed to the decreasing $T_{500\text{mm}}$ slump flow and V-funnel flow times.

However, Figure 4.9 showed that the mixes with LWCA gave higher values of L-box height ratio as compared with mixes with LWFA. This is due to the tendency of the mixes with LWFA to jam flowing, while the mixes with LWCA will flow freely without stopping (Khaleel et al., 2011). Moreover, it was observed that, the SCLC made with LWCA has better flow near the obstacles than the mixes incorporating LWFA. This deformability depends on the size and grading of LWA. The spherical shape of the LWA particles yielded a “ball bearing” effect that permitted coarser particles to flow more readily and decreased the surface area that should be wetted for enhanced workability (Koehler and Fowler, 2004). In other words, this is

attributed to the smooth texture of the bigger surface of LWCA that facilitates aggregates passing through obstacles (Kim et al., 2010).

4.1.5 Rheological Parameters of Self Compacting Lightweight Concretes

Certain materials like special cements, artificial aggregates, micro-fines, fiber reinforcement, new age chemical admixtures, etc. when used in conventional concretes can have some unexpected consequences on the fresh properties.

The workability of these new generation concretes such as self-compacting concrete cannot be sufficiently measured by slump test, slump flow test, J-ring test, V-funnel test, U-box filling test, L-box test or column test alone (ASTM C1611, 2005; EFNARC, 2005; ASTM C143, 2008; ASTM C1621, 2008). In fact, the workability of self-compacting concrete that flows readily under its own weight through the incorporation of special chemical admixtures as well as the utilization of enhanced particle size distributions must be determined and monitored carefully by using the concrete rheometer (Koehler and Fowler, 2004).

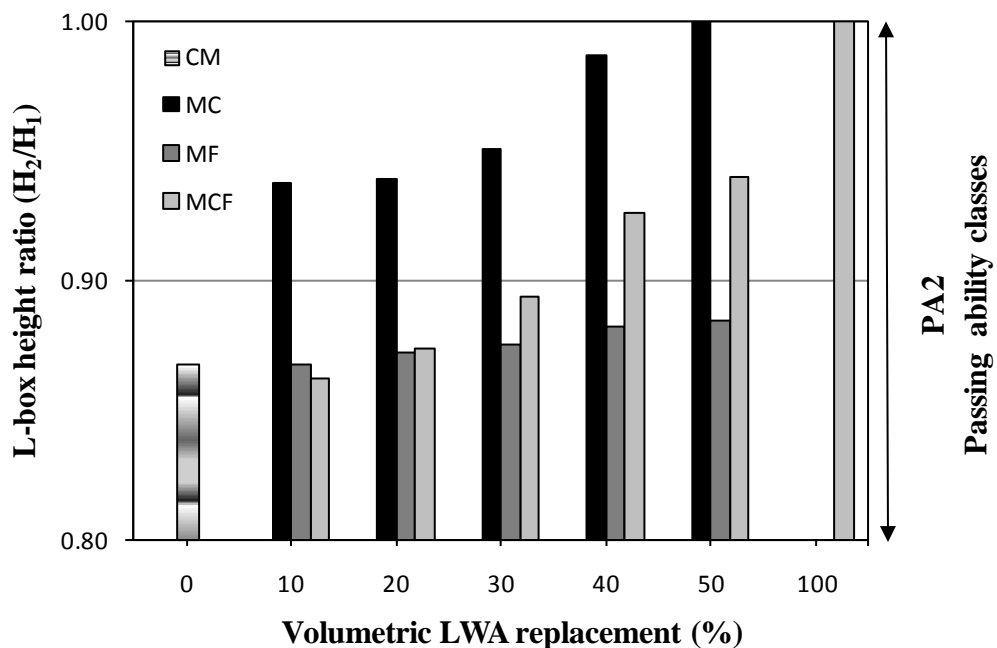


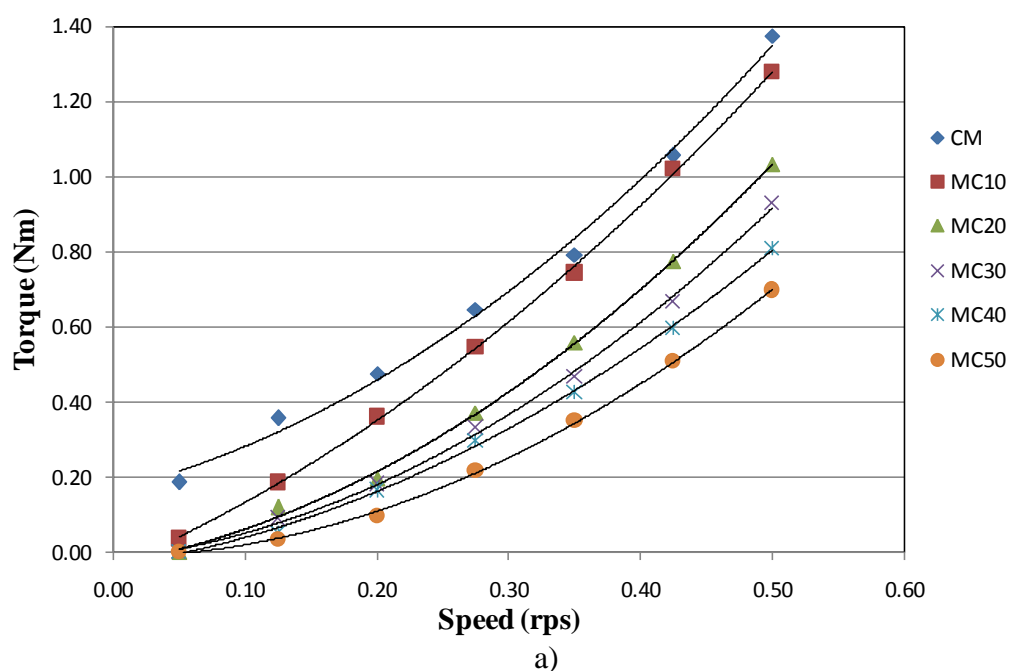
Figure 4.9 Variation of L-box height ratio values for SCLCs

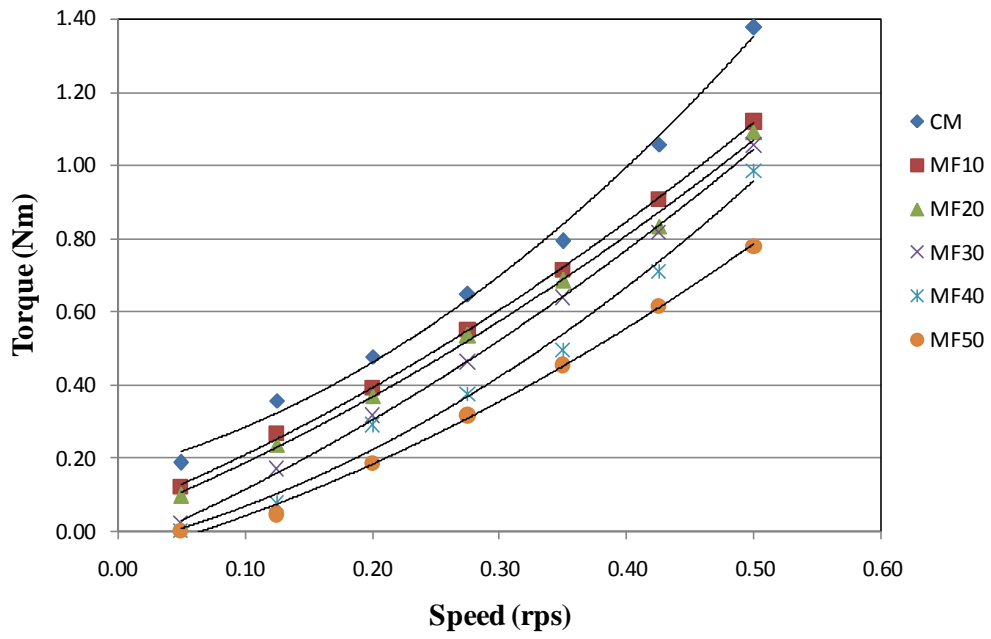
Aggregate shape and texture are strongly effective on the rheological parameters of SCCs. In concentrated suspensions, any deviation from a spherical shape results in an increased viscosity (Barnes et al., 1989). In order to ensure a high flowing ability as well as a good de-airing of the SCC, a low yield stress and moderate viscosity are required. At the same time, both characteristics have to be chosen high enough to prevent the lightweight aggregates from buoying upwards or blocking (Maghsoudi et al., 2011). Lightweight fly ash aggregate is suitable for use in SCC due to its spherical shape so as to improve the rheological properties of the fresh concrete mixture, keeping in mind, however, that the aggregate may migrate towards the surface if the paste viscosity is so low (EFNARC, 2005). This issue was resolved in this study by controlling the slump flow of the SCLC mixtures by adjusting the amount of HRWRA used.

The main and important rheological parameters for concretes are yield stress and viscosity. If yield stress stands for the pressure necessary to make concrete begin to move, viscosity expresses how fast the concrete moves, once yield stress has been exceeded. A design methodology for SCC depends upon the assumption that minimum yield stress and viscosity are needed in order to prevent segregation because the concrete will have low workability if the yield stress or viscosity is too high (Saak et al., 2001b). However, concrete with a low viscosity will have a very quick initial flow and then stop while it may continue to creep forward over an extended time for a high viscosity (EFNARC, 2005). When concrete exits in the concrete truck at a high rate of shear, the yield value of SCC is almost ineffective and the shear resistance is about 25 Pa.s for low viscosity (Nielsson and Wallevik, 2003).

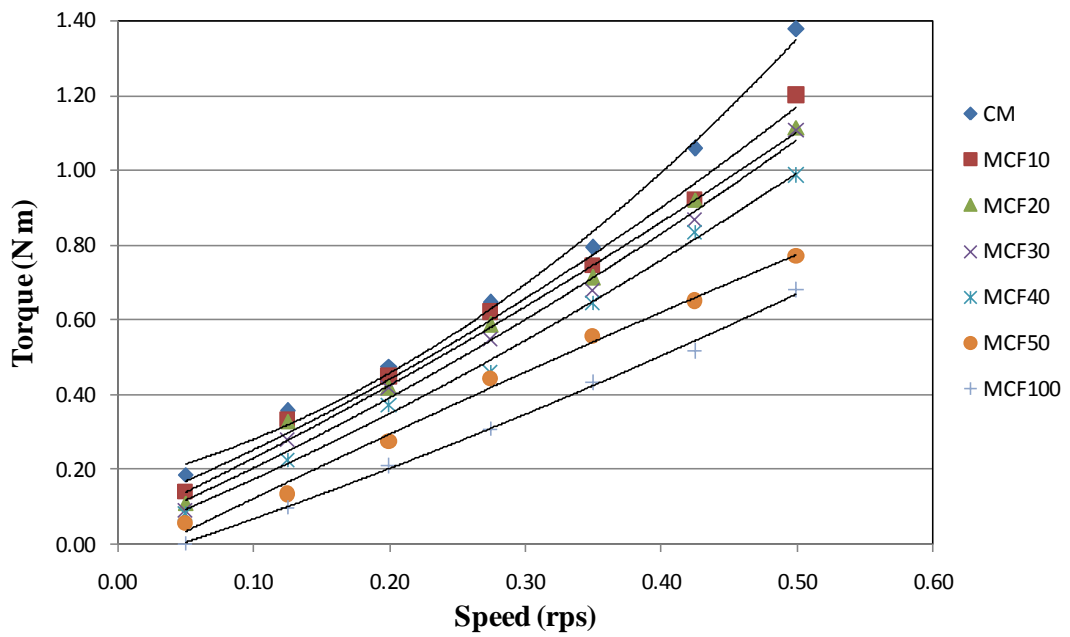
Figures 4.10 a, b and c show the flow curves of SCLCs for MC, MF, and MCF groups, respectively, plotted using data from ICAR rheometer in terms of rotational speed (in rps) and torque (in Nm) respectively, which were representing the shear strain rate and shear stress. It was observed that the control mixture showed a shear thickening behavior in line with the literature. Similarly, the concretes in MC groups incorporating varying amounts of lightweight coarse aggregates behaved as a shear thickening material with a gradual increase in the plastic viscosity. At a constant rotational speed of 0.40, the torque was measured to be 1.0 and 0.42 Nm for the control concrete and the concrete with 50% LWCA, respectively. It was evident in

Figure 4.10 that LWA replacement diminished the intensity of shear thickening of the concretes. As seen in Figure 4.10 b replacement of natural fine aggregate with lightweight one reduced the plastic viscosity and made the concretes less susceptible to shear thickening. However, the most striking effect of using LWA in SCCs was seen in Figure 4.10 c for the MCF group concretes with varying proportions of both fine and coarse LWAs such that almost all of the concretes in this group exhibited Bingham behavior, especially at higher shear rates. In fact, the concrete with 100% LWA behaved as Bingham material both at low and large shear rates. Shear thickening behavior is important because it is something that is more disadvantages than advantages. As the (apparent) viscosity increases with increasing shear rate, a larger increment in energy will be needed to further accelerate the flow of the material. Especially in processes such as mixing, pumping, extrusion, etc. where high shear rates are applied shear thickening can become significant and even dominant (Barnes, 1989; Feys et al., 2009). The findings in Figures 4.10 a, b and c well agreed with the less HRWRA demand for such concretes as shown in Figure 4.4. It may be attributed to the fact that the higher surface area to volume ratio will play a big role on decreasing the amount of HRWRA used and then decreasing the torque applied as fine LWA have bigger surface area than the coarse aggregate. Moreover, for the mixes that contained both fine and coarse LWAs together (Figure 4.10 c), they will form dual slippage effect resulting in reduced torque and HRWRA demand for keeping the slump flow constant.





b)



c)

Figure 4.10 Flow curves for a) MC group mixes, b) MF group mixes and c) MCF group mixes

When the Bingham parameters are considered, SCC has very low yield stress (near to zero as seen in Figure 2.8) so that it may be ignored. Indeed, yield stress values of SCCs of this study were well below 10 Pa, and there was no discernable trend since the slump flow diameter has been kept constant for all of the concretes. This conclusion is also approved by Feys et al. (2008), Nielsson and Wallevid (2003) that the yield values below 10 Pa can be negligible. The relative and plastic viscosities for SCLCs are presented in Table 4.2. However, Figure 4.11 displays the plastic viscosity of the Bingham model ranging from 21 to 51 Pa.s for fully LWA concrete (MCF100) and NWA concrete (CM), respectively. There was a good correlation between the LWA and the plastic viscosity, irrespective of the group mixes produced. If the viscosity of concrete expresses how fast the concrete moves, any percentage increase of LWA is accompanied by reduction of plastic viscosity owing to the reduced inter-particle friction. The correlation is highest in MCF concretes followed by MC and MF, even though the difference of R^2 is so little between them (Figure 4.11).

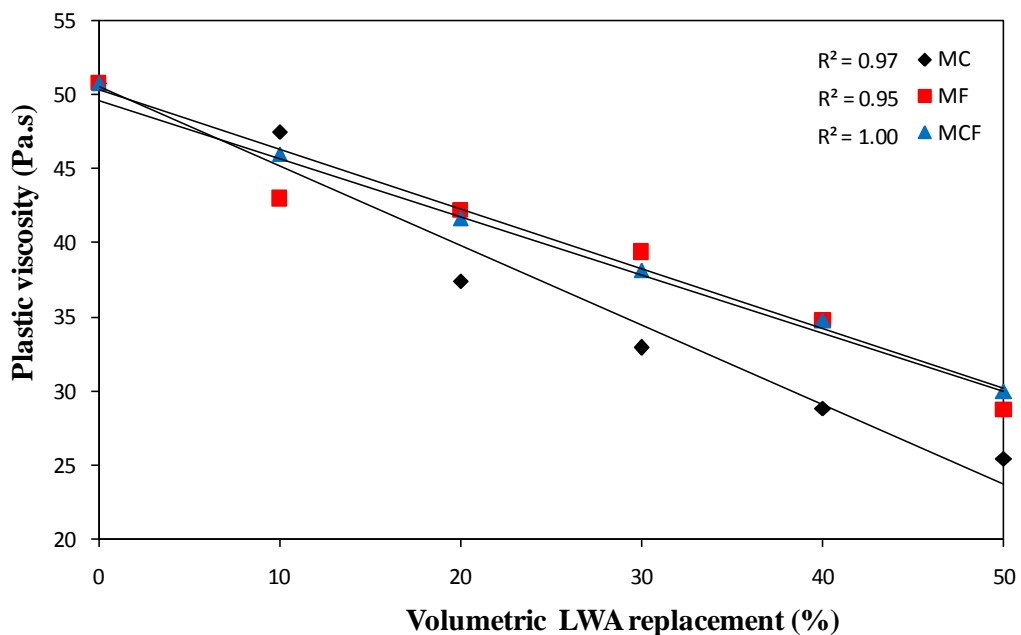


Figure 4.11 Variation of plastic viscosity with increasing LWA content

Table 4.2 Plastic and relative viscosity values for SCLCs

Code Number	Plastic viscosity (Pa.s)	Relative viscosity (Nm.s)
CM	50.8	2.83
MC10	47.5	2.29
MC20	37.4	2.24
MC30	32.9	2.14
MC40	28.8	1.84
MC50	25.4	1.80
MF10	43	2.73
MF20	42.2	2.45
MF30	39.4	2.21
MF40	34.8	2.05
MF50	28.7	1.79
MCF10	46.0	2.53
MCF20	41.7	2.33
MCF30	38.2	1.83
MCF40	34.8	1.69
MCF50	30.0	1.46
MCF100	20.8	1.01

4.2 Mechanical Properties of Self Compacting Lightweight Concretes

4.2.1 Compressive Strength

The compressive strength at 28 and 90 days for SCCs produced with LWCA and LWFA having different mix proportions are shown in Table 4.3 and graphically presented in Figure 4.12. It was observed that the compressive strength increases with the age regardless of replacement level of LWA. But, there was a gradual decrease in the compressive strength with increasing rate of LWA. The 28-day compressive strength of the CM was 75.8 MPa whereas that of MCF100 was as low as 43 MPa, indicating a 43% strength loss. When the concretes contained 100% LWCA or LWFA, the compressive strength loss at 28 days was about 25 and 38%, respectively compared to the control mixture. As seen Figure 4.12 a and b, although having higher fresh densities with respect to MC and MCF mixes, the lowest

compressive strength was observed on MF mixes without MCF100. For instance, the decreased percentage for the 28 days compressive strength with respect to CM were 23.7%, 31.6% and 26.3% for MC40 (SCLC produced with 40% LWCA), MF40 (SCLC produced with 40% LWFA) and MCF40 (SCLC produced with 20% LWCA and 20% LWFA) mixes, respectively. This may be attributed to the fact that the high specific surface area plays a bigger role the rate of decreasing in compressive strength as LWFA have greater surface area than LWCA. As seen from Table 3.3, crushed sand had smallest fineness modulus of 2.38 with respect to others. Therefore, the decreasing ratio of natural fine aggregate may lead the weakness of cement matrix in MF mixes due to the decreasing filler effect of LWFA. A similar trend was seen in 90 day compressive strength of the concretes (Figure 4.12 b). Indeed, when compared to CM at 90 days MC, MF, and MCF group concretes had lower compressive strengths by as much as 7 to 24%, 12 to 37%, and 11 to 31%, respectively depending on the replacement level of natural aggregates with artificial aggregates. The reason for the decrease in compressive strength was caused by some physical properties of the LWA. The lower specific gravity of used LWA in comparison with NWA, made the strength of aggregate less. Additionally, the water absorption ratio of LWCA and LWFA of 17.09% and 21.15% respectively are significantly higher than the absorption of NWA. However, the reason for reduction in compressive strength may be related to the presence of unfilled micro-voids in SCC with increase of LWA. These micro-voids might have acted as the weak zones offering a lower compressive strength for the hardened composites. In other words, this is due to the decreasing rate of NWA with roughness surface that has the larger surface area comparison with LWA that results in a lower bonding strength in the transition zone (ITZ) around aggregate particles (Duruta, 2003; Khaleel et al., 2011). Therefore, SCCs with LWA were fallen due to the weakness of LWA.

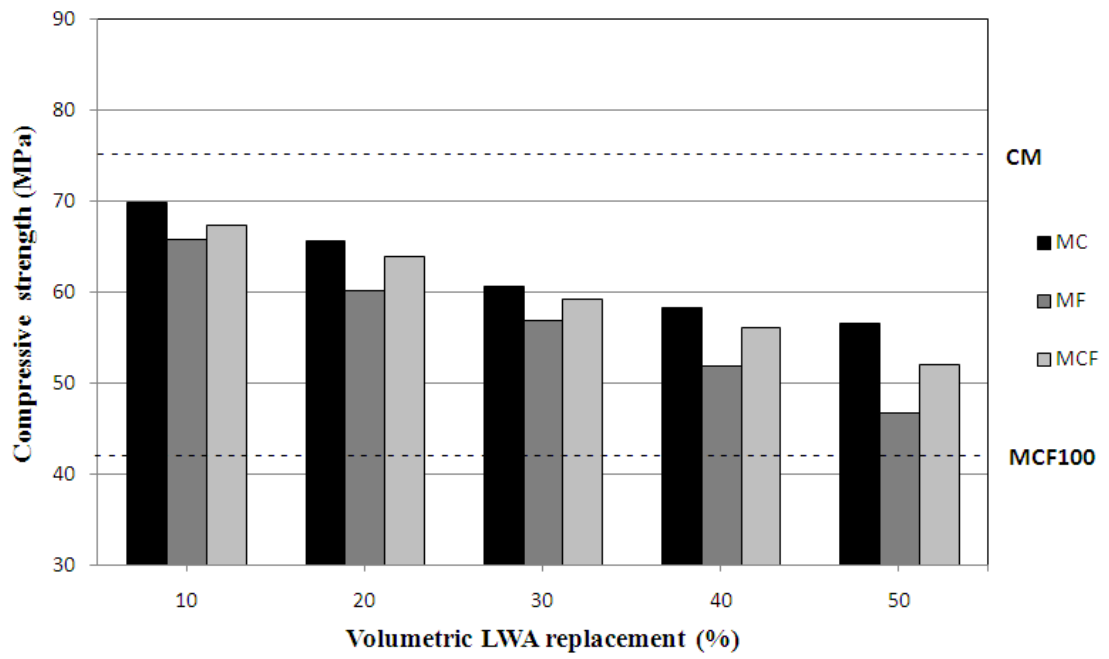
However, the effect of replacement level for LWAs on the 28 and 90 days of relative compressive strength for SCLCs is given in Figure 4.13 a and b, respectively. Relative strength is the percentage of the strength of SCLCs by the strength of the control concrete at each specified curing time. This value is calculated by division of compressive strength of each LWA replacement level incorporated SCLC by the compressive strength of the control concrete at the same age. When observing Figure 4.13 a, it was found that the highest relative strength values were ranged between

74.5%-92% in MC mixes. However, as seen Figure 4.13 b, similar to these of 28 days, the lowest relative strength changed between 62%-87% belonged to the MF mixes at 90 days. The lowest relative strength value of MF mixes is due to its lower filler effect which in turn corresponds to lower surface area than that of natural ones. However, the greatest relative difference of strength was observed between MC20-MC30, MF40-MF50 and MCF20-MCF30 at 28 days whereas the relative strength differences between MC10-MC20, MF30-MF40, and MCF10-MCF20 was the greatest value at 90 days. Moreover, from the critical observations of Figure 4.13 a and b, it was found that MC30 exhibited best performance for 90 days when compared to that of 28 days. This situation was approved by the study of Wesserman and Bentur (1996) explaining that chemical procedure related to pozzolanic activity of LWA was the reason to get the best performance at later ages. It was shown that this process was effective only in the later stages, beyond 28 days.

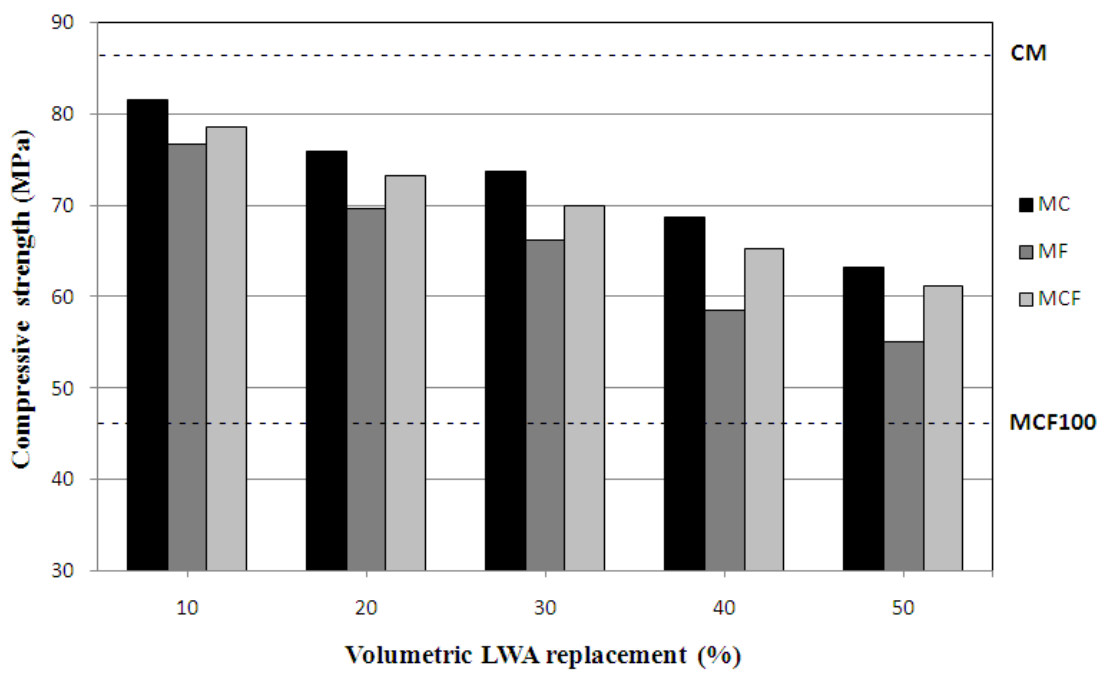
Since the compressive strength of SCCs incorporating LWA decreases in accordance with the lower density, such tendency can be assessed in terms of the structural efficiency which is the ratio of the compressive strength to the dry density of concrete at a specific age (i.e. 28 days in this study) (Choi et al., 2006; Kim et al., 2010). Table 4.4 and Figure 4.14 show the structural efficiency of SCLCs having different mix ratio of LWA. The maximum and minimum structural efficiency were attained at CM and MF50 mixes such that the difference between the latter and the former being as high as 26.6%. However, MC50 and MCF50 mixes exhibited 10.8% and 17.7% decrease in structural efficiency, respectively, compared to CM. The reason for the lowest value of structural efficiency in MF50 appears to be the greater reduction rate in compressive strength than in concrete density (Kim et al., 2010). Since density of MCF100 is about 28.4% less than that of CM, it was possible to produce SCC with LWA with higher structural efficiency (Bogas et al., 2012).

Table 4.3 Compressive strength of SCLCs

Code Number	Compressive Strength (MPa)	
	28 days	90 days
CM	75.89	87.53
MC10	69.76	81.56
MC20	65.60	75.92
MC30	60.65	73.84
MC40	58.21	68.81
MC50	56.56	63.28
MF10	65.81	76.76
MF20	60.09	69.63
MF30	56.87	66.21
MF40	51.92	58.60
MF50	46.75	55.15
MCF10	67.35	78.65
MCF20	63.92	73.33
MCF30	59.29	70.09
MCF40	56.07	65.28
MCF50	52.10	61.30
MCF100	43.00	46.69

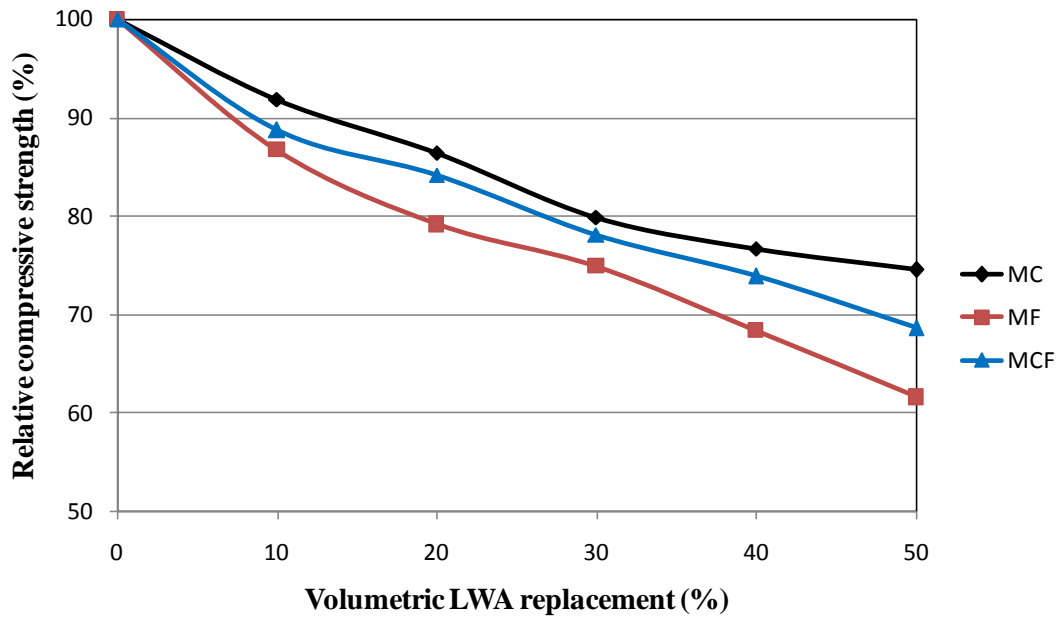


a)

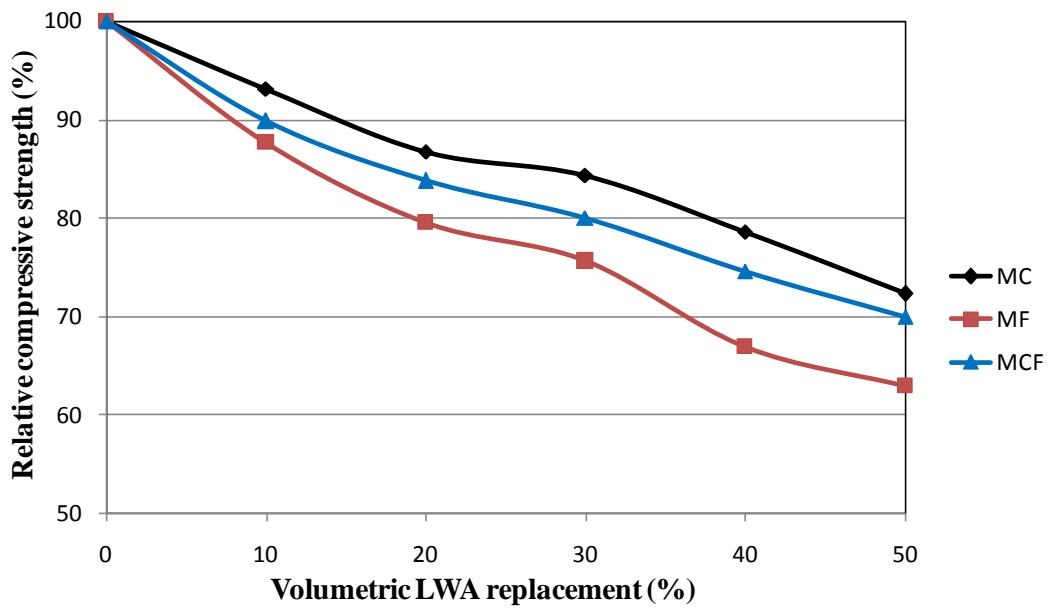


b)

Figure 4.12 Compressive strengths of SCLCs at a) 28 days and b) 90 days



a)



b)

Figure 4.13 Effect of replacement level of LWA on compressive strength of SCLCs at a) 28 days and b) 90 days (Compressive strength for control concrete is 100%)

Table 4.4 The variations of air dry density and structural efficiency for SCLCs

Code Number	Air Dry Density (kg/m ³)	Structural Efficiency (10 ⁻³ .MPa.m ³ /kg)
CM	2279.0	33.3
MC10	2154.8	26.3
MC20	2084.7	32.4
MC30	2017.2	31.5
MC40	1940.9	30.1
MC50	1905.5	30.0
MF10	2153.2	29.7
MF20	2095.3	30.6
MF30	2032.8	28.7
MF40	1971.5	28.0
MF50	1913.5	26.3
MCF10	2153.9	24.4
MCF20	2090.6	31.3
MCF30	2024.2	30.6
MCF40	1961.6	29.8
MCF50	1901.9	28.6
MCF100	1632.1	27.4

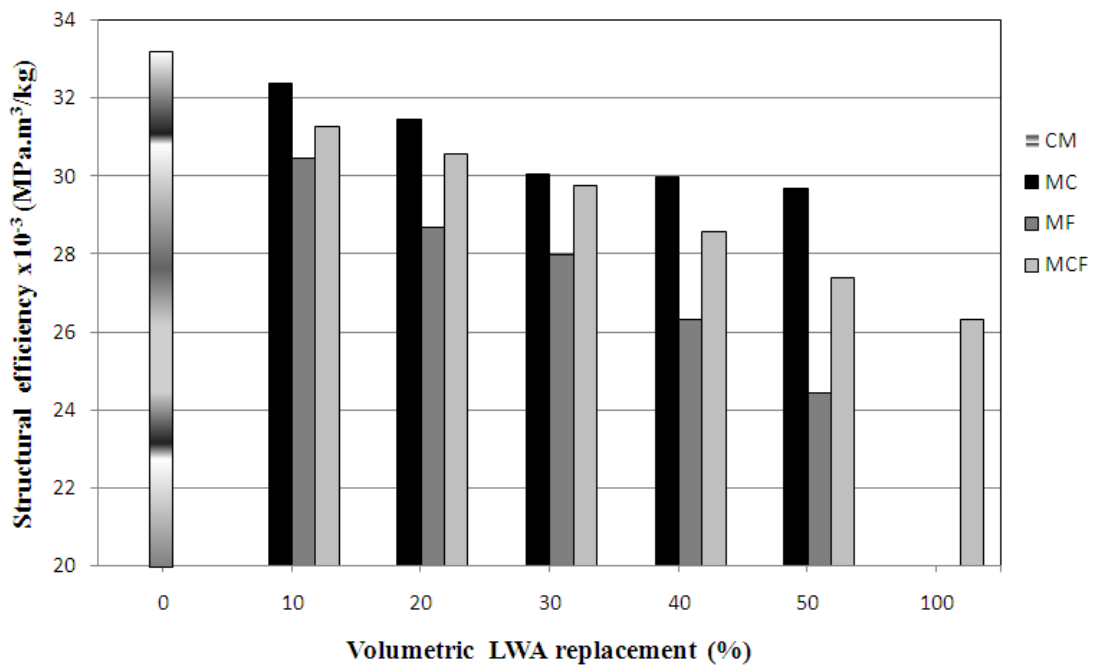


Figure 4.14 Structural efficiency of SCLCs

4.2.2 Splitting Tensile Strength

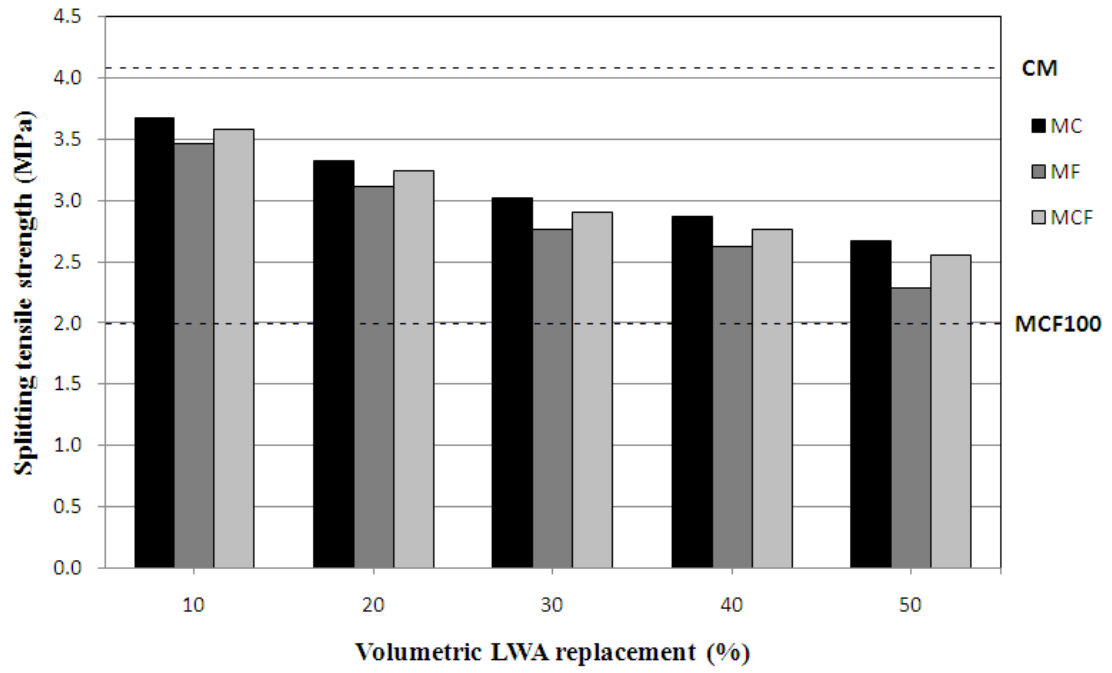
Splitting tensile strength values measured at 28 and 90 days are given in Table 4.5 and are also graphically presented in Figure 4.15. It was seen that tensile strength of the SCLCs decreased with increasing LWFA and LWCA in the mixtures. For instance, the 28-day splitting tensile strength was 4.1 MPa for CM, while this value was measured as 2.67, 2.29, 2.55 and 2.10 MPa for MC50, MF50, MCF50 and MCF100, respectively. Similarly at 90 days, the effect of using LWA was to reduce the tensile strength of the concretes. Indeed, MC40, MF40, and MCF40 mixes had lower strength values by 22.1%, 30.4%, and 25.6%, respectively in comparison to that of CM. All MC, MF and MCF mixes showed similar trends for the variation of splitting tensile strength with replacement level of LWA at both 28 and 90 days. SCC with LWA had lower splitting strength than that of CM owing to splitting tension occurring mostly through lightweight aggregates rather than cement paste since the strength of the former seemed to be lower than that of the latter (Gerrits, 1998; Choi et al., 2006). This finding agreed the Euro Light Concrete Project (2000) in that the splitting tensile strength of concretes decreased with increasing artificial aggregate content. However, it is reported in the literature that a significant reduction in tensile strength is because of the formation of the greater moisture gradients in drying attributed to the increased total water content as high water absorbent artificial aggregates used in the production of concrete (Clarke, 1993). Moreover, when considering the overall splitting tensile strength variation, it can be determined that the influence of LWFA on splitting tensile strength development of MF mixes is similar to that of compressive strength. The reduced splitting tensile strength of MF mixes among all SCLCs may be explained by the fracture path propagating throughout much more LWA grains leading to shorter fracture path. The unfilled micro-voids occurred by the weakness of LWFA lead to the initiation and propagation of tensile cracks offering a lower ultimate tensile strength for the hardened composites.

In addition, the effect of replacement level for LWAs on the 28 and 90-day of relative splitting tensile strength for SCLCs is given in Figure 4.16 a and b, respectively. Relative splitting tensile strength is calculated by the same way as the relative compressive strength values. As seen in Figure 4.16 a and b, the highest

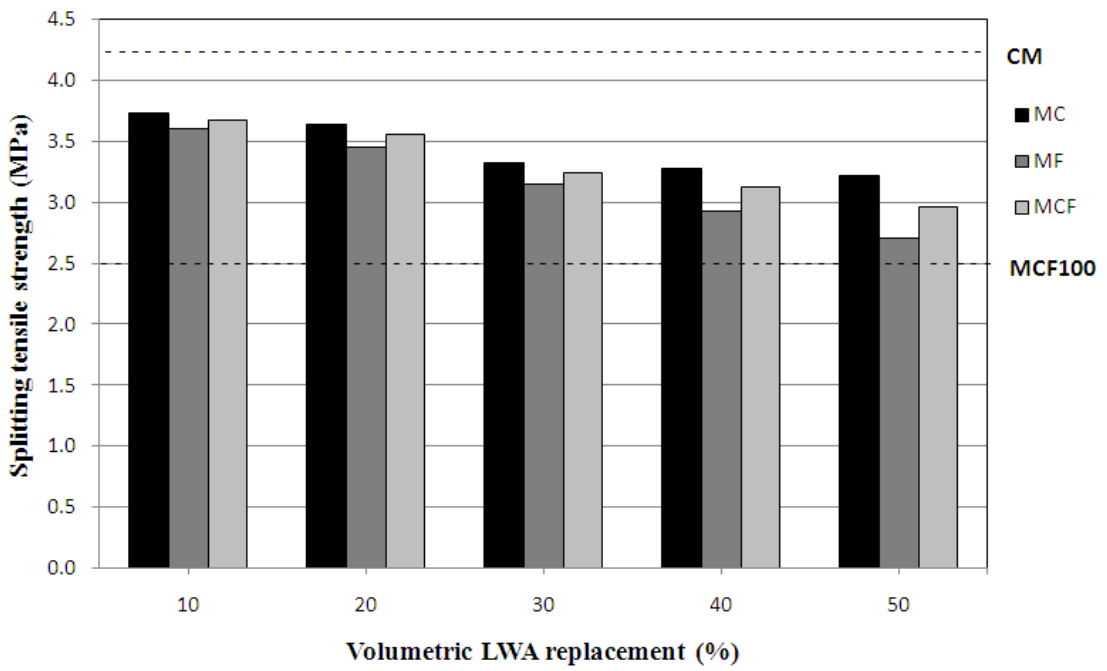
relative splitting tensile strength value was for MC10 while MF50 had the lowest one. The variations of relative compressive strength and also relative splitting tensile strength of SCLCs were very similar to each other owing to the same factors of LWA (Clarke, 1993; Mindness, 2003). However, at 90 days, MC, MF and MCF mixes for each replacement level of LWFA and/or LWCA had better performance in the term of relative splitting tensile strength than that of 28 days. Especially, MC50 mix exhibited better performance by getting the biggest difference of relative splitting tensile between 28 and 90 days. It was indicated that the adhesion of the aggregate between cement paste was improved by the pore size and surface characteristics of LWAs (Lo et al., 2007a).

Table 4.5 Splitting tensile strength of SCLCs

Code Number	Splitting Tensile Strength (MPa)	
	28 days	90 days
CM	4.14	4.21
MC10	3.67	3.73
MC20	3.32	3.64
MC30	3.02	3.33
MC40	2.87	3.28
MC50	2.67	3.22
MF10	3.47	3.61
MF20	3.12	3.46
MF30	2.76	3.15
MF40	2.63	2.93
MF50	2.29	2.71
MCF10	3.58	3.68
MCF20	3.24	3.56
MCF30	2.91	3.25
MCF40	2.76	3.13
MCF50	2.55	2.97
MCF100	2.06	2.50

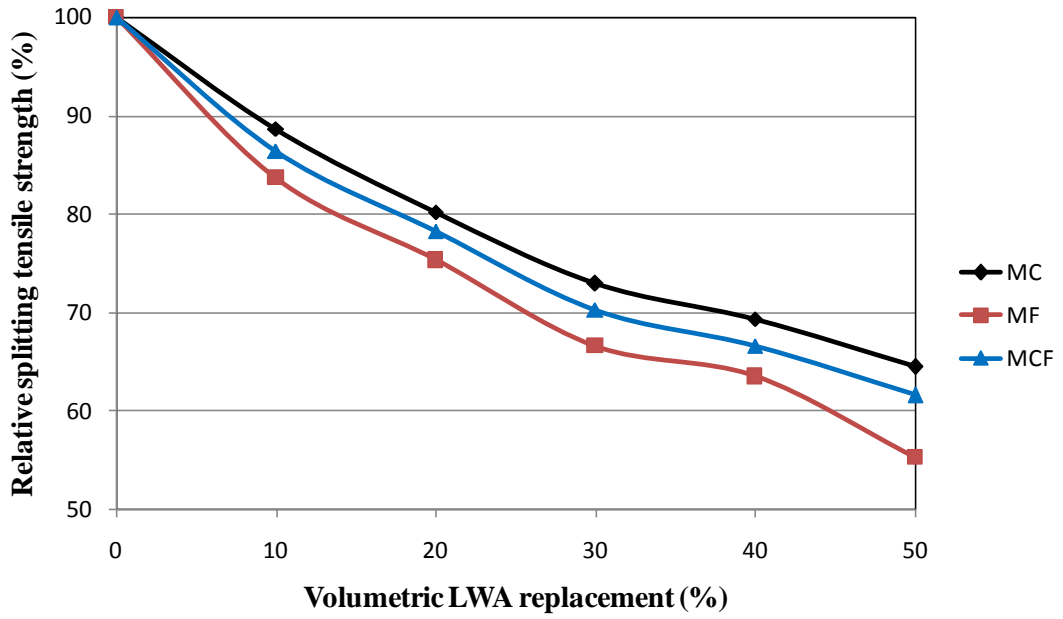


a)

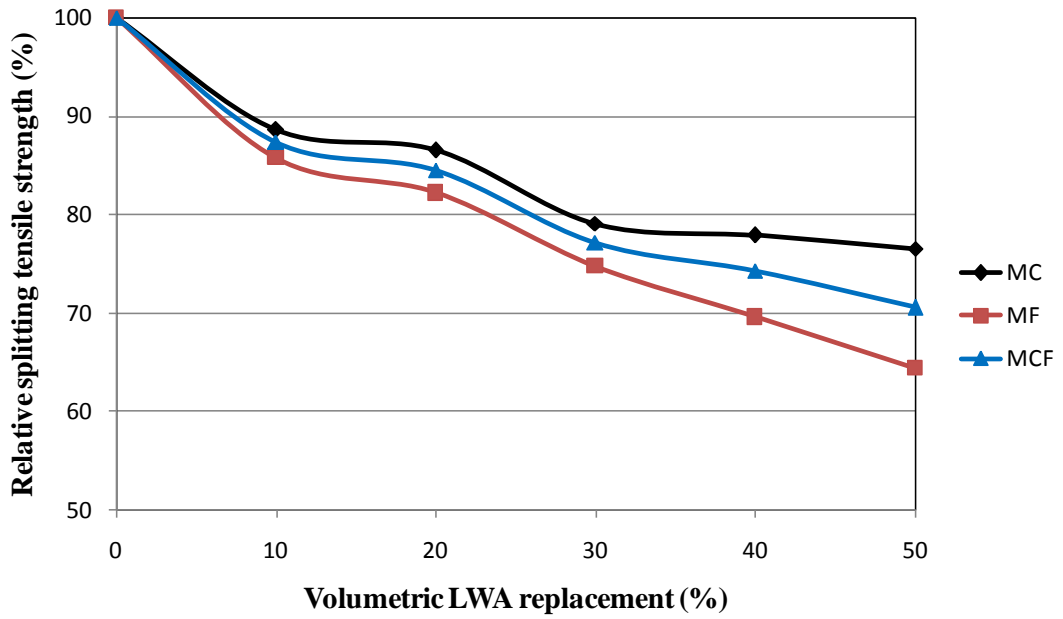


b)

Figure 4.15 Splitting tensile strength of SCLCs at a) 28 days and b) 90 days



a)



b)

Figure 4.16 Effect of replacement level of LWA on splitting tensile strength of SCLCs at a) 28 days and b) 90 days (Splitting tensile strength for control concrete is 100%)

4.2.3 Net Flexural Strength

The variation of the net flexural strength values found by Equation 3.4 with respect to the gradation size of LWA is given in Table 4.6 and graphically presented in Figure 4.17 for 90 days. The change in the relative net flexural strength values of LWA incorporated concretes was also demonstrated in Figure 4.18. The net flexural strength of CM and MCF100 were measured as 5.02 and 2.71 MPa, respectively. The volume concentration of LWA had a similar effect on the net flexural strength that observed on the compressive and splitting tensile strength tests. So, the net flexural strength decreased with increasing the lightweight aggregate content, irrespective of size of LWA due to the matrix being harder than artificial cold bonded fly ash aggregates. These findings correlate the results found by Akçay and Taşdemir (2009), İpek (2013) in that the weak lightweight aggregate behaved as defects in the matrix phase. However, this reduction was more dramatic for MF mixes. For instance, when compared to CM, increasing LWA volume fraction from 20% to 100% with 20% increment resulted in reduction of the flexural strength in the range of 10.8%-37.7%, 12.7%-46.4% and 11.9%-43.0% for MC, MF and MCF mixes, respectively. As for compressive and splitting tensile strength, decreasing natural fine aggregate content resulted in a systematic decrease in net flexural strength with respect to coarse one. Due to spherical surface of LWFA, it can cause the weaker zones at the interface between cement paste and aggregate. Moreover, as shown in Figure 4.18, the effect of size of LWA on the net flexural strength of SCLCs has been found insignificant up to 30% replacement level. This statement was approved by Akçay and Taşdemir (2009) such that the bending tensile strength was not affected significantly by the size of LWA. Nonetheless, for 100% replacement level of LWA, the highest relative net flexural strength value was obtained for MC50 while MF50 had the lowest one.

Table 4.6 Ultimate load and flexural strength of SCLCs

Code Number	P_{max} (kN)	Net Flextural Strength (MPa)
CM	3.01	5.02
MC10	2.69	4.48
MC20	2.43	4.05
MC30	2.23	3.71
MC40	2.03	3.38
MC50	1.88	3.13
MF10	2.63	4.38
MF20	2.39	3.99
MF30	2.18	3.63
MF40	1.82	3.03
MF50	1.61	2.69
MCF10	2.65	4.42
MCF20	2.42	4.03
MCF30	2.21	3.68
MCF40	1.99	3.32
MCF50	1.72	2.86
MCF100	1.63	2.71

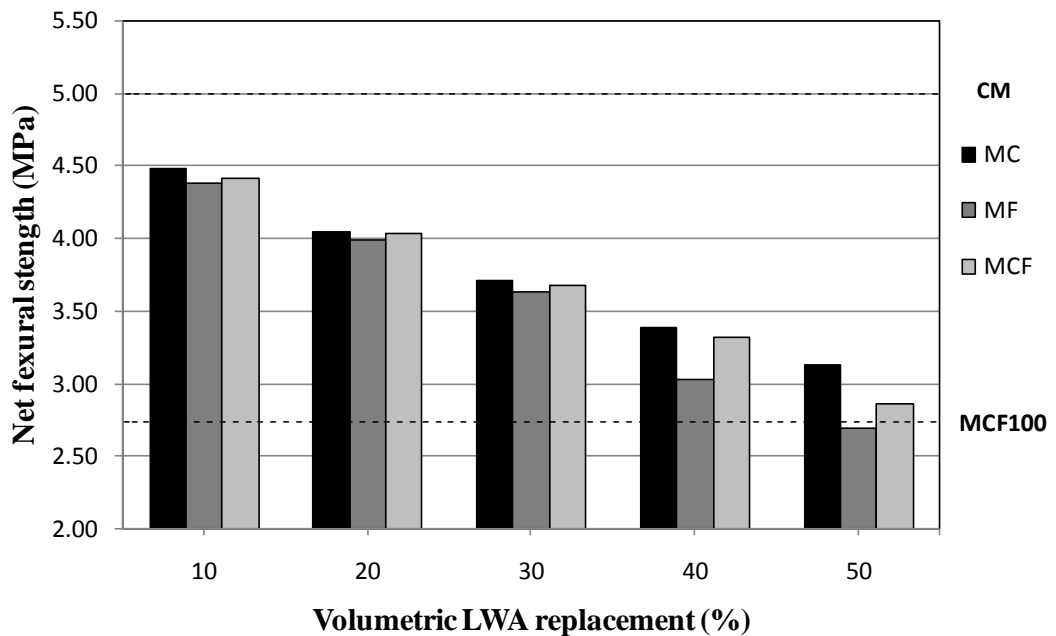


Figure 4.17 Net flexural tensile strength values for SCLCs at 90 days

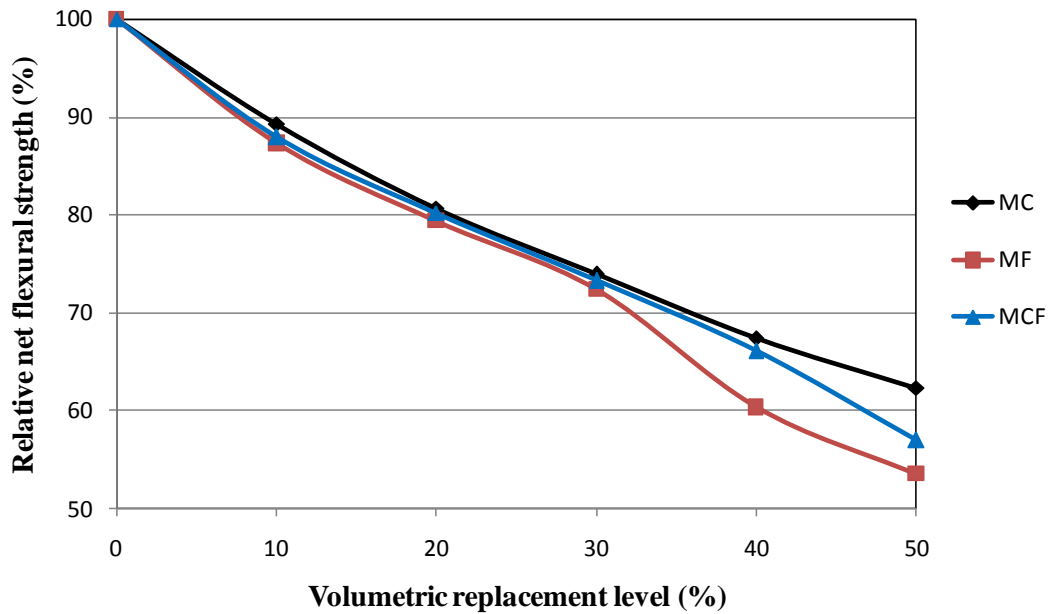


Figure 4.18 Effect of replacement level of LWA on net flexural strength of SCLCs at 90 days (Net flexural strength for control concrete is 100%)

4.3 Fracture Parameters of Self Compacting Lightweight Concretes

Qualitatively, it is easy to characterize the ductility of a material which may be determined via the post peak behavior of the stress strain curve. However, numerically, there is no uniformly accepted measure. In this part of the study, the ductility of SCLCs was evaluated in the terms of characteristic length as well as fracture energy. Since LWAs produce more microcracks, the concrete containing these aggregates can behave more ductile (i.e. less brittle) than normal cementitious materials (Akçay and Taşdemir, 2006a). On the other hand, the use of LWA instead of dense aggregate is expected to result in a lower strength. Some previous studies showed that the characteristics length from fictitious crack model was a more appropriate indication of the ductility such as the smaller the characteristics length, the more brittle is the material (Lange-Kornbak and Karihaloo, 1998; Taşdemir and Karihaloo, 2001; Gesoğlu, 2004; Akçay, 2007; İpek, 2013).

4.3.1 Fracture Energy

The calculation of fracture energy consists of two parts; energy supplied by the actuator and by the own weight of the beam. The area under the load versus displacement curve is used in the calculation of fracture energy as the energy

supplied by the actuator, and the weight of the beam is used in the calculation as the energy supplied by own weight of the beam. For SCLCs, the final displacement of the specimens is used in the calculation of energy supplied by own weight. Therefore, fracture energy (G_F) values at 90 days, evaluated with Equation 3.3 from notched beams subjected to three-point bending test, are presented in Table 4.7 and graphically shown in Figure 4.19. The variations of relative fracture energy for SCLCs are also presented in Figure 4.20. The fracture energy of CM and MCF100 were 189.01 and 8.81 N/m, respectively. It is clear from Table 4.7 and Figure 4.19 that the fracture energy decreased with LWA content due to artificial fly ash aggregates being weaker than the matrix. Similarly, the utilization of LWA in SCLCs significantly decreased the area under the load versus displacement curve as well as the ultimate load as shown in Figure 4.21-4.22 a, b and c. İpek (2013) used the cold bonded fly ash coarse aggregate in LWC and reported the same conclusion for the effect of lightweight aggregate on the fracture energy. Depending on the replacement level of LWA, the ranges of reduction were 28.7%-79.1%, 35.3%-81.8% and 35.7%-80.2% for MC, MF and MCF mixes, respectively. On the other hand, serious reductions in fracture energy were measured for MF mixes. For example, fracture energy of MC50, MF50 and MCF50 were calculated as 39.46, 34.35 and 37.45 N/m, respectively. However, in the literature, the effect of LWFA on fracture energy was contradictory. Akçay and Taşdemir (2009) showed that the 10% replacement of LWFA (2-4 mm) increased the fracture energy of concrete, while further replacement decreased. Also, they reported that concretes with LWFA (2-4 mm) had greater area under the curve that increased with respect to that of the coarser fractions (4-8 mm) for substitution of NWA with LWAs by 10, 20 and 30%. The reason that lies behind, the fine pumice aggregate only replaced in the size of 2-4 mm, while natural sand of 0-2 mm were used constantly in the rest of volume in the concrete mix. In addition the crushed fine pumice aggregate had irregular shape than LWFA produced with cold-bonding process. Similarly, the above test results (compressive strength, splitting tensile strength and net flexural energy), the decreasing natural fine aggregate content may lead to the weakness of cement matrix in MF mixes due to the decreasing filler effect of LWFA with spherical shape. However, Figure 4.20 showed that the best performance was obtained for MC10 while MF50 had the worst performance in terms of relative fracture energy. Due to negative effect of LWFA, MF and MCF had very similar trends up to 20%

replacement level. This statement proved that the negative effect of LWFA was more pronounced on fracture energy than that of coarse one.

Moreover, as observed in Figure 4.22 a, b and c, the final displacement decreased significantly with increasing the replacement level of LWA. In addition, it can be said from the figures that the displacement at the peak load generally decreased with increasing LWA content, especially in MC mixes. This is probably due to the fact that there are not enough amounts of stiffer natural aggregate around which the cracks could progress; thus the cracks can easily penetrate into the LWAs and matrix phases the displacement at peak load decreased with increasing LWA content. This statement was approved by Akçay and Taşdemir (2009) in that after 10% replacement of crushed fine pumice (2-4 mm), the final displacement of concretes at midspan began to decrease.

Table 4.7 The variations of final displacements and fracture energy of SCLCs

Code Number	Final Displacement (mm)	Fracture Energy (N /m)
CM	1.500	189.01
MC10	1.126	134.71
MC20	1.017	99.92
MC30	0.836	78.01
MC40	0.731	60.03
MC50	0.596	39.46
MF10	1.054	122.32
MF20	0.780	85.09
MF30	0.693	68.30
MF40	0.550	47.99
MF50	0.409	34.35
MCF10	1.088	121.56
MCF20	0.810	86.51
MCF30	0.713	75.67
MCF40	0.565	56.62
MCF50	0.490	37.45
MCF100	0.115	8.81

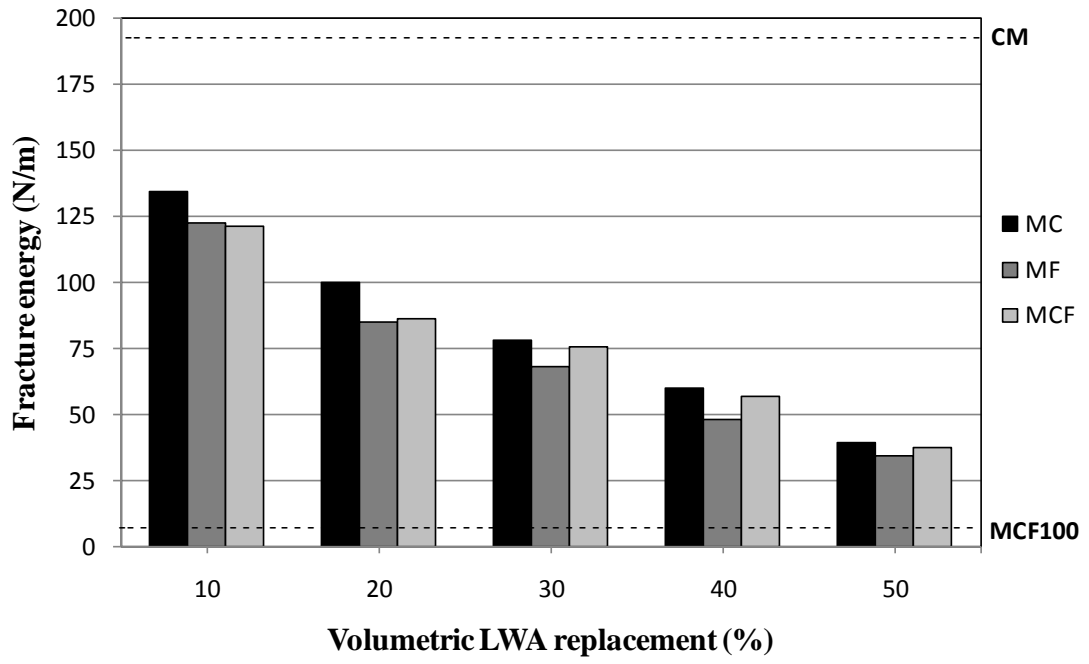


Figure 4.19 Fracture energies of SCLCs at 90 days

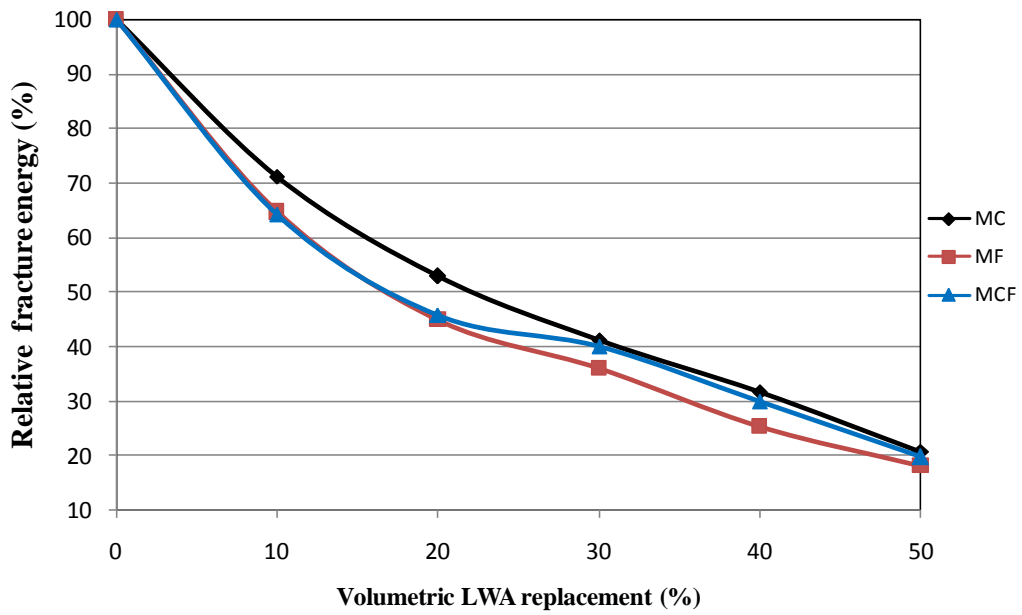


Figure 4.20 Effect of replacement level of LWA on fracture energy of SCLCs at 90 days (Fracture energy for control concrete is 100%)

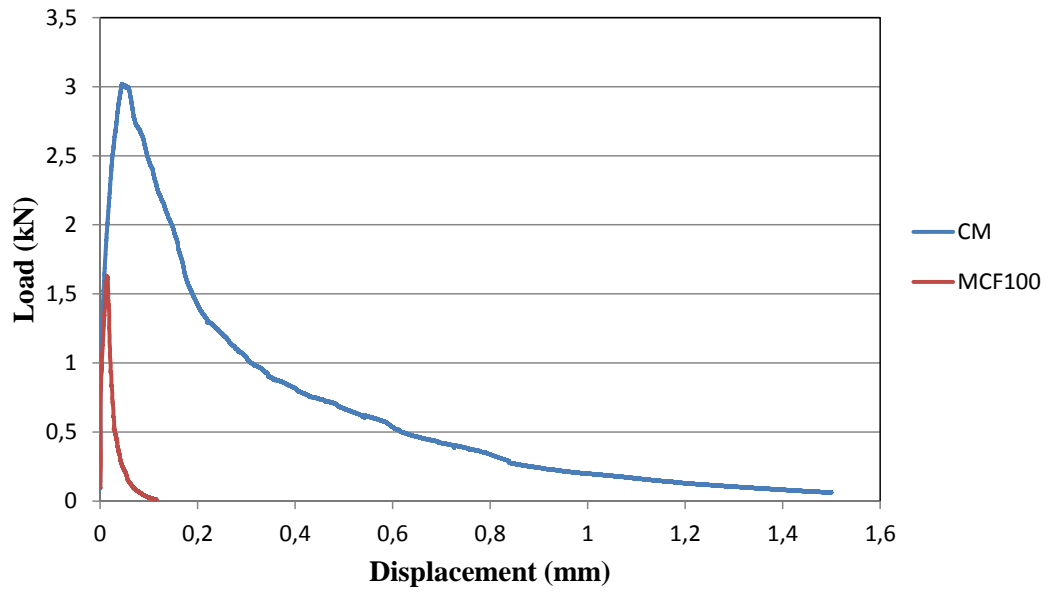
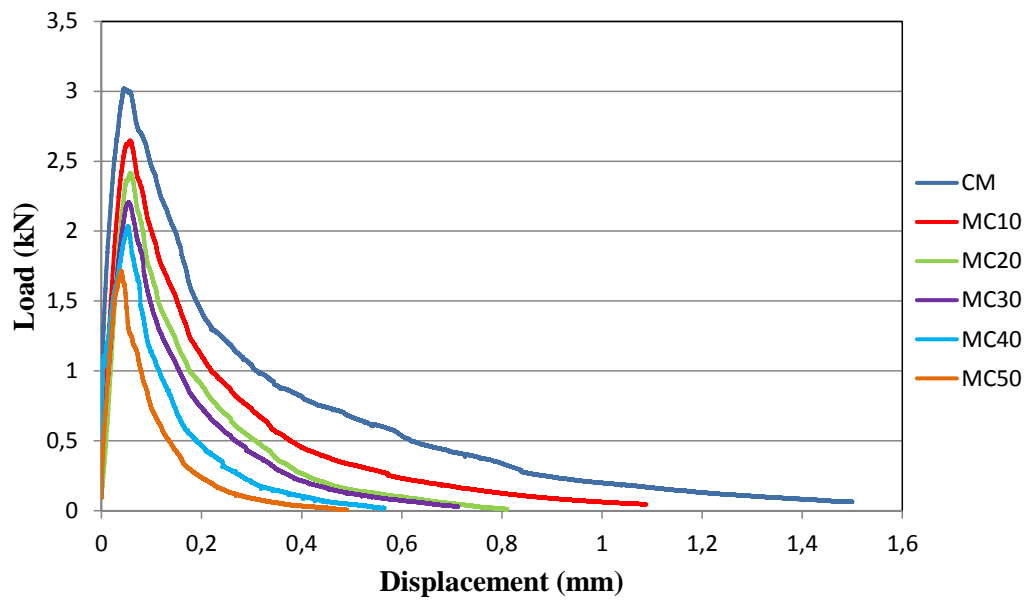
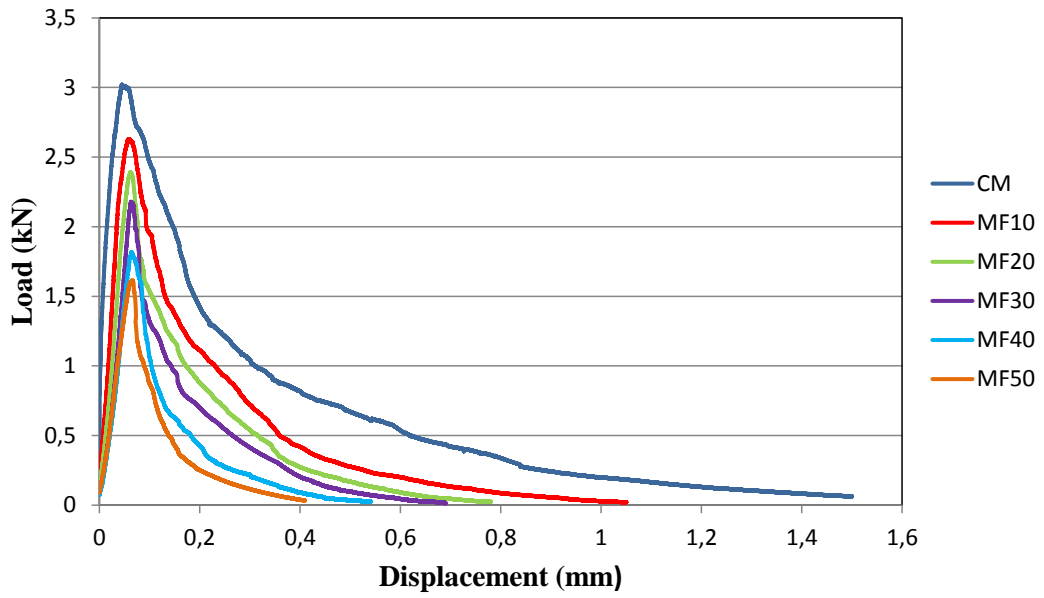


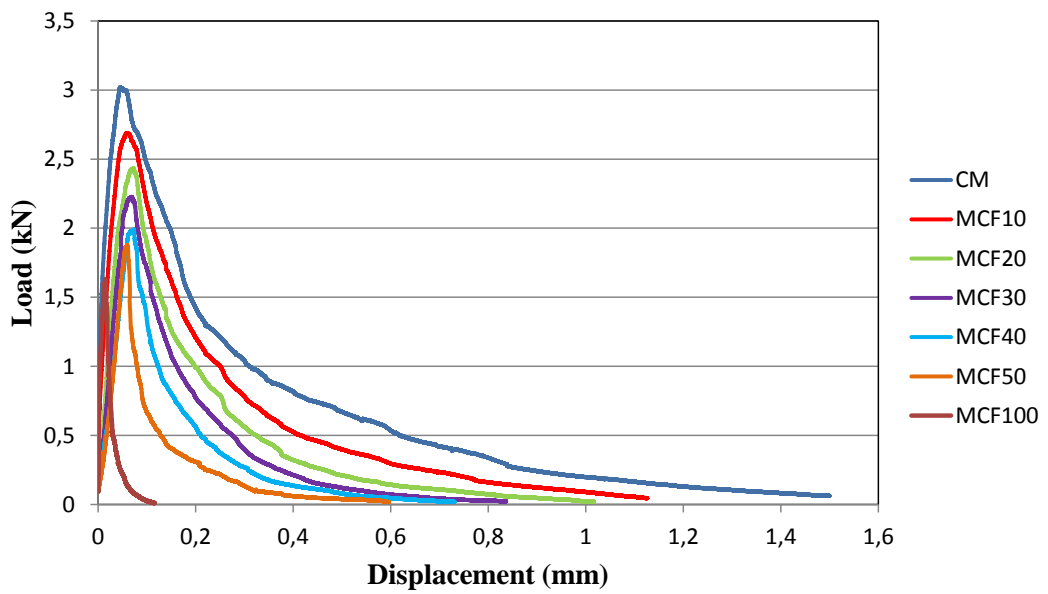
Figure 4.21 Typical load versus displacement curves of CM and MCF100



a)



b)



c)

Figure 4.22 Typical load versus displacement curves of a) MC concretes, b) MF concrete and c) MCF concretes

4.3.2 Characteristic Length

First of all, in order to determine of characteristics length as a measure of brittleness, modulus of elasticity for SCLC is required. Therefore, modulus of elasticity was determined numerically depending on the corresponding compressive strength. The broad relation between the modulus of elasticity of concrete and its compressive strength is well known but there is no unique relation because the modulus of elasticity of concrete is affected primarily by the stiffness and volume content of aggregate as well as the aggregate-paste interface. For this, Equation 4.1 proposed by ACI 318 (1995) was applied to the 28 and 90 day compressive strengths obtained in this study.

$$E = 4.15q^{1.5}\sqrt{f_c} \quad (4.1)$$

Where, E modulus of elasticity (MPa), q is the air dried density of concrete (kg/m^3), f_c is the cylinder compressive strength measured on 150x300 specimens (MPa).

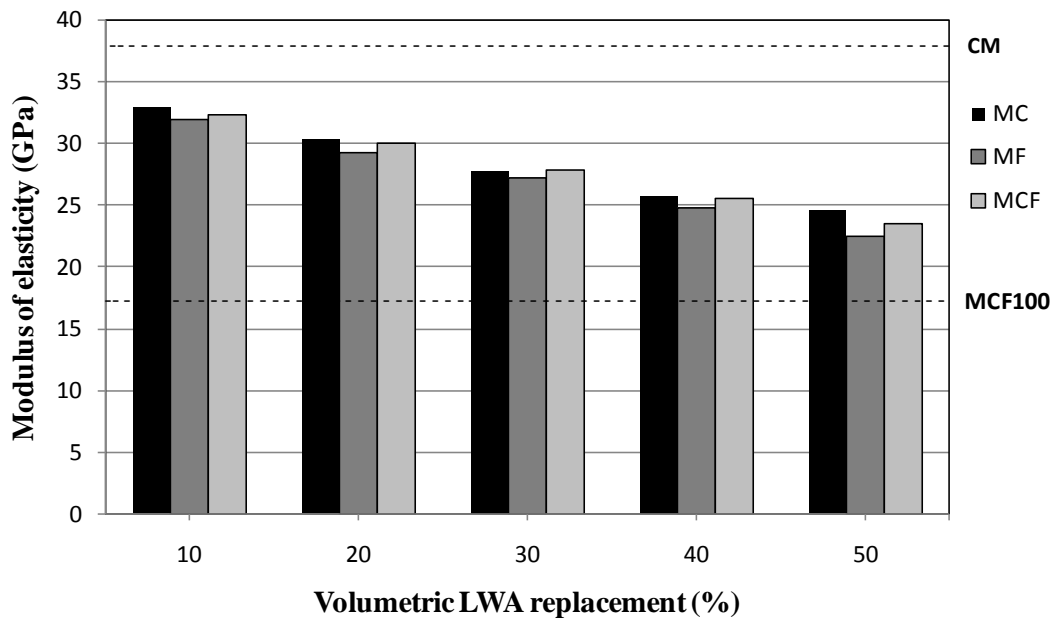
In order to apply this equation on the test results, the 150 mm cube compressive strength was converted to the 150x300 mm cylinder specimens by a shape and size factor of 0.9 (Zhang and Gjorv, 1991c). The calculated modulus of elasticity of SCLCs is presented in Table 4.8 and shown in Figures 4.23 a and b for 28 and 90 days, respectively. As in the case of compressive strength, the static elastic modulus was the highest for MC which was followed by those with MCF and MF concretes. As observed in Figure 4.23 a and b, the aggregate strength is the primary factor affecting the modulus of elasticity of SCLCs (Gesoglu et al, 2004). Considering the control mixture, replacing 20% of natural aggregate with LWA resulted in a decrease in the modulus of elasticity as low 18.6%, 21.4%, and 19.4% at 28 days, and 18.5%, 21.4%, and 19.6% at 90 days for MC, MF and MCF concretes, respectively. Although the change in the size of LWA had no significant effect on the modulus of elasticity of SCLCs as expected, a slight decrease in the modulus of elasticity (E) was recorded with increasing the replacement volume of the LWAs (Taşdemir et al., 2002).

Thereafter, the variation in characteristic lengths for SCLCs is shown in Table 4.8 and graphically depicted in Figure 4.24 depending on 90-day modulus of elasticity of SCLCs. The change in the relative characteristic values of concrete incorporated LWA is also presented in Figure 4.25. The characteristic length of CM (427.3 mm) was found to be higher than those of SCLC with LWAs while MCF100 (25 mm) had the lowest one. As seen in Figure 4.24, the characteristic lengths of MC50, MF50 and MCF50 were 99.1, 114.5 and 108.5 mm, respectively, indicating that the material became more brittle with the use of LWA. Although increasing the amount of LWFA and/or LWCA caused a decrease in compressive strength, it does not make the concrete more ductile because LWA being weaker than matrix. Similar to test results of fracture energy of MF and MCF mixes, MF and MCF mixes had similar trend up to 30% replacement level as seen in Figure 4.25. However, MC10 had the best performance in the terms of characteristics length while the worst performance was obtained for MF50. This means that LWFA decreased the characteristics length more than LWCA.

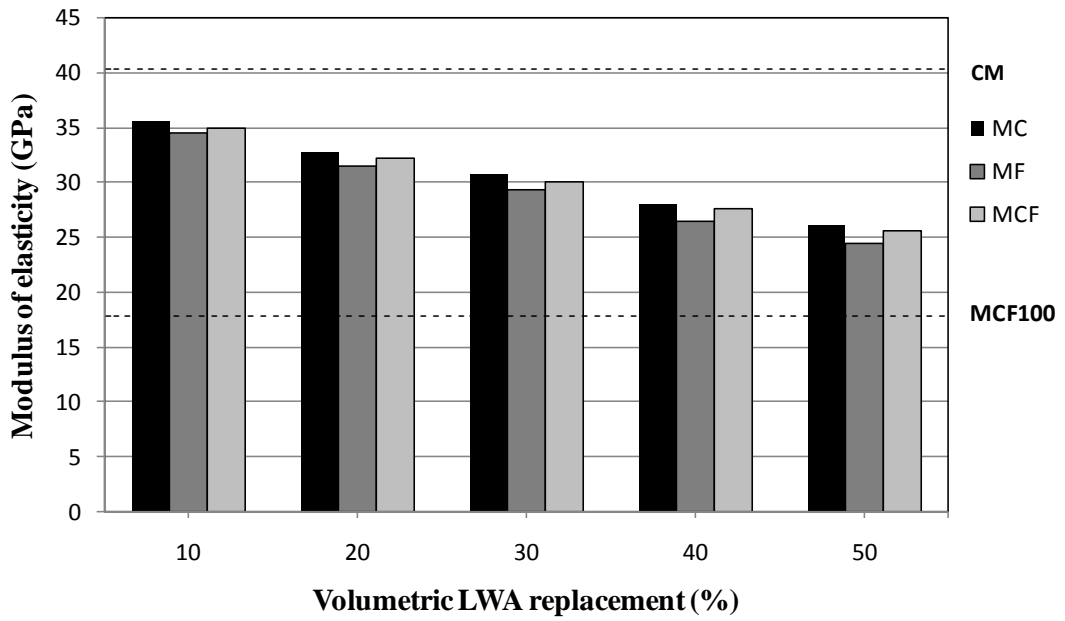
The natural sand replacement with LWFA adversely affected the ductility of MF and MCF mixes owing to the larger decrease in the tensile strength than the failure load of the beam specimens. As a result of this, MF mixes had only a modest increase for characteristic length than that of MCF mixes. However, the characteristic length of MC mixes seemed to be higher for all replacement level compared to MF and MCF mixes. Since the bond between the layers of the aggregate particle weakens as the particle gets larger during the pelletization, the crack followed a path through the weakest layer of aggregate rather than the relatively stronger interface between the aggregate and surrounding cement paste. Therefore, a more tortuous crack path was achieved, thus giving more ductile concrete with respect to MF and MCF mixes. This type of behavior was also observed in normal weight concrete. Zhou et al. (1995) and Taşdemir et al. (1996) stated that the larger particle size yielded higher characteristic length for a given type of aggregate.

Table 4.8 Modulus of elasticity and characteristic length of SCLCs

Code Number	Modulus of Elasticity (GPa)		Characteristics Length (mm)
	28 days	90 days	
CM	37.3	40.1	427.3
MC10	32.9	35.6	344.3
MC20	30.4	32.7	246.1
MC30	27.8	30.6	215.6
MC40	25.7	27.9	155.8
MC50	24.6	26.1	99.1
MF10	31.9	34.5	323.5
MF20	29.3	31.5	224.0
MF30	27.2	29.4	202.1
MF40	24.8	26.4	147.5
MF50	22.5	24.5	114.5
MCF10	32.3	34.9	313.3
MCF20	30.1	32.2	220.0
MCF30	27.8	30.0	215.0
MCF40	25.6	27.6	159.7
MCF50	23.6	25.6	108.5
MCF100	17.0	17.7	25.0



a)



b)

Figure 4.23 Modulus of elasticity of SCLCs at a) 28 days and b) 90 days

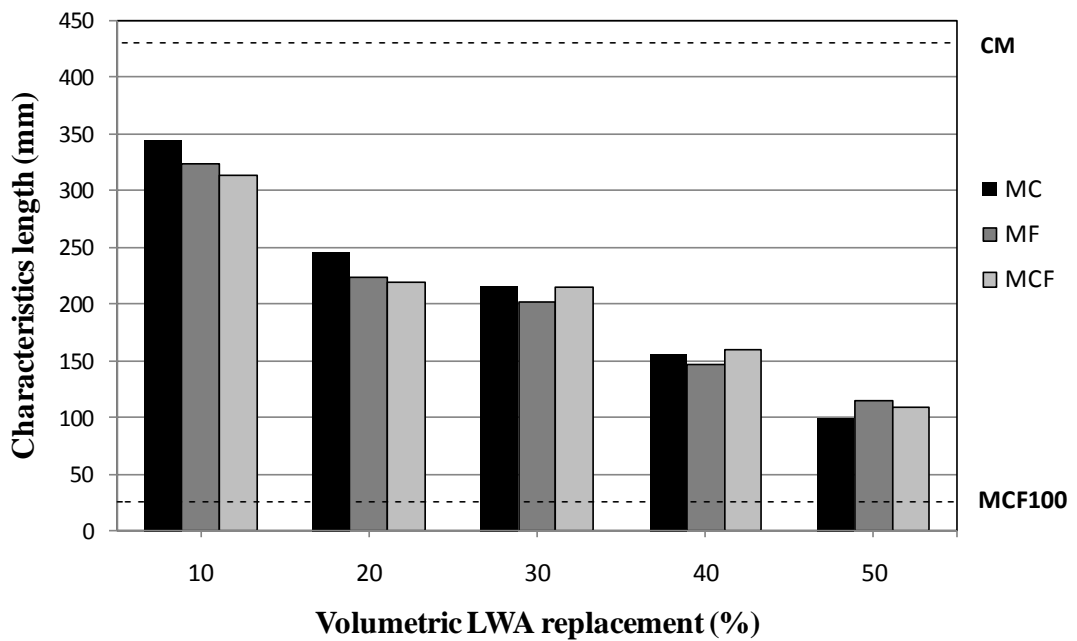


Figure 4.24 Characteristic lengths of SCLCs

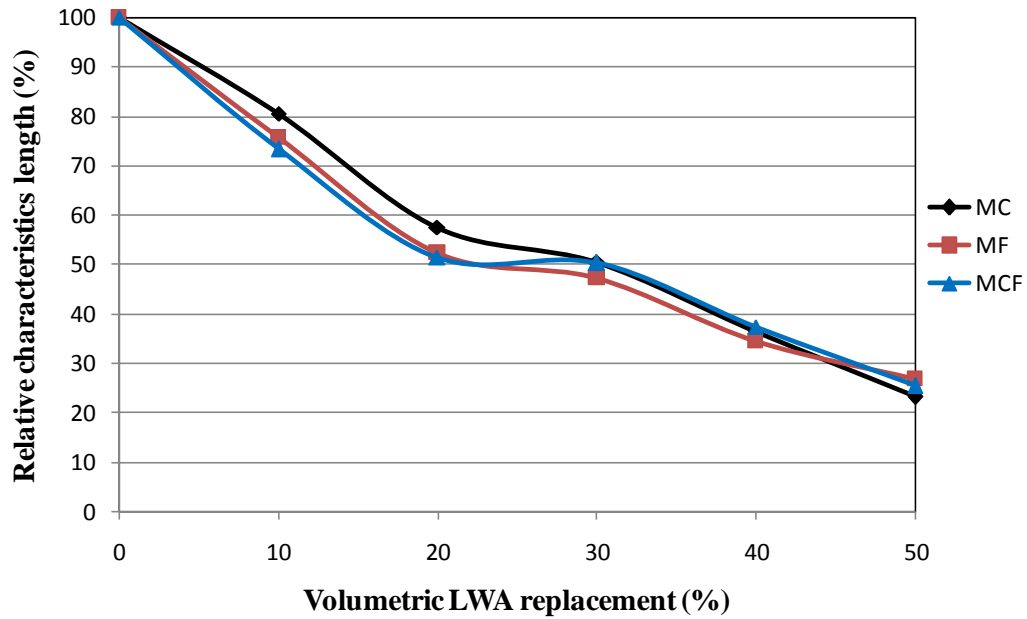


Figure 4.25 Effect of replacement level of LWA on characteristic lengths of SCLCs at 90 days (Characteristics length for control concrete is 100%)

4.4 Physical Properties of Self Compacting Lightweight Concretes

4.4.1 Drying Shrinkage and Weight Loss

Drying shrinkage tests can ensure the knowledge on how the drying shrinkage stresses develop although all concrete structures are restrained in some way, internally by reinforcement bars, aggregate and externally by foundation, adjacent structural members (Wiegrink, 1996). The highest values of the shrinkage strain for SCLCs at the end of the 60 days drying period is given in Table 4.9. Also typical drying shrinkage versus time curves for SCLC incorporating with LWFA and/or LWCA are depicted in Figures 4.26 a, b and c for MC, MF and MCF concretes, respectively. According to the curves of MC, MCF and MF, drying shrinkage of concretes containing cold-bonded LWFA and/or LWCA decreased in this order, but all of the concretes showed higher shrinkage than the control mixture (CM). Similar test results were observed by other researches such that high absorption as well as the lower modulus of elasticity of LWA was accompanied with higher shrinkage strain in concrete as verified from the increase in drying shrinkage with increasing volume of LWA in SCLC (Neville and Brooks 1987; Kayali 1999; Gesoğlu et al., 2004; Zhang et al., 2005). In addition, SCLC containing LWA was prone to have higher

shrinkage strain due to its lower tensile strength with respect to CM. Furthermore, the study of Hwang and Khayat (2008) showed that SCCs can develop higher shrinkage in comparison with NWC due to its greater volume of cement paste and relatively low coarse aggregate content.

It can be shown in Figure 4.26 a, b and c that drying shrinkage strains of MC, MF and MCF mixes were comparable at the early age of drying period. The major part of the increment of total shrinkage occurred approximately in the first three week. The lowest shrinkage strains of 402 microstrain at 60 days was measured for CM while SCC including 100% LWFA and LWCA (MCF100) had the highest shrinkage value as found to be 675 microstrain. This is also approved by the results of Kayali et al. (1999) and Zhang et al. (2005) who observed that LWC exhibited higher shrinkage than that of NWC. Al-Khaiyat and Hague (1998) showed that LWC including Lytag aggregate exhibited moderately higher drying shrinkage as 640 microstrain at three months of drying. Gesoğlu et al. (2004) reported that LWC with cold-bonded fly ash coarse aggregate had higher shrinkage for all w/b ratio, but this impression was more indicative for high w/b ratio. It was found that the maximum increase in shrinkage strain observed in MC mixes ranged between 9.5%-50.5% whereas the 60 days drying shrinkage of MF mixes increased by about 6.5%-39.5% with respect to CM. However, the usage both LWCA and LWFA made MCF mixes have increased shrinkage strain of by about 8.2%-43.5% compared to CM. Owing to the larger specific surface of LWFA with respect to LWCA, MF mixes had lower shrinkage strains than both MC and MCF mixes. For example, at a constant LWA replacement ratio of 30%, shrinkage strain were found to be 525, 498, and 506 microstrain for MC30, MF30 and MCF30, respectively indicating the lower shrinkage of LWFA.

The weight loss graphs of MC, MF and MCF are illustrated in Figures 4.27 a, b and c, respectively. It was observed that the total weight loss increased with increasing LWA content in SCLC regardless the size of LWA. As a result, the increased weight loss led to a higher total drying shrinkage of SCLC. During 60 days of drying period, clear difference of weight loss for SCLC including LWA was more distinctive after approximately one week. However, for the same replacement level of LWA, higher amount of LWFA induced to the greatest weight loss of MF mixes compared to CM inasmuch as LWAs used in SSD condition leading to increased unit water content

despite the fact that the corresponding shrinkage strains being smaller than those of MC and MCF mixes. This may be attributed to the fact that drying shrinkage is related to other factors in addition to weight loss (Wiegrink et al., 1996; Gesoğlu et al., 2004). Therefore, the weight loss alone cannot provide sufficient information on the variation in the drying shrinkage of concretes.

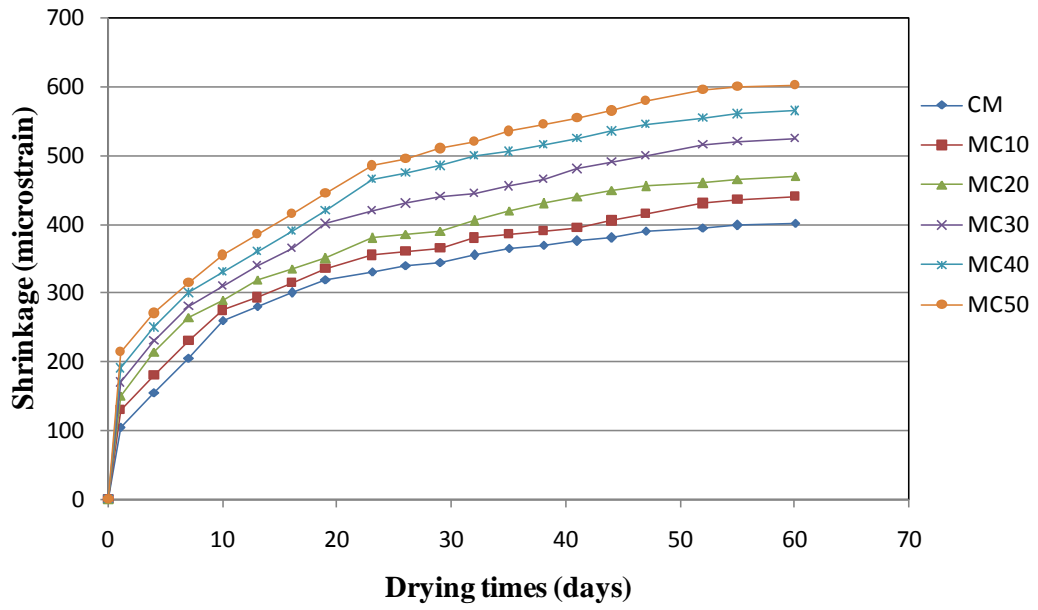
4.4.2 Restrained Shrinkage

Shrinkage cracking age and maximum crack width of MC, MF and MCF mixes are given in Table 4.9, and the crack developments of restrained shrinkage specimens within time are shown in Figure 4.28 a, b and c. Although LWAs in SSD condition provided water into the drying matrix at the very early ages, and thus extended the cracking time by reducing the autogenous shrinkage, higher unit water content resulted in higher shrinkage values at later ages (Gesoğlu et al., 2004). SCLC including low LWA volume fractions cracked at earlier, however, as the replacement level of LWA increased; the time of cracking greatly extended irrespective of size of LWA. The initial cracking was first seen at 12 days for CM, however, the initiation of cracking for MCF100 (SCC with 100% LWFA and LWCA) was prolonged to 17 days. Furthermore, for a given similar LWA volume replacement used (i.e. 30%), the time of cracking was delayed to 15, 16 and 16 days for MC30, MF30 and MCF30 respectively. This finding was approved by Gesoğlu et al. (2004) in that LWA produced with cold bonding process extended the cracking time by reducing autogenous shrinkage. Though the cracking time was extended, the crack opening for SCLC including LWA was faster in the first day, due to the weakness of LWA. The lowest crack propagation was observed for CM irrespective of drying time, while the maximum crack widths at the end of 60 days were found to be 2.2 mm for MCF100. On the other hand, considering the overall drying period, SCLC with LWA displayed higher crack propagation with respect to CM. Nevertheless, MF mixes exhibited more reduction in crack width at the end of drying period than that of MC and MCF mixes. The effect of LWFAs on the reduction of autogenous shrinkage and restraining stresses in MF mixes is a clear demonstration in their internal curing efficiency much more than that of LWCA. The results of current study agreed with the findings of study performed by Dale et al. (2010). They concluded that LWAs with a fineness modulus smaller than 3.2 would protect much more than 90% of the

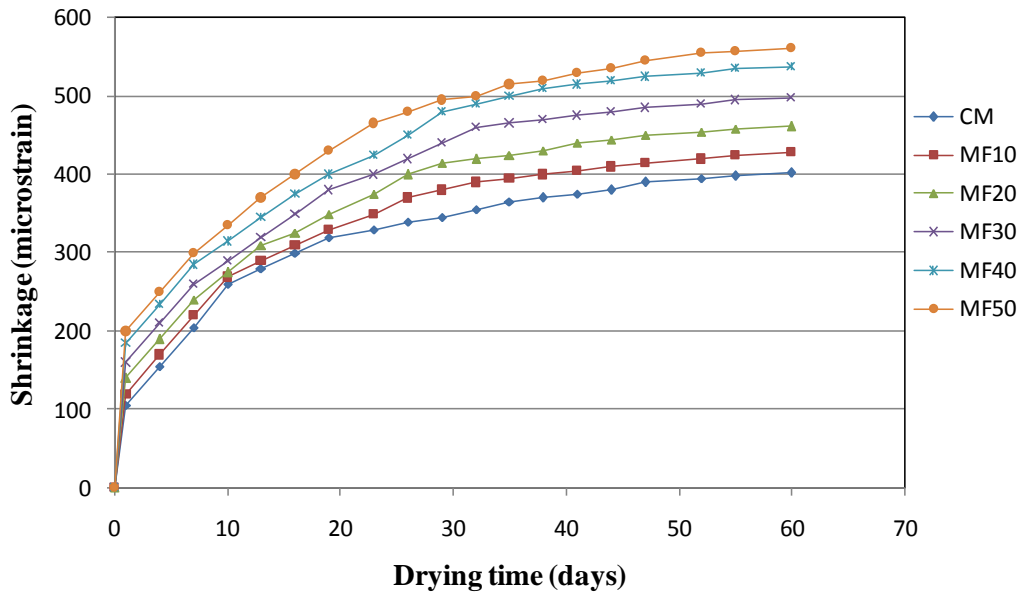
cement paste against the self-desiccation. Thus, the usage of LWFA in MF mixture showed the beneficial effect of extending cracking time and reducing the crack width with respect to MC and MCF mixes (Wiegrink et al., 1996; Henkensiefken et al., 2009; Dale et al., 2010; Goliasa et al., 2012).

Table 4.9 Drying and restrained shrinkage performance of SCLCs

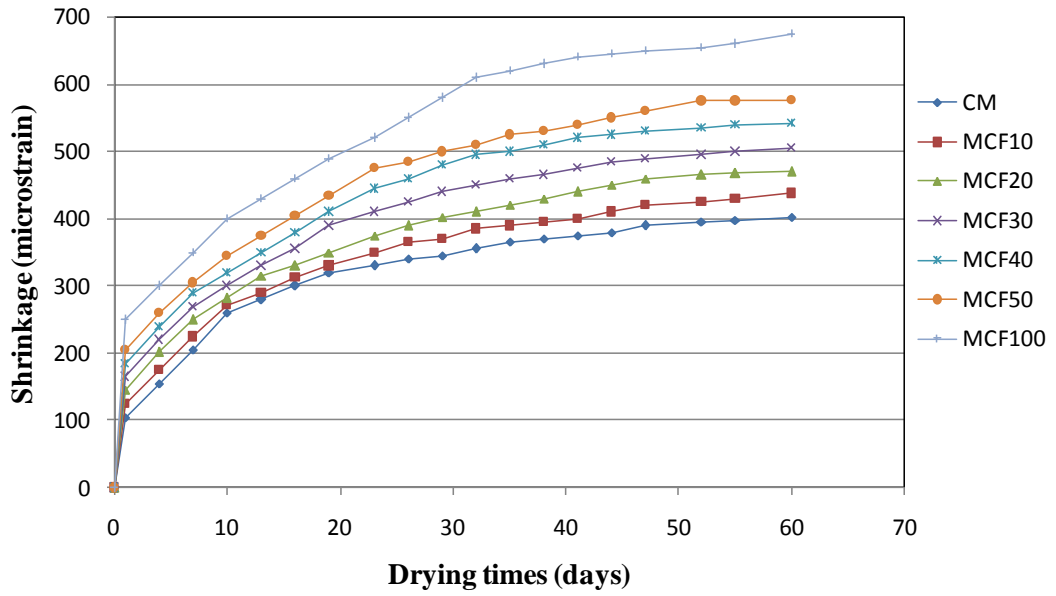
Code Number	Maximum free shrinkage (microstrain)	Maximum weight loss (g)	Average cracking age (days)	Maximum crack width (mm)
CM	402	73.3	12	0.62
MC10	440	85.7	13	0.83
MC20	475	97.2	14	0.97
MC30	525	115.8	15	1.15
MC40	565	137.8	16	1.44
MC50	605	167.5	16	1.61
MF10	428	91.4	14	0.79
MF20	461	101.5	15	0.88
MF30	498	127.3	16	1.03
MF40	508	153.3	16	1.18
MF50	561	187.3	17	1.40
MCF10	438	88.1	14	0.80
MCF20	470	101.6	15	0.92
MCF30	506	120.1	16	1.06
MCF40	542	148.7	17	1.26
MCF50	577	175.2	17	1.51
MCF100	675	240.9	18	2.20



a)

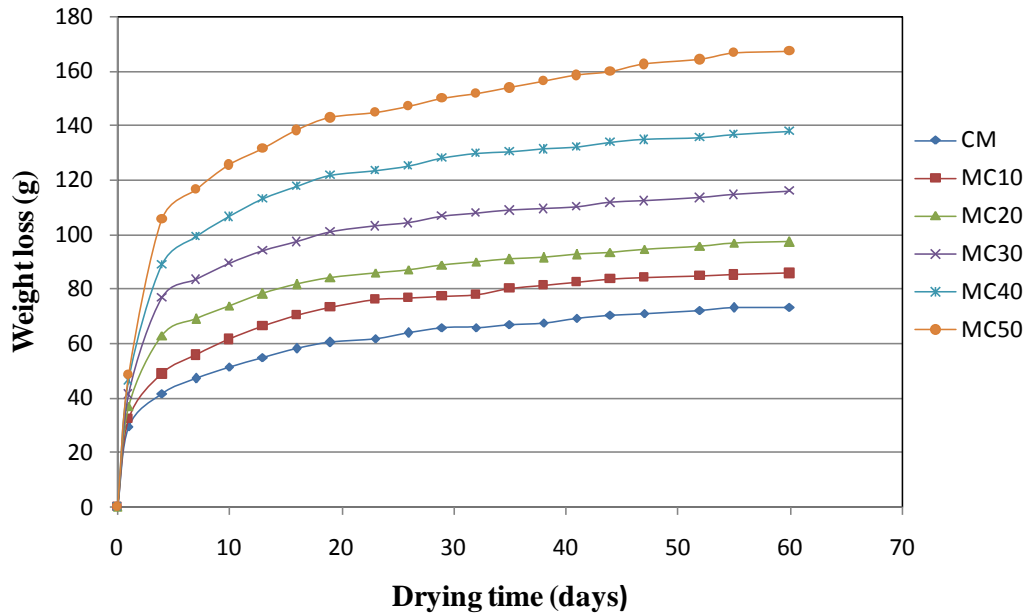


b)

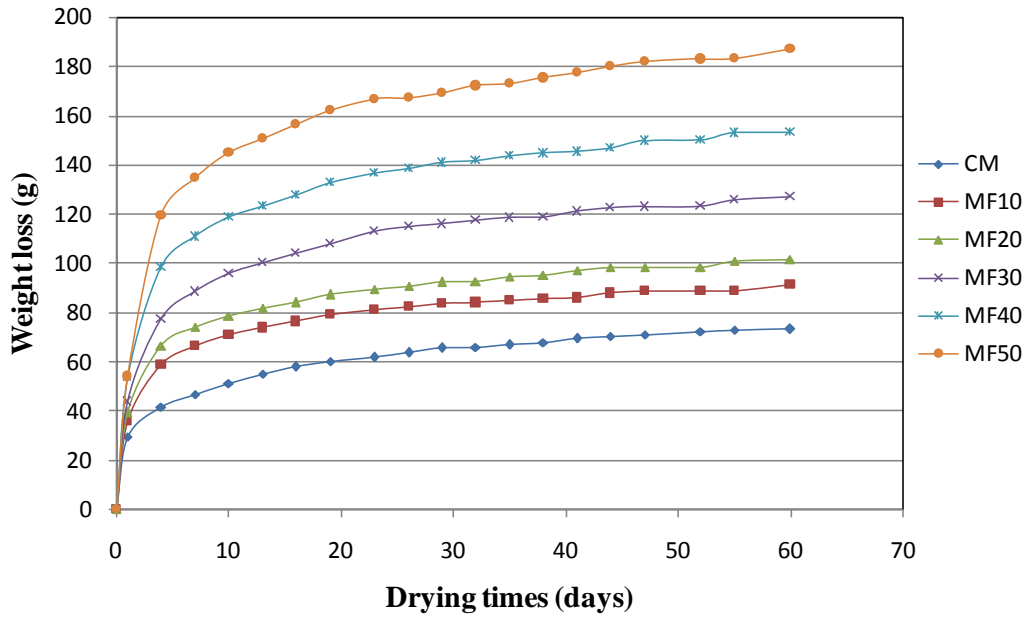


c)

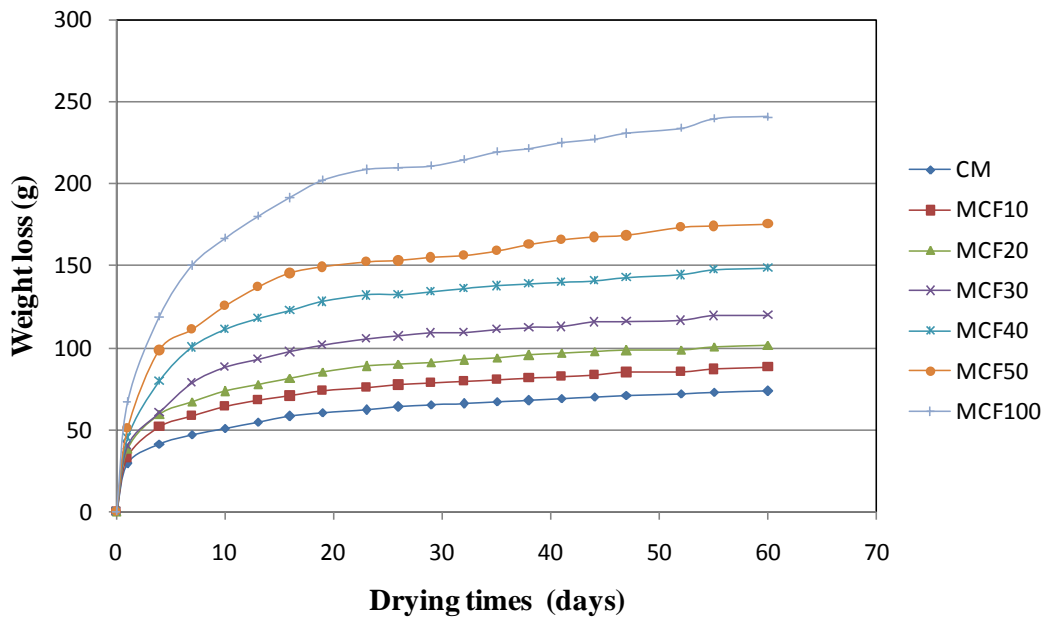
Figure 4.26 Drying shrinkage strain development of a) MC concretes, b) MF concretes and c) MCF concretes



a)

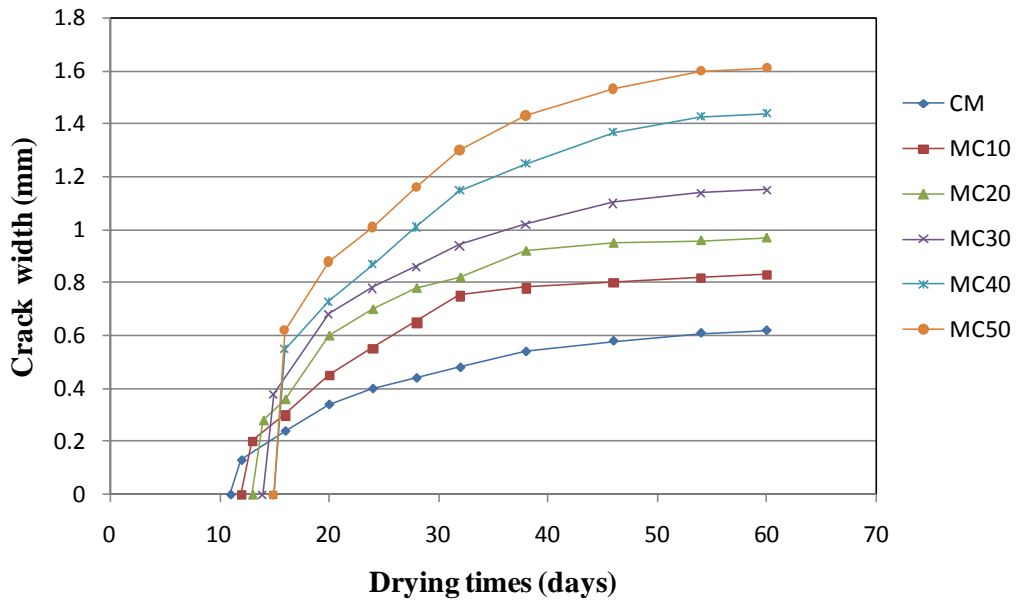


b)

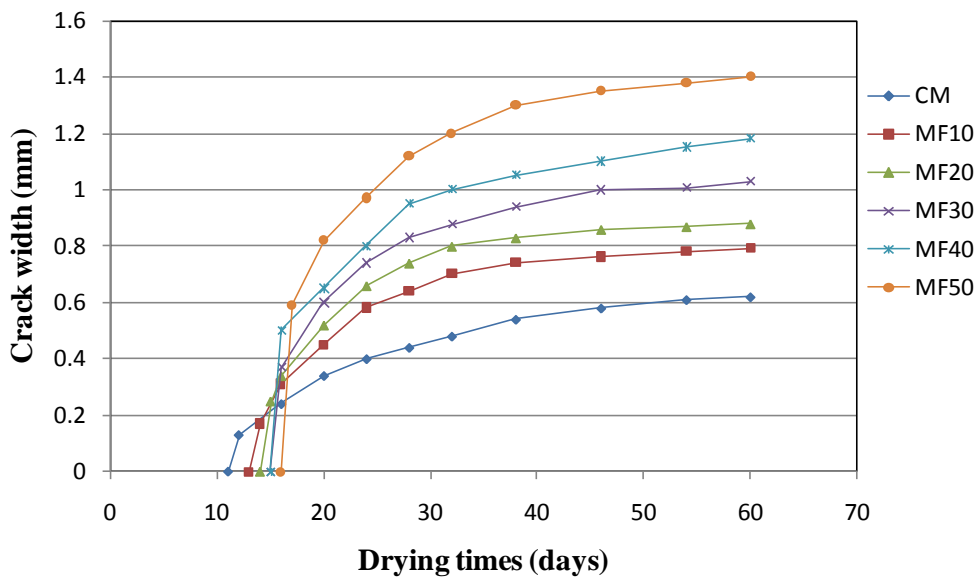


c)

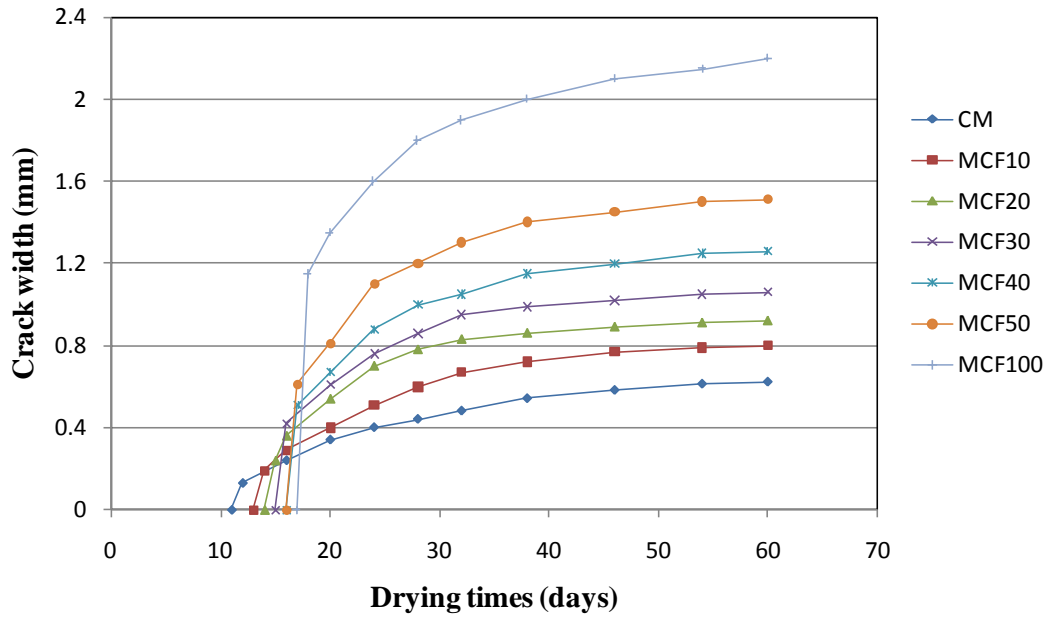
Figure 4.27 Variations in weight loss of a) MC concretes, b) MF concretes and c) MCF concretes



a)



b)



c)

Figure 4.28 Shrinkage cracking performance of a) MC concretes, b) MF concretes and c) MCF concretes

4.5 Durability Properties of Self Compacting Lightweight Concretes

4.5.1 Water Sorptivity

The water sorptivity test is based on the water flow into concrete by capillary action. Therefore, this test of a concrete surface depends on many factors depending on concrete mix design, such as concrete mixture proportions, presence of chemical admixtures, supplementary cementitious materials, and physical characteristics of the cementitious components of the aggregates. The relation used for calculation of sorptivity is given in Equation 4.2.

$$I = S'\sqrt{t} \quad (4.2)$$

Where S' is sorptivity ($\text{mm}/\text{min}^{1/2}$) and I is cumulative infiltration (mm) at time t (min).

The variations of the water sorptivity coefficient at 28 and 90 days according to the replacement level of LWCA and LWFA are demonstrated in Table 4.10 and Figure 4.29. However, the variation of the relative sorptivity coefficient values for SCLCs

with respect to CM at 28 and 90 days are shown in Figures 4.30 a and b, respectively. SCLC incorporating with LWA revealed a systematic increase in water sorptivity coefficients with increasing replacement level of LWA at both ages. The sorptivity coefficients of $0.070 \text{ mm/min}^{0.5}$ and $0.027 \text{ mm/min}^{0.5}$ of the control mixture (CM) at 28 and 90 days respectively increased to $0.195 \text{ mm/min}^{0.5}$ and $0.095 \text{ mm/min}^{0.5}$ when all the natural aggregates were replaced with lightweight aggregates (MCF100) at 28 and 90 days, respectively. As seen in Figure 4.29 b, sorptivity coefficients measured at 90 days displayed a reduction as compared with those of the 28 days. When LWFA and/or LWCA replaced 40% of the NWA in SCLCs, the 90 days sorptivity coefficients was 0.057 , 0.051 and $0.052 \text{ mm/min}^{0.5}$ for MC40, MF40 and MCF40 respectively.

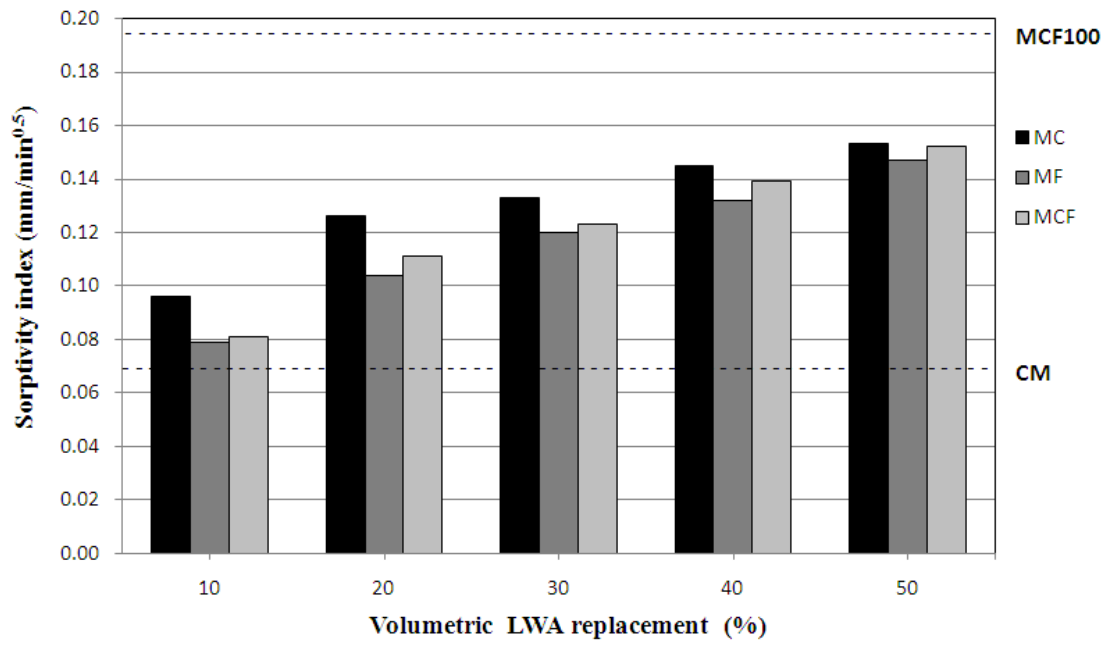
Critical observation of Figure 4.29 a and b indicated that when considering the fixed replacement level of LWA, changing the type of LWA remarkably affected the sorptivity behavior of concrete. This may be attributed to the quality of matrix which affected the capillarity of concrete by the porosity of LWAs. Therefore, the increasing mean pore size and total porosity leads to increased capillarity of SCLC with LWA (Liu et al., 2011; Güneyisi et al., 2013).

The relative sorptivity index describes the rate of sorptivity of any concrete to that of control one at a given age. SCCs including LWA revealed a systematic increase in sorptivity coefficients with increasing replacement level of LWA at both ages. As observed from Figure 4.30 a, MF mixes had the lowest relative sorptivity index ranged between 1.1-2.1%, whereas, the highest relative sorptivity coefficient values ranged between 1.4-2.2% for MC mixes at 28 days. However, it was observed from Figure 4.30 b that considering 30% LWA replacement level, the relative sorptivity index value at 90 days was found to be 1.9%, 1.6% and 1.8% for MC30, MF30 and MCF30, respectively. Although having lower compressive strength compared to MC mixes, MF mixes had better sorptivity coefficient than that of MC mixes for the same replacement level of LWA. Moreover, Figure 4.30 a clearly showed that the variation trends of relative sorptivity index for MF and MCF mixes were close to each other at 28 days. But, the enhancement of relative sorptivity index at 90 days was more pronounced for MF mixes as seen in Figure 4.30 b. These findings point out that the contribution of LWFA on sorptivity for SCLCs at later age is dominantly due to the

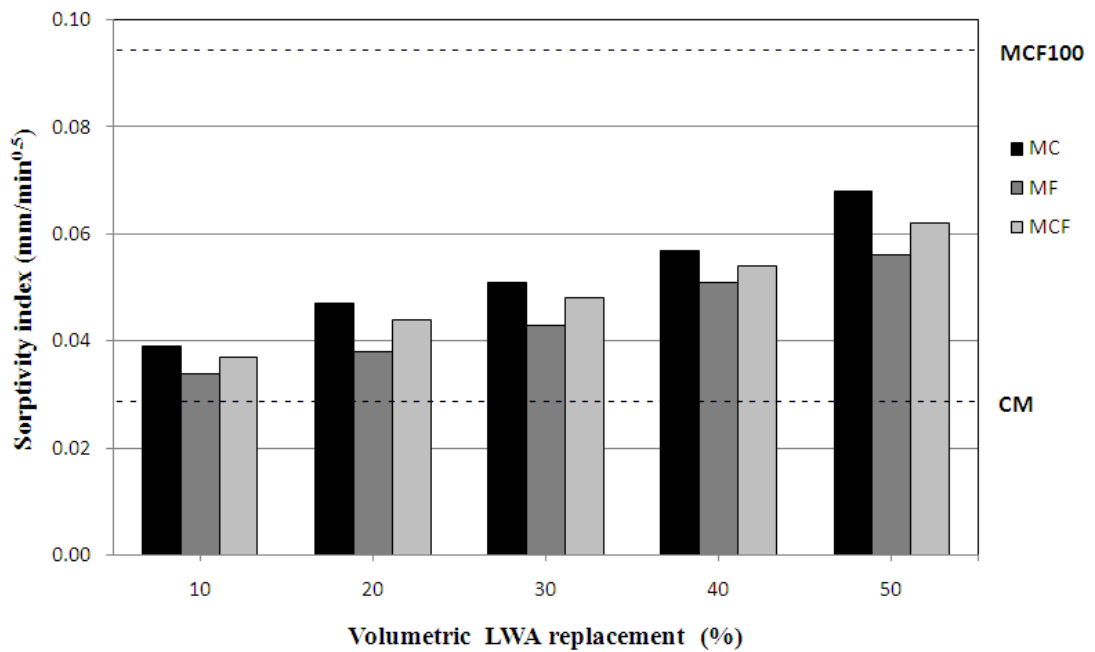
chemical process emerged by internal curing effect of LWFA increased with the larger surface area. The degree of cement hydration in these concretes would probably be higher compared with that in MC mixes, since the water inside the LWFA with bigger surface area contributed to internal curing (Wasserman and Bentur, 2006; Liu et al., 2011).

Table 4.10 28 and 90 days sorptivity values of SCLCs

Code Number	Sorptivity Index (mm/min ^{0.5})	
	28 days	90 days
CM	0.070	0.027
MC10	0.096	0.039
MC20	0.126	0.047
MC30	0.133	0.051
MC40	0.145	0.057
MC50	0.153	0.068
MF10	0.079	0.034
MF20	0.104	0.038
MF30	0.120	0.043
MF40	0.132	0.051
MF50	0.147	0.056
MCF10	0.081	0.037
MCF20	0.111	0.044
MCF30	0.123	0.048
MCF40	0.139	0.054
MCF50	0.152	0.062
MCF100	0.195	0.095

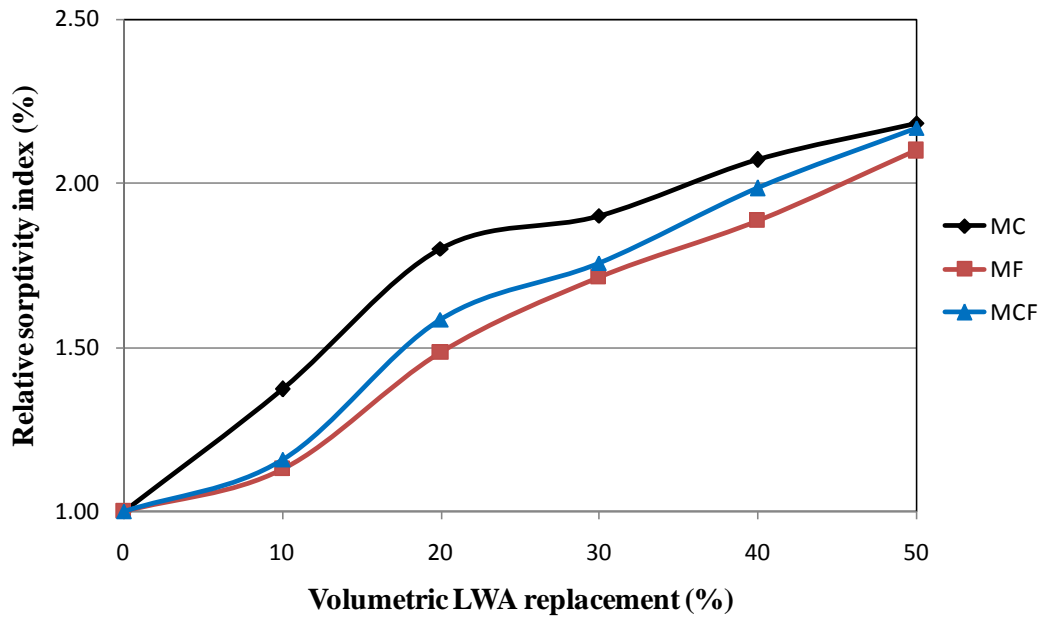


a)

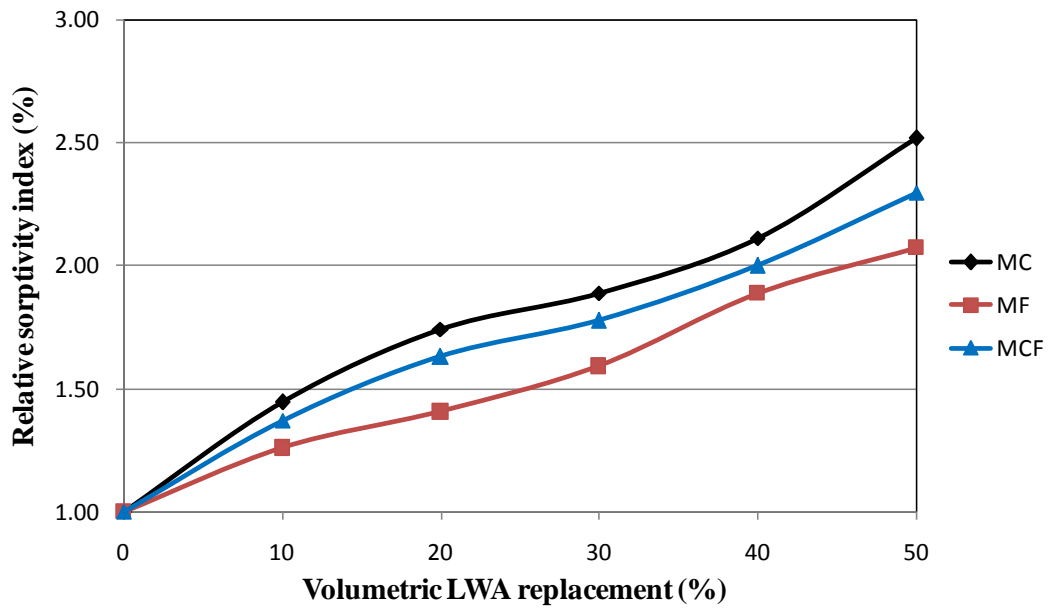


b)

Figure 4.29 Water sorptivity test results at a) 28 days and b) 90 days



a)



b)

Figure 4.30 Effect of replacement level of LWA on sorptivity index of SCLCs at a) 28 days and b) 90 days (Sorptivity index for control concrete is 1)

4.5.2 Water Permeability

Water permeability test measures the depth of water penetration into concrete in which a fluid may flow throughout a permeable body as a result of differential pressure. The variations of the water penetration depth with respect to type and replacement level of LWA are given Table 4.11, also graphically shown in Figure 4.31 a and b at 28 and 90 days, respectively. Additionally, the relative changes in water penetration depth with respect to CM are depicted in Figure 4.32 a and b for different ages. Test results revealed that using LWA made the concretes more water absorbent, irrespective of the LWA size, but the effect being more indicative with increasing the LWA content. The highest penetration depth was measured for MCF100 as 33.5 mm and 26 mm, whereas, the lowest penetration depth was measured for CM as 15.5 mm and 11 mm at 28 and 90 days, respectively. Due to the porous structure of LWAs, water may easily penetrate into and through the aggregates under pressure which in turn resulted in a deeper penetration water of into the SCCs containing LWAs than that of CM. The increased porosity can result in an increment of pore connectivity of concrete. As water can penetrate through porous media, the porous LWA may reduce the concrete resistance to water penetration (Liu et al., 2011). The results showed that the SCLCs with LWCA (MC mixes) had higher water penetration depth, depending on the amount of the porous LWA particles used, with respect to MF and MCF mixes. For instance, as compared with CM for 30% replacement level, the penetration depth had an increase of 63.3%, 35.4% and 48.4% for MC30, MF30, and MCF30 respectively at 28 days. This may be attributed to interior open pores in the LWCA probably contributed to the higher water penetration depth.

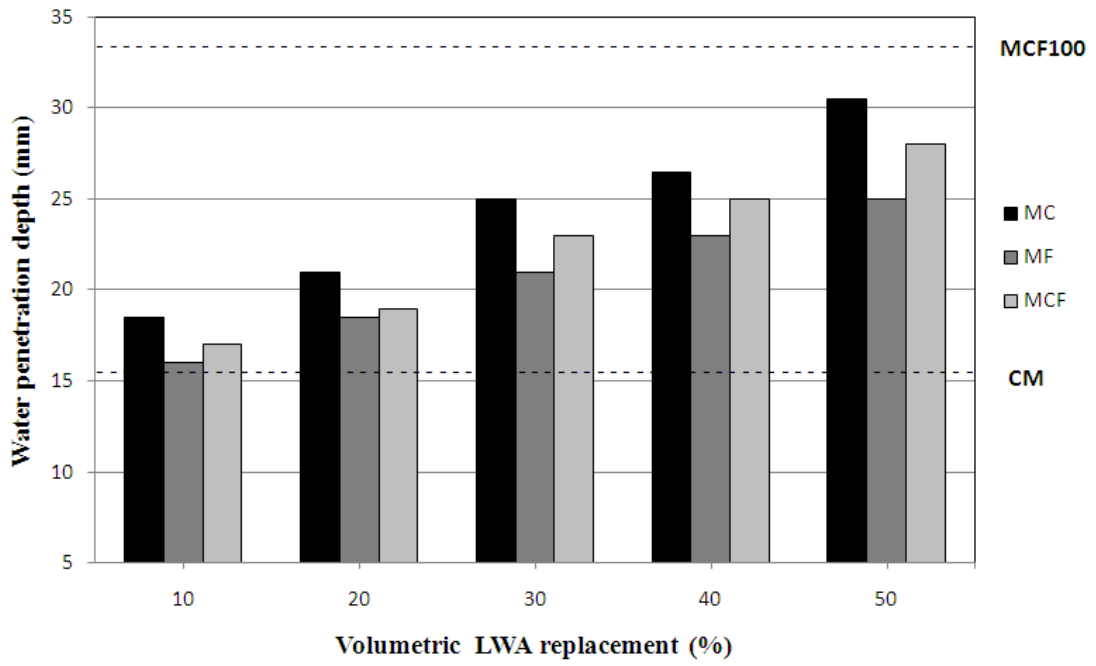
However, SCLCs containing LWFA exhibited a comparable performance with MC and MCF mixes at both age. For instance, water ingress measured at 28 days was deeper by 1.71%, 1.48% and 1.61 times at MC40, MF40 and MCF40 concretes, respectively compared to the control one. As seen in Figure 4.31 b, the results of the water permeability test indicated that the substantial reductions in water penetration depths were obtained at 90 days. A similar finding was observed in 90 days that MF mixes had lower relative water penetration depth among the concretes containing LWAs. The lower penetration depth of MF mixes with respect to MC and MCF

mixes was probably a result of enhanced hydration due to internal curing provided by additional pre-wetted LWA. Therefore, the improved ITZ between LWFA paste matrixes is improved the cement hydration by the water absorbed in LWFA leading to reduced capillary pores in MF mixes compared to MC and MCF mixes (Liu et al., 2011; Wasserman and Bentur 1996; 1997).

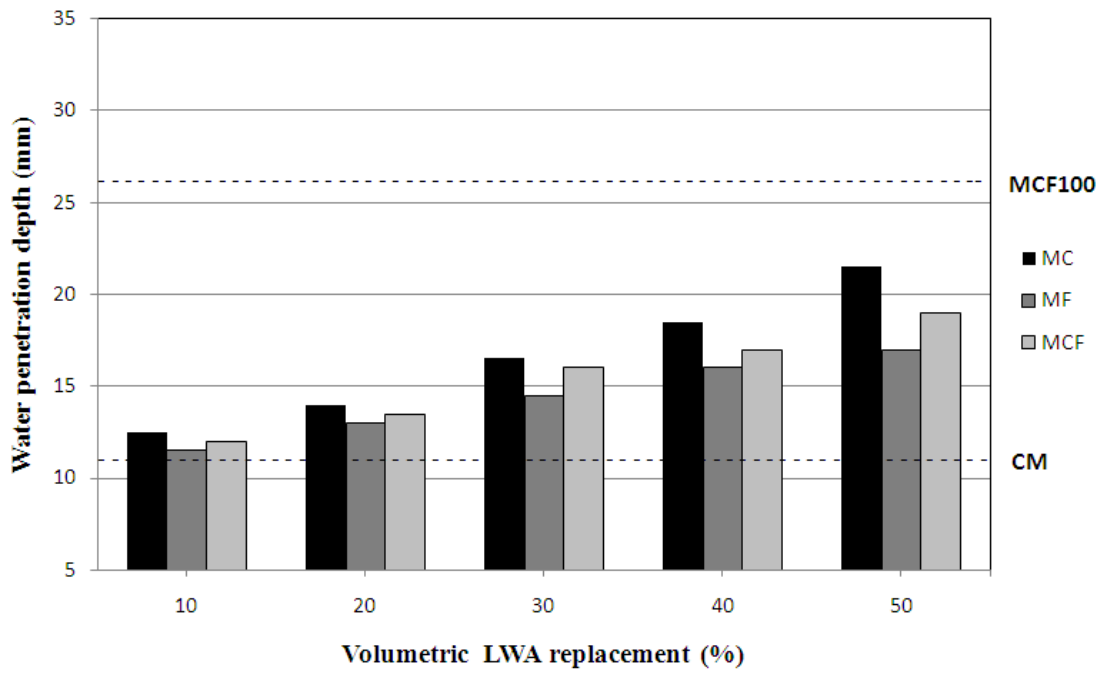
The water permeability test may also provide some information about the pore structure of the concrete, the continuity of the pores, and concrete's potential durability against the aggressive media. According to DIN 1048 (1991) and TS EN 12390/8 (2002) guidelines, concretes can be considered resistant to chemical attacks if the water penetration depth was less than 30 mm when in contact with aggressive media. From test results it can be concluded that SCLCs including LWA except MC50 and MCF100 can be considered resistant to chemical attacks, since water does not penetrate to a depth of more than 30 mm.

Table 4.11 Water penetration depths measured at 28 and 90 days

Code Number	Water Penetration Depth (mm)	
	28 days	90 days
CM	15.5	11.0
MC10	18.5	12.5
MC20	21.0	14.0
MC30	25.0	16.5
MC40	26.5	18.5
MC50	30.5	21.5
MF10	16.0	11.5
MF20	18.5	13.0
MF30	21.0	14.5
MF40	23.0	16.0
MF50	25.0	17.0
MCF10	17.0	12.0
MCF20	19.0	13.5
MCF30	23.0	16.0
MCF40	25.0	17.0
MCF50	28.0	19.0
MCF100	33.5	26.0

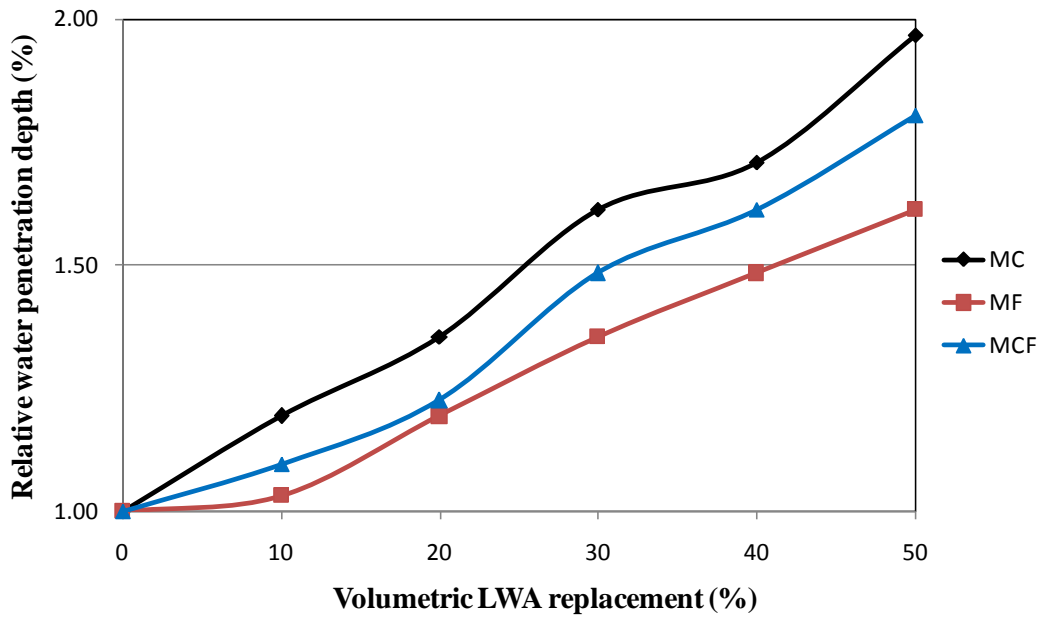


a)

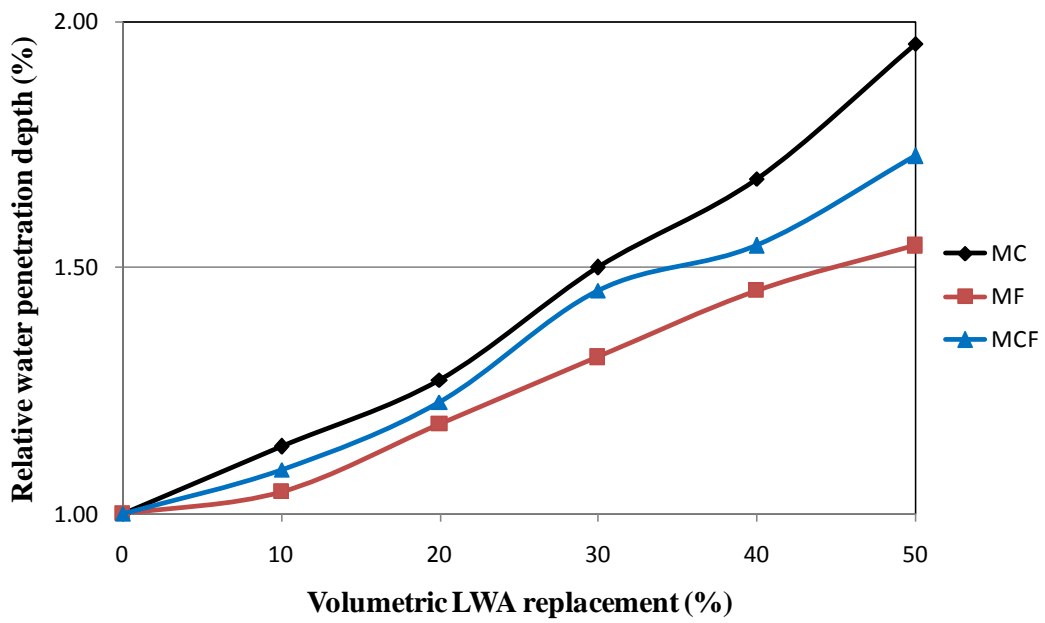


b)

Figure 4.31 Water penetration depths of SCLCs at a) 28 days and b) 90 days



a)



b)

Figure 4.32 Effect of replacement level of LWA on water penetration depth of SCLCs at a) 28 days and b) 90 days (Water penetration depth for control concrete is 1)

4.5.3 Rapid Chloride Permeability

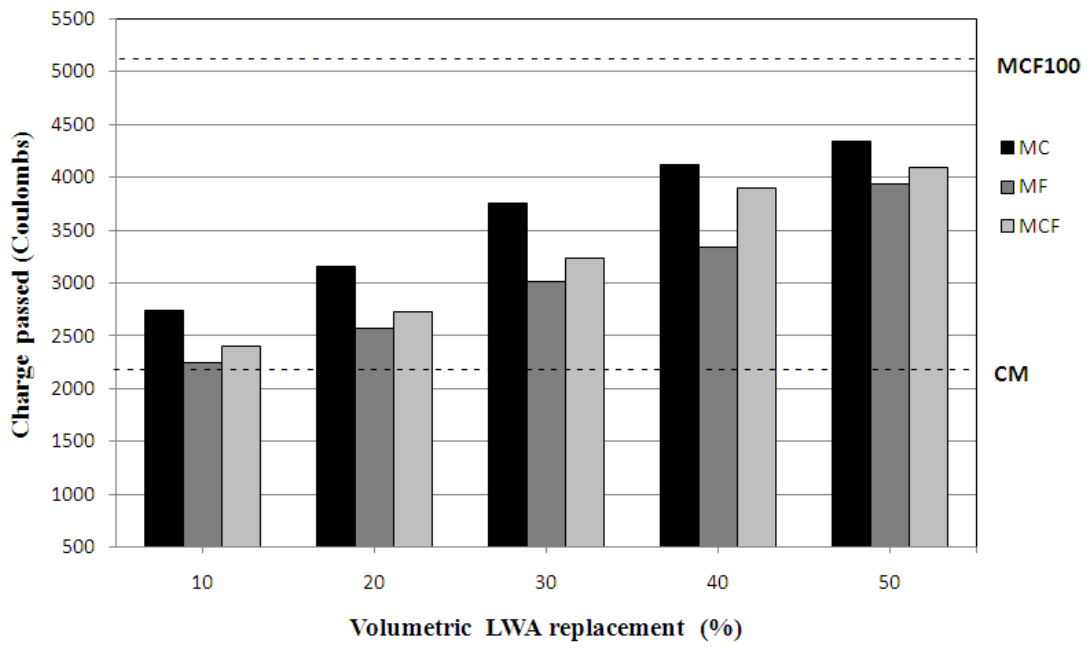
The penetration of water with chloride and other aggressive ions into concrete is the most important factor affecting the physical and chemical process of deterioration. The microstructure of concrete that is mainly controlled by this process is associated with water permeation and the transport of ions in concrete (Oh et al., 2002). According to the chloride ion penetrability recommended by ASTM C 1202 (2012), the variation of the chloride ion permeability with respect to the type of LWA is given in Table 4.12 and graphically presented in Figure 4.33 a and b. The change in relative chloride ion permeability in comparison to CM was also demonstrated in Figure 4.34 a and b at 28 and 90 days, respectively. There was a symmetric increase in chloride-ion permeability with increasing cold-bonded aggregate content. It was observed that the concrete with full lightweight aggregate (MCF100) had the highest total charged passed of 5083 and 1472 C whereas the lowest values of 2150 and 809 C were achieved at CM at 28 and 90 days, respectively. As seen in Figure 4.33 a, the total charge values ranged between 2840–4038 C, 2150–3378 C and 2201–4093 C for MC, MF and MCF groups, at 28 days respectively. At 28 days, the total charge passed through the SCCs including LWAs less than 40% of total aggregate volume fell in the range between 2000 and 4000 C, thus leading to moderate classification of chloride penetrability with respect to ASTM C 1202 (2012). At 90 days, however, chloride ion penetration of all SCCs except MCF100 diminished to as low as 1000 C indicating very low rating of chloride permeability. Moreover, the rating of MCF100 concrete shifted from high to low at 90 days. This finding suggested that the negative effect of LWAs on the chloride ion permeability remarkably diminished with the prolonged testing ages from 28 to 90 days.

As illustrated in Figures 4.34 a and b, increasing the replacement level of LWA caused a substantial increase in relative chloride ion permeability at 28 days whereas the relative charges passed increased moderately at 90 days for MC, MF and MCF mixes, respectively. However, LWFA seemed to be effective at both ages. Figures 4.34 a and b indicated that the relative charge passed values of MF mixes were lower than those of MC mixes. The utilization of LWFA appeared to be the more effective for chloride ion permeability than LWCA, especially when increasing LWFA content. The higher porosities of LWCA might be attributed to the higher surface

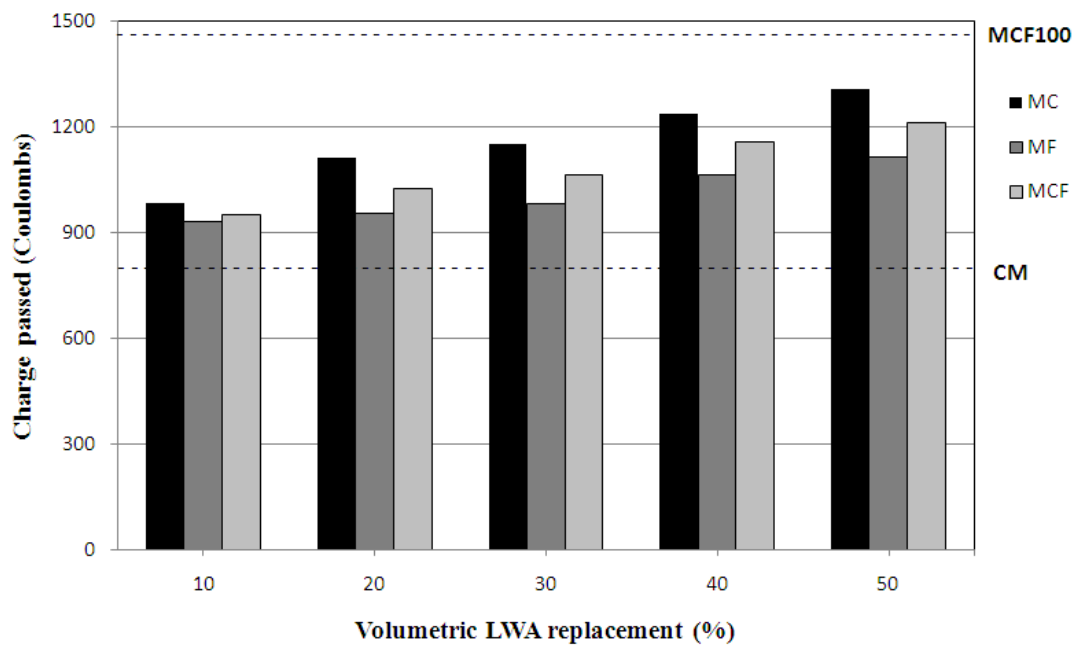
chloride content of MC mixes. However, this result is questionable as the compressive strength of MC mixes being higher than that of MF mixes at the same replacement level of LWA. The results presented herein are consistent with the findings of the previous research. LWCA affected adversely the chloride ion permeability with respect to LWFA due to the increased pore size in the paste and also in the ITZ. The water absorption of LWFA reduces the wall effect and improves the quality of ITZ, which in turn refine the pore structure of MF to have only a modest increase for the ingress of chloride ions with respect to MC and MCF mixes. Although the poor performance of MF50 in MF mixes, the greatest relative difference between 28 and 90 days of MF50 proved that the pozzolanic activity of LWFA was more effective at later ages than at early ages (Wasserman and Bentur, 1996; Oh et al., 2002; Liu et al., 2011). Moreover test results were conformed to values obtained from water permeability tests. This statement was approved by Zhang and Gjorv (1991b) showed that there was a relation directly between water permeability and chloride ion penetration.

Table 4.12 Total charge values measured at 28 and 90 days

Code Number	Charge Passed (Coulombs)	
	28 days	90 days
CM	2150.6	809.5
MC10	2740.0	981.3
MC20	3154.7	1110.9
MC30	3754.1	1151.7
MC40	4127.1	1235.1
MC50	4338.5	1307.0
MF10	2250.8	928.4
MF20	2571.7	955.4
MF30	3014.5	980.4
MF40	3337.9	1062.7
MF50	3944.2	1112.3
MCF10	2402.6	949.6
MCF20	2730.9	1024.3
MCF30	3239.7	1063.5
MCF40	3898.6	1157.3
MCF50	4093.2	1209.8
MCF100	5083.0	1472.0

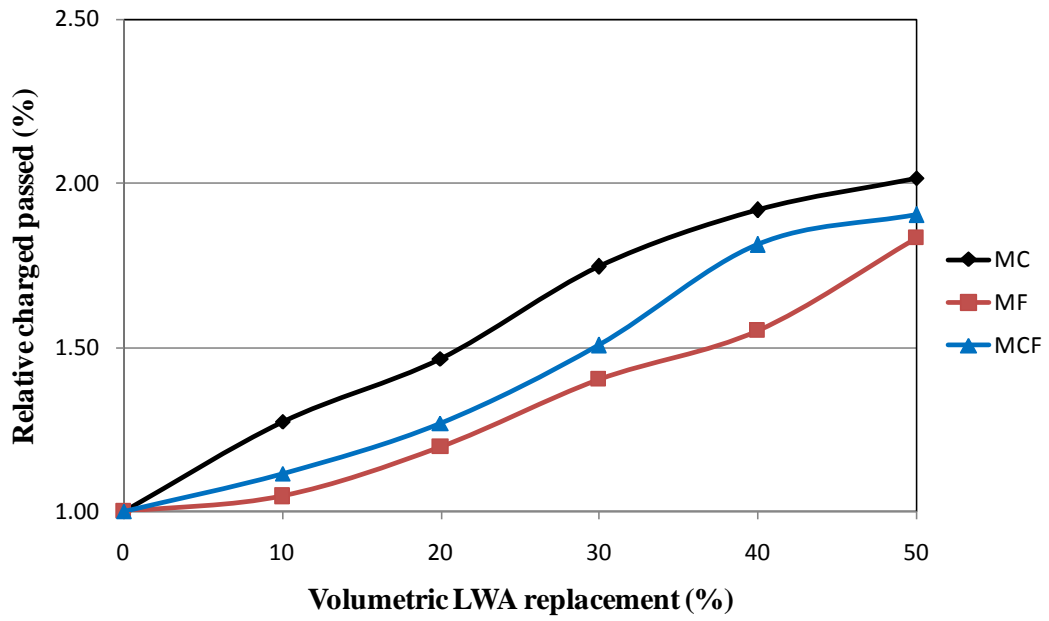


a)

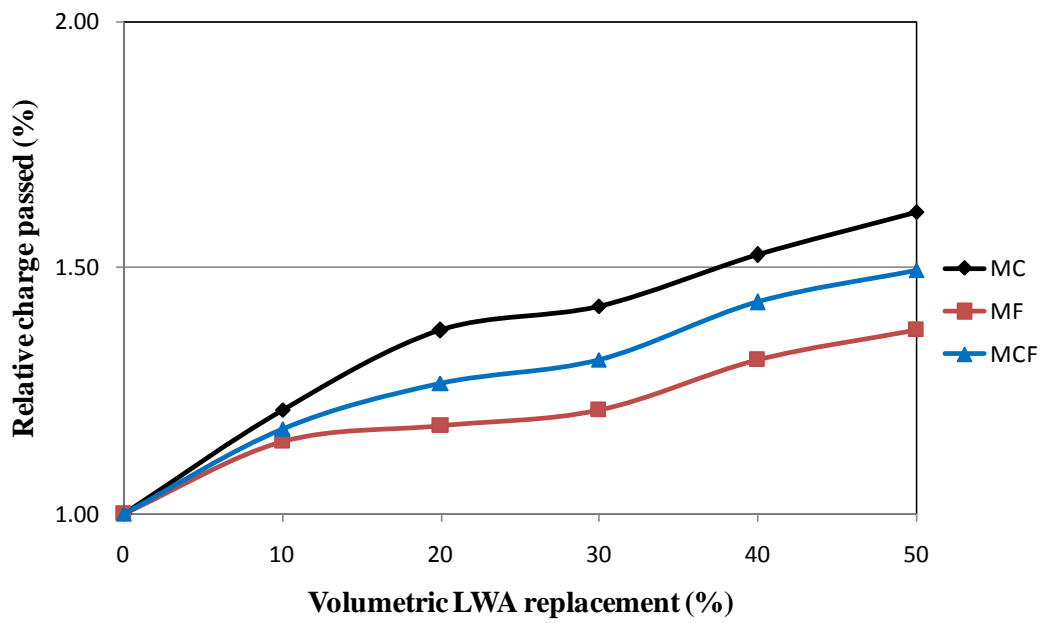


b)

Figure 4.33 RCPT test results of SCLCs at a) 28 days and b) 90 days



a)



b)

Figure 4.34 Effect of replacement level of LWA on chloride resistance of SCLCs at
a) 28 days and b) 90 days (Charge passed for control concrete is 1)

4.5.4 Gas Permeability

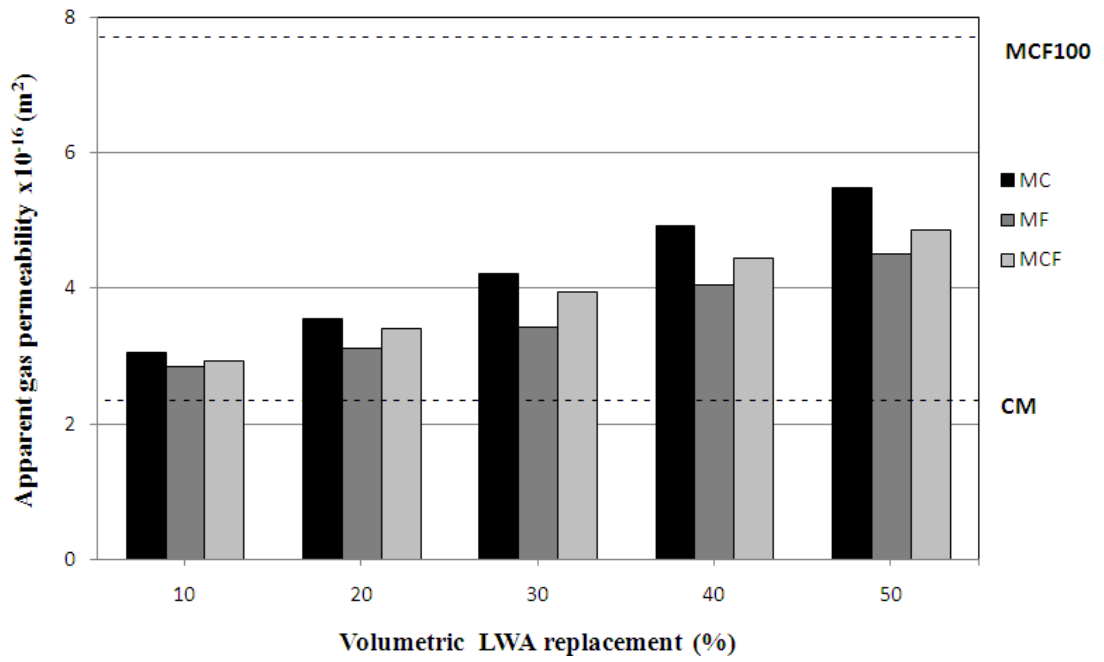
The usage of 150, 200, and 300 kPa inlet pressures for computing the average gas permeability coefficient is recommended by RILEM (1999). Therefore, the apparent gas permeability coefficients of SCLCs measured at 28 and 90 days are determined accordingly and given in Table 4.13, Figures 4.35 a and b. Moreover, taking into account the apparent gas permeability coefficient for CM as $2.35 \times 10^{-16} \text{ m}^2$ and $1.97 \times 10^{-16} \text{ m}^2$ at 28 and 90 days, the relative apparent gas permeability value of SCLCs at 28 and 90 days are depicted in Figure 4.36 a and b, respectively. The test results clearly demonstrated that substitution of natural aggregate with LWFA and/or LWCA considerably increased the apparent gas permeability coefficient depending on the replacement level of LWA. The highest gas permeability coefficients at 28 and 90 days were quantified at MCF100 as $7.76 \times 10^{-16} \text{ m}^2$ and $6.93 \times 10^{-16} \text{ m}^2$, respectively. Since the transport properties of concretes are strongly depending on its pore structure, the raising of gas permeability of concrete can be attributed to the increased pore structure in concrete due to LWA addition. But, LWCA seemed to be more liable to cause increase in gas permeability coefficient. For instance, the variation of apparent gas permeability coefficients for MC, MF mixes was changed between 3.05×10^{-16} - $5.48 \times 10^{-16} \text{ m}^2$ and 2.84×10^{-16} - $4.51 \times 10^{-16} \text{ m}^2$ at 28 days, respectively. However, as seen in Figure 4.35 a and b, this value for MCF mixes (MCF10-MCF50) ranged between 2.82×10^{-16} - $4.86 \times 10^{-16} \text{ m}^2$ and 2.33×10^{-16} - $4.17 \times 10^{-16} \text{ m}^2$ at 28 and 90 days, respectively.

In addition to the mentioned test results, when Figures 4.36 a and b were concerned, the highest relative gas permeability was found to be 2.3% at 28 days for MC100 was evident that LWCA was governing the increment in apparent gas permeability coefficients of SCLCs when used at higher amounts. Nonetheless, it can be interfered from Figures 4.36 a and b that the effectiveness of LWFA was observed to be persistent at both ages. For instance, MC40 had 2.10% of relative gas permeability value, however, the relative gas permeability value decreased to 1.89% and 1.72% for MCF40 (SCLC incorporated 20% LWFA and 20% LWCA) and MF40 (SCLC including 40% of LWFA), respectively. This may be attributed to the bigger surface of LWFA that giving the opportunity to improve more pozzolanic reaction between ITZ and matrix. Additionally, the porous LWFA can reduce the thickness of the

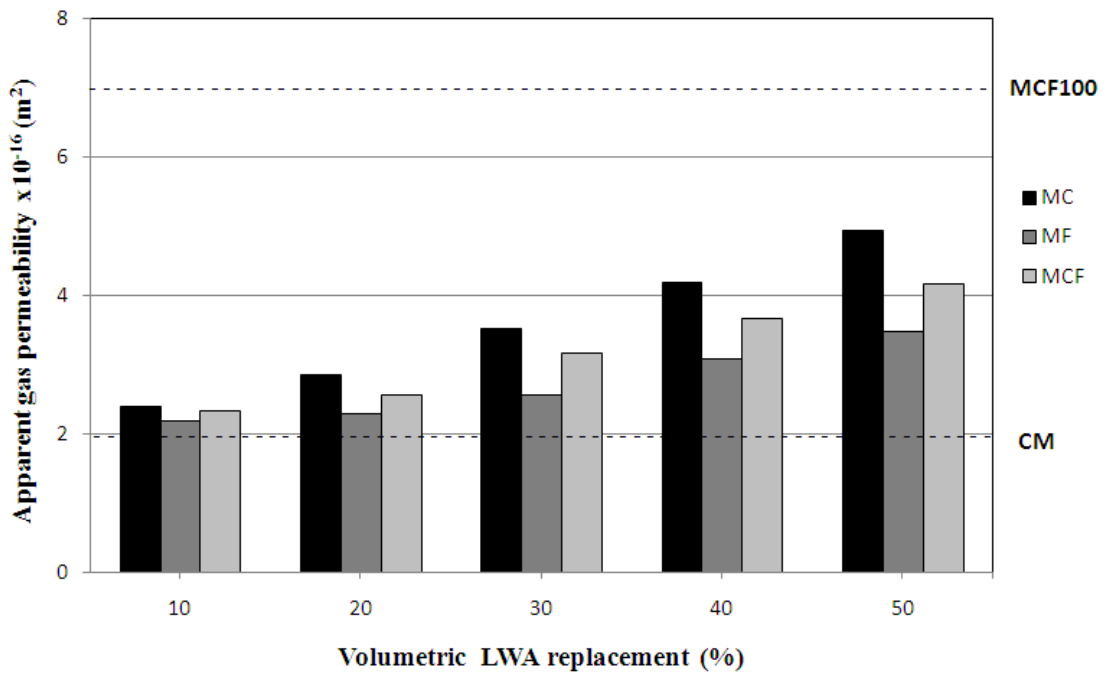
dense matrix among the aggregates and possibly increased interconnectivity (Liu et al., 2011). As a result of this, MF mixes had lowest apparent gas permeability coefficient irrespective of replacement level. However, at 90 days, the concretes incorporating LWFA seemed to have a more consistent variation of the relative apparent gas permeability values with the change in replacement level than those of values for 28 days. For instance, the relative gas permeability coefficient value of MF30 was found to be 1.46% and 1.29% at 28 and 90 days, respectively. The concretes containing LWFA exhibited better performance than MC and MF group concretes due to fact that smaller size of such aggregates reduced the width of the interfacial transition zone apart from the chemical process associated with pozzolanic activity of LWFA which in turn diminished the permeability with respect to MC and MCF mixes (Zhang and Gjorv, 1990; Wasserman and Bentur, 1996; Oh et al., 2002; Liu et al., 2011).

Table 4.13 Apparent gas permeability coefficient average of that value for 150, 200, and 300 kPa inlet pressures as recommended per RILEM (1999)

Code Number	Apparent Gas Permeability Coefficient (10^{-16}xm^2)	
	28 days	90 days
CM	2.35	1.97
MC10	3.05	2.39
MC20	3.56	2.86
MC30	4.21	3.52
MC40	4.93	4.18
MC50	5.48	4.93
MF10	2.84	2.18
MF20	3.11	2.28
MF30	3.43	2.55
MF40	4.05	3.09
MF50	4.51	3.48
MCF10	2.92	2.33
MCF20	3.40	2.55
MCF30	3.95	3.16
MCF40	4.44	3.66
MCF50	4.86	4.17
MCF100	7.76	6.93

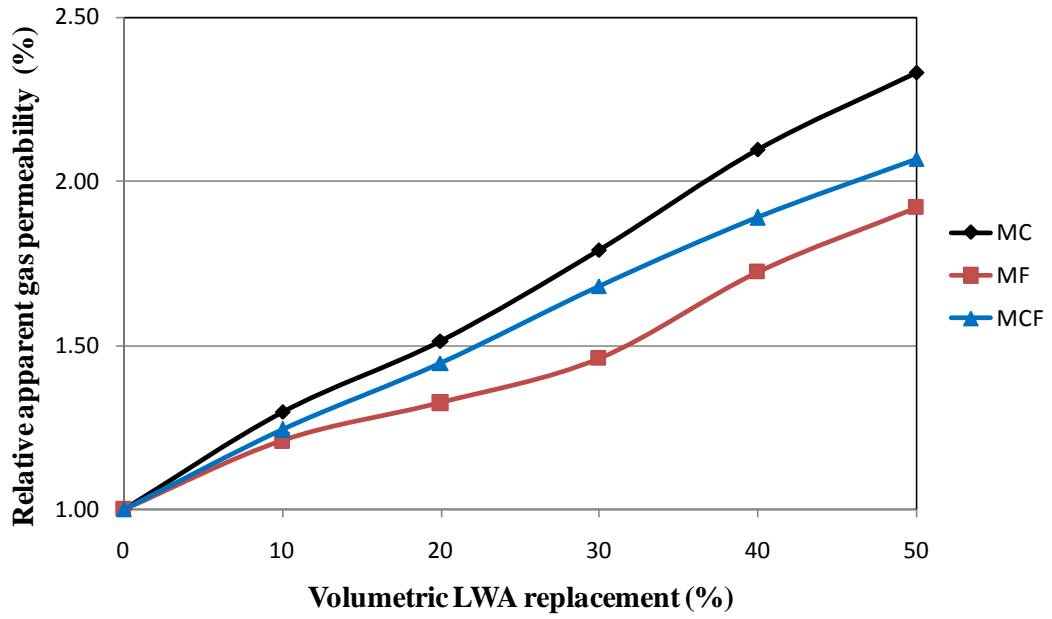


a)

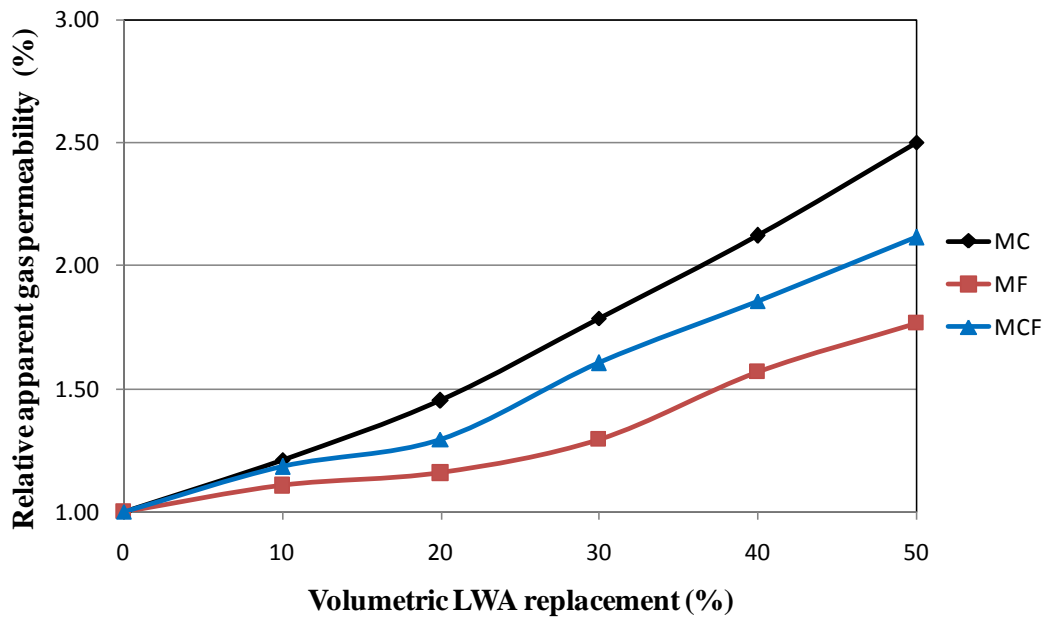


b)

Figure 4.35 Variation of apparent gas permeability coefficients of SCLCs at a) 28 days and b) 90 days



a)



b)

Figure 4.36 Effect of replacement level of LWA on apparent gas permeability of SCLCs at a) 28 days and b) 90 days (Apparent gas permeability coefficient for control concrete is 1)

CHAPTER 5

CONCLUSIONS

An experimental program was conducted to investigate the effects of cold bonded lightweight fine and coarse aggregates on the fresh, mechanical, fracture, physical, and durability properties of self-compacting lightweight aggregate concretes. In this context, a total of 17 self-compacting concrete mixtures were designed at 0.32 w/b ratio. Based on the findings of this study the following conclusions were drawn:

- It is very clear from the test results that all the mixes satisfy the requirements of SCC with respect to EFNARC (2005). Thus, all the mixes are assumed to have good consistency, workability, filling and passing ability. Moreover, spherical artificial LWA with saturated specific gravity of 1.76 g/cm^3 may be used in producing LWC to achieve lower unit weight. Uniform and non-segregating SCLCs with varying densities in the range of $2392\text{-}1827 \text{ kg/m}^3$ were produced. MCF100 mix including 100% of LWA was of nearly 25% less unit weight than CM with 100% of natural aggregate.
- All of SCLCs were designed to give a slump flow diameter of $720\pm 20 \text{ mm}$ which was acquired by adjusting the dosage of HRWRA used. The required HRWRA to obtain the aimed slump flow substantially decreased with increasing the amount of LWCA and LWFA. MCF100 had lower demand for HRWRA than CM by as low as 43%. The higher specific surface area played a big role on decreasing the amount of HRWRA used as LWFAs have bigger surface area than the coarse one.
- The spherical shape as well as relatively smooth surface of LWCA and LWFA provided ease in flow of the aggregate particles and paste. Therefore, both the time required to reach 500 mm slump-flow and the time required to

flow through the V-funnel apparatus decreased as the proportion of LWA increase.

- It was observed that increasing the replacement ratio of LWA resulted in a gradual increase in the L-box height ratio of SCLCs mixes. Moreover, the height ratio reached to 1.0 for MC50 and MCF100, revealing the highest fluid behavior.
- Test results of the rheological properties of fresh SCLC indicated that the flow curves of SCLCs were not linear, resulting in apparently negative yield stresses or the results were below 10 Pa. On the other hand, of plastic viscosity of concretes produced ranged from 21 to 51 Pa.s for fully LWA concrete (MCF100) and fully NWA concrete (CM), respectively.
- Flow curves indicated a shear thickening behavior for SCC with natural aggregates (CM). However, the material showed less susceptibility against shear thickening as LWAs replaced the natural ones. In the case of SCLC with 100% LWA (MCF100), the behavior was much similar to that of Bingham material.
- The compressive strength showed a considerable decrease depending on the replacement level of LWA. The 28 days compressive strength of the CM was 75.8 MPa whereas the 28 days compressive strength of MCF100 was found to be 43 MPa. However, the 28 days compressive strength of MC50 (SCLC with 50% of LWCA) was 25% lower than that of the CM, while the 28 days compressive strength of MF50 (SCC with 50% of LWFA) had 38% decrease compared with CM.
- Due to strength limitation of LWA, SCCs including LWA had lower splitting strength than that of CM. Splitting tension occurred through LWA, since the strength of LWA is lower than that of cement and slurry. The 28 days splitting tensile strength was 4.1 MPa for CM, while this value was measured as 2.67, 2.30, 2.55 and 2.1 MPa for MC50, MF50 and MCF50 and MCF100 respectively.

- The volume concentration of LWA had a similar effect on the net flexural strength that observed on the compressive and splitting tensile strengths. So, the net flexural strength decreased with increasing the lightweight aggregate content irrespective of size of LWA due to being the matrix harder than artificial cold bonded fly ash aggregates. Decreasing the volume of natural fine aggregate resulted in a systematic decrease of net flexural strength with respect to coarse one. Moreover, the effect of size for LWA on the net flexural strength of SCLCs has been found insignificant up to 30% replacement level.
- The fracture energy decreased with increasing LWA content due to artificial fly ash aggregates being weaker than the matrix. Similarly, the utilization of LWA in SCLCs significantly decreased the area under the load versus displacement curve as well as the ultimate load. This is probably due to the fact that there are not enough amount of stiffer natural aggregate around which the cracks could progress; thus the cracks can easily penetrate into the LWAs and matrix phases so that the displacement at peak load decreased with increasing LWA content. On the other hand, serious reductions in fracture energy were measured for MF mixes. Similar to the above mentioned test results (compressive strength, splitting tensile strength and net flexural energy), the decreasing natural fine aggregate content may lead to the weakness of cement matrix in MF mixes due to the decreased filler effect of LWFA with spherical shape.
- The characteristic length decreased with the use of LWA indicating that the material became more brittle. Although increasing the amount of LWFA and/or LWCA cause a decreasing in compressive strength of SCLCs, it does not make the concrete more ductile because of LWA being weaker than matrix.
- Irrespective of size of LWA, it was observed that drying shrinkage strains at 60 days were higher for SCLCs for all replacement levels of LWAs with respect to CM. The drying shrinkage of MCF100 up to a period of 60 days was 675 microstrains. This might be attributed to the fact that high absorption

as well as the lower modulus of elasticity of LWA was accompanied with higher drying shrinkage in concrete as verified from the increase in shrinkage with increase of the amount LWA in SCLC.

- Considering the overall drying period, MF mixes had lower shrinkage strains than that of MC and MCF mixes. This may be attributed to internal curing effect of LWA in which water supplied from the outer surface of LWA to the matrix. Though SCC with LWA had higher crack propagation with respect to CM, the time of cracking was greatly extended with the increased replacement level of LWA.
- SCC incorporating LWA revealed a systematic increase in sorptivity coefficient values with increasing replacement level of LWA at both ages. Although having lower compressive strength compared with MC mixes, MF mixes had better sorptivity coefficient than that of MC mixes for same replacement level of LWA. The degree of cement hydration in these concretes would probably be higher compared with that in MC mixes, since the water inside the LWFA with bigger surface area contributed to internal curing.
- The highest penetration depth was measured for MCF100 as 33.5 mm and 26 mm whereas the lowest penetration depth was measured for CM as 15.5 mm and 11 mm at 28 and 90 days, respectively. Moreover, MF mixes, had the lowest penetration depth in produced SCCs at 28 and 90 days. The lower penetration depth of MF mixes was probably a result of enhanced hydration due to internal curing provided by additional pre-wetted LWA.
- There was a symmetric increase in chloride-ion permeability with increasing cold-bonded aggregate content. The charges passed through the SCCs including LWA (except for MCF100), however, were all within the range from 2000 to 4000 C which was classified as “moderate” chloride penetrability with respect to ASTM C 1202 (2012). However, the total charges passed of MF mixes are lower than those of MC mixes.

- The highest gas permeability coefficients at 28 and 90 days were measured at MCF100 as $7.76 \times 10^{-16} \text{ m}^2$ and $6.93 \times 10^{-16} \text{ m}^2$, respectively. Compared to MC mixes, MF mixes had lower apparent gas permeability coefficient, irrespective of testing age.

REFERENCES

- ACI Committee 213R. American Concrete Institute. (2003). Guide for structural lightweight aggregate concrete. *Manual of Concrete Practice*. Farmington Hills, Michigan, USA.
- Akçay B. (2007). Effects of lightweight aggregates on autogenous deformation and fracture of high performance concrete. *PhD Thesis*, Istanbul Technical University, Turkey.
- Akçay, B., Taşdemir, M. A. (2009). Optimization of using lightweight aggregates in mitigating autogenous deformation of concrete. *Construction and Building Materials*. **23**, 353-363.
- Al-Khaiyat, H., Haque, M. N. (1998). Effect of initial curing on early strength and physical properties of a lightweight aggregate concrete. *Cement and Concrete Research*. **28**, 859-866.
- Alonso, J. L., Wesche, K. (1991). Characterization of fly ash. *Report of Technical Committee 67-Fab*. RILEM, London.
- Arslan, H., Baykal, G. (2006). Utilization of fly ash engineering pellet aggregates. *Environmental Geology*. **50**, 761-770.
- ASTM C1202. American Society for Testing and Materials. (2012). Standard test method for electrical indication of concrete's ability to resist chloride ion penetration. *Annual book of ASTM standards*, vol. **04.02**. West Conshohocken, PA: ASTM.
- ASTM C127. American Society for Testing and Materials. (2007). Standard test method for specific gravity and absorption of coarse aggregate. *Annual book of ASTM standards*, vol. **04.02**. West Conshohocken, PA: ASTM.

ASTM C143. American Society for Testing and Materials. (2008). Standard test method for slump of hydraulic-cement concrete. *Annual book of ASTM standards*, vol. **04.02**. West Conshohocken, PA: ASTM.

ASTM C157. American Society for Testing and Materials. (2008). Standard test method for length change of hardened hydraulic-cement mortar and concrete. *Annual book of ASTM standards*, vol. **04.02**. West Conshohocken, PA: ASTM.

ASTM C1611. American Society for Testing and Materials. (2005). Standard test method for slump flow of self-consolidating concrete. *Annual book of ASTM standards*, vol. **04.02**. West Conshohocken, PA: ASTM.

ASTM C1621. American Society for Testing and Materials. (2008). Standard test method for passing ability of self-consolidating concrete by j-ring. *Annual book of ASTM standards*, vol. **04.02**. West Conshohocken, PA: ASTM.

ASTM C330. American Society for Testing and Materials. (2009). Standard specification for lightweight aggregates for structural concrete. *Annual book of ASTM standards*, vol. **04.02**. West Conshohocken, PA: ASTM.

ASTM C39. American Society for Testing and Materials. (2012). Standard test method for compressive strength of cylindrical concrete specimens. *Annual book of ASTM standards*, vol. **04.02**. West Conshohocken, PA: ASTM.

ASTM C496. American Society for Testing and Materials. (2011). Standard test method for splitting tensile strength of cylindrical concrete specimens. *Annual book of ASTM standards*, vol. **04.02**. West Conshohocken, PA: ASTM.

ASTM C618. American Society for Testing and Materials. (2008). Standard specification for coal fly ash and raw or calcined natural pozzolan for use as a mineral admixture in concrete. *Annual book of ASTM standards*, vol. **04.02**. West Conshohocken, PA: ASTM.

Baker, M. (1984). Evaluation on the utilization options. *Coal Combustion By-Product Utilization Manual*. **EPRI Report No. CS-3122**.

- Barnes HA, Hutton JF, Walters K. (1989). An introduction to rheology. New York: Elsevier.
- Barnes, H. A. (1989). Shear-thickening (“Dilatancy”) in suspensions of nonaggregating solid particles dispersed in Newtonian liquids. *Journal of Rheology*. **33(2)**, 329-366.
- Baykal, G., Döven, A. G. (2000). Utilization of fly ash by pelletization process; theory, application areas and research results. *Resources, Conservation and Recycling*. **30(1)**, 59-77.
- Baykal, G., Döven, A. G., Savaş, M. A., Özturan, T., Atay, Z. (1997). Uçucu külden pelet agrega üretimi için laboratuvarında model tesis kurulması ve peletleme işleminin optimizasyonu. *The Scientific and Technical Research Council of Turkey, Construction Technologies Research Grant Committee. Project No: INTAG 627*. Ankara.
- Bentur, A., Igarashi, S., Kovler, K. (2001). Prevention of autogenous shrinkage in high-strength concrete by internal curing using wet lightweight aggregates. *Cement and Concrete Research*. **31**, 1587-1591.
- Bentz, D. P., Weiss, W. J. (2010). Internal curing: A 2010 state-of-the-art review. *National Institute of Standards and Technology U.S. Department of Commerce. NISTIR 7765*.
- Bogas, J. A., Gomes, A., Pereira, M. F. C. (2012). Self-compacting lightweight concrete produced with expanded clay aggregate. *Construction and Building Materials*. **35**, 1013-1022.
- Booya E. (2012). Improving fresh and hardened properties of self compacting cold bonded fly ash lightweight aggregate concretes with binary and ternary blends of silica fume and fly ash. *MSc Thesis*. Gaziantep University, Turkey.
- Bradbury, H. W. (1982). The use of fly ash in pre-blended cement. *Silicates Industrials*. **No.12**, 283-288.

Bremner, T. W., Thomas, M. D. A. Learning module on traditional and nontraditional uses of coal combustion products (CCP). http://www.unb.ca/fredericton/engineering/depts/civil/_resources/pdf/textofcourse.pdf, 31.10.2013.

BS812-part 110. British Standards. (1990). Methods for determination of aggregate crushing value (ACV).

Chang, T. P., Shieh, M. M. (1996). Fracture properties of lightweight concrete. *Cement and Concrete Research*. **26**, 181-188

Cheeseman, C. R., Makinde, A., Bethanis, S. (2005). Properties of lightweight aggregate produced by rapid sintering of incinerator bottom ash. *Resources, Conservation and Recycling*. **43(2)**, 147-162.

Chia, K. S., Zhang, M. H. (2002). Water permeability and chloride penetrability of high-strength lightweight aggregate concrete. *Cement and Concrete Research*. **32**, 639-645.

Choi, Y. W., Kim, Y. J., Shin, H. C., Moon, H. Y. (2006). An experimental research on the fluidity and mechanical properties of high-strength lightweight self-compacting concrete. *Cement and Concrete Research*. **36**, 1595-1602.

Clarke JL. 1993. Structural lightweight aggregate concrete. Blackie Academic and Professional, Berkshire.

Cohen, M. D., Olek, J., Dolch, W. L. (1990). Mechanism of plastic shrinkage cracking in portland cement and portland cement–silica fume paste and mortar. *Cement and Concrete Research*. **20(1)**, 103-119.

DIN 1048 Part 5. German Standard. (1991). Testing concrete; Testing of hardened concrete.

Douglas RP. (2004). Properties of self-consolidating concrete containing type F fly ash. *Master of Science*. PCA R&D Serial No. 2619.

Döven AG. (1996). Lightweight fly ash aggregate production using cold bonding agglomeration process. *PhD Thesis*. Boğaziçi University, Turkey.

Druta C. (2003). Tensile strength and bonding characteristics of self-compacting concrete. *MSc Thesis*. Louisiana State University.

EFNARC. European Federation of National Associations Representing for Concrete. (2005). Specification and guidelines for self-compacting concrete. UK: EFNARC.

Erdoğan, T. Y. (1993). Atık malzemelerin inşaat endüstrisinde kullanımı-uçucu kül ve yüksek fırın cürufu. *Endüstriyel Atıkların İnşaat Sektöründe Kullanımı Sempozyumu*. TMMOB, pp. 1-8, Ankara.

Euro Light Concrete Project (1998). LWAC material properties state-of-the-art. *Economic Design and Construction with Light Weight Aggregate Concrete*. **Document BE96-3942/R2**.

Euro Light Concrete Project (2000). Mechanical properties of lightweight aggregate concrete. *Economic Design and Construction with Light Weight Aggregate Concrete*. **Document BE96 3942/R23**.

Feys, D., Verhoeven, R., Schutter, G. D. (2008). Fresh self-compacting concrete, a shear thickening material. *Cement and Concrete Research*. **38**, 920-929.

Feys, D., Verhoeven, R., Schutter, G. D. (2009). Why is fresh self-compacting concrete shear thickening? *Cement and Concrete Research*. **39**, 510-523.

Gaarder N. (2010). Coal ash will fight flooding. Omaha World-Herald.

Gambhir ML. (1993). Concrete technology. Tata McGraw-Hill Publishing Co. Ltd.

Gerrits, A. (1998). Design considerations for reinforced lightweight concrete. *International Journal of Cement Composites and Lightweight Concrete*. **3(1)**, 57-69.

Gesoğlu M. (2004). Effects of lightweight aggregate properties on mechanical, fracture, and physical behavior of lightweight concretes. *PhD Thesis*. Boğaziçi University, Turkey.

Gesoğlu, M., Güneyisi, E., Öz, H. Ö. (2012a). Properties of lightweight aggregates produced with cold-bonding pelletization of fly ash and ground granulated blast furnace slag. *Materials and Structures*. **45**, 1535-1546.

Gesoğlu, M., Güneyisi, E., Mahmood, S. F., Öz, H. Ö., Mermerdaş, K. (2012b). Recycling ground granulated blast furnace slag as cold bonded artificial aggregate partially used in self-compacting concrete. *Journal of Hazardous Material*. **235-236**, 352-358.

Gesoğlu, M., Özturan, T., Güneyisi, E. (2004). Shrinkage cracking of lightweight concrete made with cold-bonded fly ash aggregates. *Cement and Concrete Research*. **34**, 1121-1130.

Gesoğlu, M., Özturan, T., Güneyisi, E. (2006). Effects of cold-bonded fly ash aggregate properties on the shrinkage cracking of lightweight concretes. *Cement and Concrete Composites*. **28**, 598-605.

Gesoğlu, M., Özturan, T., Güneyisi, E. (2007). Effects of fly ash properties on characteristics of cold-bonded fly ash lightweight aggregates. *Construction and Building Materials*. **21**, 1869-1878.

Goliassa, M., Castro, J., Weiss, J. (2012). The influence of the initial moisture content of lightweight aggregate on internal curing. *Construction and Building Materials*. **35**, 52-62.

Gonzalez-Corrochano, B., Alonso-Azcarate, J., Rodas, M. (2009). Production of lightweight aggregates from mining and industrial wastes. *Journal of Environmental Management*. **90**, 2801-2812.

Grzybowski, M., Shah, S. P. (1990). Shrinkage cracking of fiber reinforced concrete. *ACI Materials Journal*. **87(2)**, 138-148.

Güneyisi, E., Gesoğlu, M., Booya, E. (2012). Fresh properties of self-compacting cold bonded fly ash lightweight aggregate concrete with different mineral admixtures. *Materials and Structures*. **45**, 1849-1859.

Güneyisi, E., Gesoğlu, M., Pürsünlü, Ö., Mermerdaş, K. (2013). Durability aspect of concretes composed of cold bonded and sintered fly ash lightweight aggregates. *Composites: Part B*. **53**, 258-266.

- Hammer, T. A., Sandvik, M. (1995). Use of high performance lightweight aggregate concrete in Norwegian marine structures. *2nd CANMET/ACI Int. Symposium Advances in Concrete Technology*. **201-226**, Las Vegas, Nevada.
- Haque, M. N., Al-Khaiat, H., Kayali, O. (2007). Long-term strength and durability parameters of lightweight concrete in hot regime: importance of initial curing, *Building and Environment*. **42(8)**, 3086-3092.
- Hela, R., Hubertova, M. (2005). Development of self-compacting lightweight concrete using lightweight liapor aggregate, *The financial support of the Ministry of Education, Youth and Sports of the Czech Republic*, **project No. 1M0579**.
- Henkensiefken, R., Castro, J., Bentz, D., Nantung, T., Weiss, J. (2009). Water absorption in internally cured mortar made with water-filled lightweight aggregate. *Cement and Concrete Research*. **39**, 883-892.
- Hillerborg, A. (1985). Theoretical basis of method to determine fracture energy G_F of concrete. *Materials and Structures*. **18**, 291-296.
- Husem, M. (2003). The effects of bond strengths between lightweight and ordinary aggregate-mortar aggregate-cement paste on the mechanical properties of concrete. *Material Science and Engineering: A*. **363(1-2)**, 152-158.
- Hwang, C. L., Lin, R. Y., Hsu K. M., Chan, J. F. (1992). Granulation of fly ash lightweight aggregate and accelerated curing technology. *Fourth CANMET/ACI Int. Conference on Fly Ash, Silica Fume, Slag and Natural Pozzolans in Concrete*. **SP 132-24**, 419-438.
- Hwang, S. D., Khayat, K. H. (2008). Effect of mixture composition on restrained shrinkage cracking of self-consolidating concrete used in repair. *ACI Materials Journal*. **105(5)**, 499-509.
- İpek S. (2013). Improving the ductility properties of lightweight concretes by steel fiber addition. *MSc Thesis*. Gaziantep University, Turkey.
- Jaroslav S, Ruzickova Z. 1987. Pelletization of fines. Ore Research Instituted-Prague, Elsevier Science Publishing Company. New York.

Joseph, G., Ramamurthy, K. (2009). Influence of fly ash on strength and sorption characteristics of cold-bonded fly ash aggregate concrete. *Construction and Building Materials*. **23**, 1862-1870.

Josephson, J. (2010). Coal ash under fire from Portland resident. *Observer Today*.

Kabay, N., Aköz, F. (2012). Effect of prewetting methods on some fresh and hardened properties of concrete with pumice aggregate. *Cement and Concrete Composites*. **34**, 503-507.

Kayali, O. (2008). Fly ash lightweight aggregates in high performance concrete. *Construction and Building Materials*. **22**, 2393-2399.

Kayali, O., Haque, M. N., Zhu, B. (1999). Drying shrinkage of fibre-reinforced lightweight aggregate concrete containing fly ash. *Cement and Concrete Research*. **29**, 1835-1840.

Ke, Y., Beaucour, A. L., Ortola, S., Dumontet, H., Cabrillac, R. (2009). Influence of volume fraction and characteristics of lightweight aggregates on the mechanical properties of concrete. *Construction and Building Materials*. **23**, 2821-2828.

Khaleel, O. R., Al-Mishhadan, S. A., Razak, H. A. (2011). The effect of coarse aggregate on fresh and hardened properties of self-compacting concrete (SCC). *Procedia Engineering*. **14**, 805-813.

Kılıç, A., Atış, C. D., Yaşar, E., Özcan, F. (2003). High-strength lightweight concrete made with scoria aggregate containing mineral admixtures. *Cement and Concrete Research*. **33**, 1595-1599.

Kim, Y. J., Choi, Y. W., Lachemi, M. (2010). Characteristics of self-consolidating concrete using two types of lightweight coarse aggregates. *Construction and Building Materials*. **24**, 11-16.

Kim, Y., Kim, J. H., Lee, K. G., Kang, S. G. (2005). Recycling of dust wastes as lightweight aggregates. *Journal of Ceramic Processing Research*. **6(2)**, 91-94.

Koçkal NU. (2008). Effects of lightweight fly ash aggregate properties on the performance of lightweight concretes. *PhD Thesis*. Boğaziçi University, Turkey.

- Koçkal, N. U., Özturan, T. (2010). Effects of lightweight fly ash aggregate properties on the behavior of lightweight concretes. *Journal of Hazardous Materials*. **179**, 954-965.
- Koehler, E. P., Fowler, D. W. (2004). Development of a portable rheometer for fresh portland cement concrete. *Aggregates foundation for technology, research and education* (AFTRE).
- Koehler EP. (2004). Development of a portable rheometer for Portland cement concrete. *MSc Thesis*. University of Texas at Austin.
- Koehler, E. P. (2003). Use of rheology to design, specify, and manage self-consolidating concrete. *Tenth CANMET/ACI International Conference on Recent Advances in Concrete Technology and Sustainability Issues*.
- Lange-Kornbak, D., Karihaloo, B. L. (1998). Design of fiber reinforced DSP mixes for minimum brittleness. *Advanced Cement-Based Materials*. **7**, 89-101.
- Li, Y., Wu, D., Zhang, J., Dhang, L., Wu, D., Fang, Z., Yahua, S. (2000). Measurement and statistics of single pellet mechanical strength of differently shaped catalysts. *Powder Technology*. **113(1-2)**, 176-84.
- Liu, X., Chia, K. S., Zhang, M. H. (2010). Development of lightweight concrete with high resistance to water and chloride-ion penetration. *Cement and Concrete Composites*. **32(10)**, 757-766.
- Liu, X., Chia, K. S., Zhang, M. H. (2011). Water absorption, permeability, and resistance to chloride-ion penetration of lightweight aggregate concrete. *Construction and Building Materials*. **25(1)**, 335-343.
- Lo, T. Y., Cui, H. Z. (2004). Effect of porous lightweight aggregate on strength of concrete. *Materials Letters*. **58**, 916-919.
- Lo, T. Y., Cui, H. Z., Li, Z. G. (2004) Influence of aggregate pre-wetting and fly ash on mechanical properties of lightweight concrete. *Waste Management*. **24**, 333-338.
- Lo, T. Y., Tang, W. C., Cui, H. Z. (2007a). The effects of aggregate properties on lightweight concrete. *Building and Environment*. **42**, 3025-3029.

- Lo, T. Y., Tang, P. W. C., Cui, H. Z., Nadeem, A. (2007b). Comparison of workability and mechanical properties of self-compacting lightweight concrete and normal self-compacting concrete. *Materials Research Innovations*. **1(1)**, 45-50.
- Lura, P., Pease, B. J., Mazzotta, G., Rajabipour, F., Weiss, W. J. (2007). Influence of shrinkage reducing admixtures on the development of plastic shrinkage cracks. *ACI Materials Journal*. **104(2)**, 187-194.
- Maghsoudi, A. A., Mohamadpour, Sh., Maghsoudi, M. (2011). Mix design and mechanical properties of self-compacting lightweight concrete. *International Journal of Civil Engineering*. **9(3)**, 230-236.
- Mahmood SF. 2012. Use of cold-bonded blast furnace slag aggregate in the production of self-compacting concretes. *MSc Thesis*. Gaziantep University, Turkey.
- Mangialardi, T. (2001). Sintering of msw fly ash for reuse as a concrete aggregate. *Journal of Hazardous Materials*. **B87**, 225-39.
- Manikandan, R., Ramamurthy, K. (2007). Influence of fineness of fly ash on the aggregate pelletization process. *Cement and Concrete Composites*. **29**, 456-464.
- Manikandan, R., Ramamurthy, K. (2008). Effect of curing method on characteristics of cold bonded fly ash aggregates. *Cement and Concrete Composites*. **30**, 848-853.
- Matsunaga, T., Kim, J. K., Hardcastle, S., Rohatgi, P. K. (2002). Crystallinity and selected properties of fly ash particles. *Materials Science and Engineering*. **325**, 333-343.
- Mehta, K. (1998). Role of the pozzolanic and cementitious material in sustainable development of the concrete industry. *Sixth CANMET/ACI International Conference on Fly Ash, Silica Fume, Slag and Natural Pozzolans in Concrete*, Bangkok, Thailand, SP178. **1**, 1-20.
- Mindness, S, Young JF, Darwin D. (2003). *Concrete*, Second Edition, Pearson Education. Upper Saddle River, NJ 07458.
- Müller, H. S., Haist, M. (2002). Self-compacting lightweight concrete—technology and use. *Concrete Plant Precast Technology*. **71(2)**, 29-37.

- Myers, J. F., Pichumani, K., Bernadette, S. (1976). Fly ash-a highway construction material. U.S. Department of Transportation. **FHWA-IP-76-16**, Monroeville, Pennsylvania.
- Naik, T. R., Singh, S. S. (1995). Fly ash generation and utilization an overview. *Proceedings of Workshop on Flowable Slurry Containing Fly Ash, Silica Fume, Slag and Natural Pozzolans in Concrete*. **1**, 1-32, Milwaukee, Wisconsin.
- Neville AM, Brooks JJ. (1987). Concrete technology, Longman Scientific and Technical. Essex, England.
- Neville, A. M. (1997). Aggregate bond and modulus of elasticity of concrete. *ACI Materials Journal*. **94(1)**, 71-74.
- Newman J. (2003). Properties of lightweight concrete. Processes, Volume 4, 3-29.
- Nielsen, U. A., Monterio, J. M., Gjorv, O. E. (1995). Estimation of elastic moduli of lightweight aggregate. *Cement and Concrete Research*. **25**, 276-280.
- Nielsen, U., Aitcin, P. C. (1992). Properties of high strength concrete containing light, normal and heavy weight aggregate. *Cement, Concrete and Aggregate*. **1**, 8-12.
- Nielsson., I., Wallevik, O. (2003). Rheological evaluation of some empirical test methods preliminary results. *Third International Symposium on Self Compacting Concrete*, Reykjavik, Iceland, RILEM Publications S.A.R.L.
- Oh, B. H., Cha, S. W., Jang, B. S., Jang, S. Y. (2002). Development of high-performance concrete having high resistance to chloride penetration. *Nuclear Engineering and Design*. **212**, 221-231.
- Okamura H. (1999). Self-compacting high performance concrete. Tokyo: Social System Institute.
- Ozawa, K., Maekawa, K. (1989). Development of high performance concrete based on durability design of concrete structure. *Proceeding of the Second East-Asia and Pacific Conference on Structural Engineering and Construction (EASEC-2)*. **1**, 445-450.

- Pietsch W. (1991). Size enlargement by agglomeration. New York: John Wiley and Sons.
- Quiroga PN. (2003). The effect of aggregate characteristics on the performance of Portland cement concrete. *PhD Dissertation*. University of Texas at Austin.
- Raask, E. (1985). Cenospheres in pulverized fuel ash. *Journal of the Institute of Fuel*. **13**, 339-344.
- Ramadan KZ. (1995). Composite and aggregate production using high calcium fly ash. *PhD Thesis*. Boğaziçi University, Turkey.
- RILEM 50-FMC (1985). Committee of fracture mechanics of concrete. Determination of fracture energy of mortar and concrete by means of three-point bend tests on notched beams. *Materials and Structures*. **18(106)**, 285-290.
- RILEM TC 116-PCD (1999). Permeability of concrete as a criterion of its durability. *Materials and Structures*. **32**, 174-179.
- Roussel, N. (2005). Steady and transient flow behaviour of fresh cement pastes. *Cement and Concrete Research*. **35**, 1656-1664.
- Roussel, N. (2006). A thixotropy model for fresh fluid concretes: theory, validation and applications. *Cement and Concrete Research*. **36**, 1797-1806.
- Saak, A. W., Jennings, H. M., Shah, S. P. (2001a). The influence of wall slip on yield stress and viscoelastic measurements of cement paste. *Cement and Concrete Research*. **31**, 205-212.
- Saak, A. W., Jennings, H. M., Surendra, P. S. (2001b). New methodology for designing self-compacting concrete. *ACI Materials Journal*. **98(6)**, 429-439.
- Safiuddin, M. D., Salam, M. A., Jumaat, M. Z. (2011). Effects of recycled concrete aggregate on the fresh properties of self-consolidating concrete. *Archives of Civil and Mechanical Engineering*. **11(4)**, 1023-1041.
- Satapathy, L. N. (2000). A study on the mechanical, abrasion and microstructural properties of zirconia-fly ash material. *Ceramics International*. **26**, 39-45.

Schneider, U., Chen, S. (1992). The interface zone around expanded shale grain in hardened cement paste. *Interface in Cementitious Composites*. J.C. Maso, ed., **Paper no. 16**.

Schwartzentruber, L. D., Roy, R. L., Cordin, J. (2006). Rheological behaviour of fresh cement pastes formulated from a self-compacting concrete (SCC). *Cement and Concrete Research*. **36**, 1203-1213.

Sadran T. (2000). Rheology. Brite EuRam, Final Report of Task 3.

Şengül Ö. (2005). Effects of pozzolanic materials on the mechanical properties and chloride diffusivity of concrete. *PhD Thesis*. Istanbul Technical University, Turkey.

Shah, S. P., Karaguler, M. E., Sarigaphuti, M. (1992). Effects of shrinkage reducing admixtures on restrained shrinkage cracking of concrete. *ACI Materials Journal*. **89(3)**, 289-295.

Shannag, M. J. (2011). Characteristics of lightweight concrete containing mineral admixtures. *Construction and Building Materials*. **25**, 658-662.

Smadi, M., Migdady, E. (1991). Properties of high strength tuff lightweight aggregate. *Cement and Concrete Composites*. **13**, 129-135.

Su, N., Hsu, K. C., Chai, H. W. (2001). A simple mix designs method for self-compacting concrete. *Cement and Concrete Research*. **31(12)**, 1799-1807.

Taşdemir, C., Taşdemir, M. A., Lydon, F. D., Barr, B. I. G. (1996). Effects of silica fume and aggregate size on the brittleness of concrete. *Cement and Concrete Research*. **26(1)**, 63-68.

Taşdemir, M. A., Karihaloo, B. L. (2001). Effect of aggregate volume fraction on the fracture parameters of concrete: a meso-mechanical approach. *Magazine of Concrete Research*. **53**, 405-415.

Taşdemir, M. A., Taşdemir, C., Grimm, R., König, G. (2002). Role of aggregate fraction in the fracture of semi-lightweight high strength concrete. *Proceedings of the 6th International Symposium on Utilization of High Strength/High Performance Concrete*. Leipzig, June, 1453-1466.

Tattersall GH, Banfill PFG. (1983). The rheology of fresh concrete. Pitman Advanced Pub. Program, Boston.

Tattersall GH. (1991). Workability and quality control of concrete. London: E&FN Spon.

Topcu, İ. B., Uygunoğlu, T. (2010). Effect of aggregate type on properties of hardened self-consolidating lightweight concrete (SCLC). *Construction and Building Materials*. **24**, 1286-1295.

Torres, M. L., Garcia-Ruiz, P. A. (2009). Lightweight pozzolanic materials used in mortars: Evaluation of their influence on density, mechanical strength and water absorption. *Cement and Concrete Composites*. **31(2)**, 114-119.

TS EN 12390-8. Institute of Turkish Standards. (2002). Testing Hardened Concrete-Part 8: Depth of Penetration of Water under Pressure, Ankara, Turkey.

TS 706 EN 12620-A1. Institute of Turkish Standards. (2009). Aggregates for Concrete, Ankara, Turkey.

Turkish Statistical Institute, Press Release 8. <http://www.turkstat.gov.tr/> 2010.

Türkmen, İ., Kantarcı, A. (2007). Effects of expanded perlite aggregate and different curing conditions on the physical and mechanical properties of self-compacting concrete. *Building and Environment*. **42**, 2378-2383.

Videla, C., Martinez, P. (2002). Physical, mechanical and microscopic characterization of cold bonded fly ash lightweight aggregates. *Materials and Construction*. **268**, 5-18.

Wallevik JE. (2003). Rheology of particle suspensions. *PhD Dissertation*. Norwegian University of Science and Technology, Trondheim.

Wallevik, O. H. (2003). Rheology—A scientific approach to develop self-compacting concrete. *Third International RILEM Symposium on SCC*.

- Wasserman, R., Bentur, A. (1996). Interfacial interactions in lightweight aggregate concretes and their influence on the concrete strength. *Cement and Concrete Composites*. **18**, 67-76.
- Wasserman, R., Bentur, A. (1997). Effect of lightweight fly ash aggregate microstructure on the strength of concretes. *Cement and Concrete Research*. **27(4)**, 525-537.
- Wiegink, K., Marikunte, S. M., Shah, S. P. (1996). Shrinkage cracking of high strength concrete. *ACI Materials Journal*. **93(5)**, 409-415.
- Wittmann, F. (1976). On the action of capillary pressure in fresh concrete. *Cement and Concrete Research*. **6(1)**, 49-56.
- Wu, Z., Zhang, Y., Zheng, J., Ding, Y. (2009). An experimental study on the workability of self-compacting lightweight concrete. *Construction and Building Materials*. **23**, 2087-2092.
- Yamashita, T., Yamane R., Kohata, H., Sera, S., Kasami, I. I., Yonezawa, T. (1992). Fly ash lightweight aggregate sintered in a circular-grate kiln. *Fourth CANMET/ACI Int. Conference on Fly Ash, Silica Fume, Slag and Natural Pozzolans in Concrete*. Supplementary Papers, 895-915, İstanbul.
- Yang, C. C. (1997). Approximate elastic moduli of lightweight concrete. *Cement and Concrete Research*. **27**, 1021-1030.
- Yashima, S., Kanda, Y., Sano, S. (1987). Relationship between particle size and fracture energy or impact velocity required to fracture as estimated from single particle crushing. *Powder Technology*. **51(3)**, 227-282.
- Zhang, M. H., Gjorv, O. E. (1990). Microstructure of the interfacial zone between lightweight aggregate and cement paste. *Cement and Concrete Research*. **20**, 610-619.
- Zhang, M. H., Gjorv, O. E. (1991a). Characteristics of lightweight aggregates for high-strength concrete. *ACI Materials Journal*. **88(2)**, 150-158.

Zhang, M. H., Gjorv, O. E. (1991b). Permeability of high-strength lightweight concrete. *ACI Materials Journal*. **88(5)**, 463-469

Zhang, M. H., Gjorv, O. E. (1991c). Mechanical properties of high strength lightweight concrete. *ACI Materials Journal*. **88(3)**, 240-247.

Zhang, M. H., Li, L., Paramasivam, P. (2005). Shrinkage of high-strength lightweight aggregate exposed to dry environment. *ACI Materials Journal*. **102(2)**, 86-92.

Zhou, F. P., Balendran, R. V., Jeary, A. P. (1998). Size effect on flexure, splitting tensile and torsional strengths of high strength concrete. *Cement and Concrete Research*. **28(12)**, 1725-1736.

Zhu, W., Bartos, P. J. M. (2003). Permeation properties of self-compacting concrete. *Cement and Concrete Research*. **33**, 921-926.

PERSONAL INFORMATION

Name and Surname : Hatice Öznur ÖZ
Nationality : T.C.
Birth place and date : Kayseri/1983
Marial status : Married- 1 children
Phone number : 05053711923/03423172457
Fax : 03423601107
Email : oznuroz@gantep.edu.tr

EDUCATION

	Graduate School	Year
Master	University of Erciyes	2007
Second University	University of Anadolu (Department of Business)	2007
Bachelor	University of Erciyes	2005
High School	Fevzi Çakmak High School	2001

WORK EXPERIENCE

Years	Place	Enrollment
2005-2006	University of Niğde	Research Assistant
2006-2007	University of Kayseri	Research Assistant
2007-2008	University of Niğde	Research Assistant
2008-Present	University of Gaziantep	Research Assistant

PUBLICATIONS

A. International Journals

1. Mehmet Gesoğlu, Erhan Güneyisi, and **Hatice Öznur Öz** (2012), “Properties of Lightweight Aggregates Produced with Cold-Bonding Pelletization of Fly Ash and Ground Granulated Blast Furnace Slag,” *Materials and Structures*, V. 45, pp. 1535-1546.

2. Mehmet Gesođlu, Erhan Güneyisi, Swara Fuad Mahmood, **Hatice Öznur Öz** and Kasım Mermerdaş (2012), “Recycling Ground Granulated Blast Furnace Slag as Cold Bonded Artificial Aggregate Partially Used in Self-Compacting Concrete,” *Journal of Hazardous Materials*, V. 235, pp. 352–358.

3. Mehmet Gesođlu, Erhan Güneyisi, Turan Özturan, **Hatice Öznur Öz**, Diler Sabah Asaad (2014), “Self-Consolidating Characteristics of Concrete Composites Including Rounded Fine and Coarse Fly Ash Lightweight Aggregates,” *Composite Part B* (Accepted).

B. International Congress, Conference, and Symposium

1. Faruk Geyik, Mehmet Gesođlu, Erhan Güneyisi, Kasım Mermerdaş and **Hatice Öznur Öz** (2012), “Predicting the Crushing Strength of Cold-Bonded Artificial Aggregates by Genetic Algorithms,” 27th International Conference on Solid Waste Technology and Management, Philadelphia, USA, CD pp. 276–283,.

2. Mehmet Gesođlu, Erhan Güneyisi and **Hatice Öznur Öz** (2012), “Using of Fly Ash and Blast Furnace Slag in the Production of Lightweight Aggregates through Cold-Bonding Process,” 27th International Conference on Solid Waste Technology and Management, Philadelphia, USA, CD pp. 609–620.

Research Projects

1. Sođuk bađlama yöntemi ile üretilecek uçucu kül ve öđütölmüş yüksek fırın cürufu hafif agregalarının özelliklerinin incelenmesi (GUBAP, Completed, 2011).

FOREIGN LANGUAGE

Turkish (Mother language), English.

HOBBIES

Shopping, Computer, Reading.

